

Φασματοσκοπία ^1H - και ^{13}C -NMR

Βιβλιογραφία

- 1) R. M. Silverstein *et al*, "Spectrometric Identification of Organic Compounds"
- 2) R. S. Macomber, "A Complete introduction of Modern NMR Spectroscopy"
- 3) M. Hesse *et al*, "Spectroscopic Methods in Organic Chemistry"

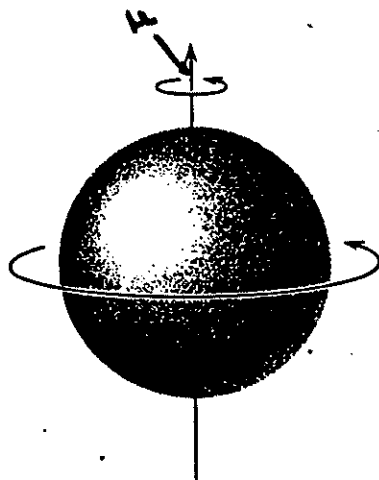


Fig. 1.
Spinning charge in proton generates magnetic dipole.

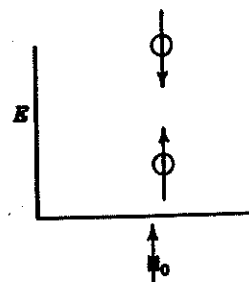


Fig. 2.
Energy levels of a proton.

1). The angular momentum of the spinning charge can be described in terms of spin numbers I ; these numbers have values of 0, 1/2, 1, 3/2, and so forth ($I = 0$ denotes no spin). The intrinsic magnitude of the generated dipole is expressed in terms of nuclear magnetic moment, μ .

Each proton and neutron has its own spin, and I is a resultant of these spins. If the sum of protons and neutrons is even, I is zero or integral (0, 1, 2, ...); if the sum is odd, I is half-integral (1/2, 3/2, 5/2, ...); if both protons and neutrons are even-numbered, I is zero. Both ^{12}C and ^{16}O fall in the latter category and give no NMR signal.

Several nuclei (^1H , ^{19}F , ^{13}C , and ^{31}P) have a spin number I of 1/2 and a uniform spherical charge distribution (Figure 1). Nuclei with a spin number I of 1 or higher have a nonspherical charge distribution. This asymmetry is

electromagnetic radiation) such that the parallel orientation (low-energy state) can be flipped to the antiparallel orientation (high-energy state) in a magnetic field of given strength H_0 . The fundamental NMR equation correlating electromagnetic frequency with magnetic field strength is

$$\nu = \frac{\gamma H_0}{2\pi}$$

The constant γ is called the magnetogyric (or more commonly but less properly, gyromagnetic) ratio and is a fundamental nuclear constant; it is the proportionality constant between the magnetic moment μ and the spin number I

$$\gamma = \frac{2\pi\mu}{hI}$$

where h is Planck's constant.

The bald statement made earlier that nuclear magnetic resonance spectrometry is akin to other forms of absorption spectrometry may now seem somewhat more plausible. The problem is how to inject electromagnetic energy into

Όπως ή περιστροφή του ηλεκτρονίου δημιουργεί το spin αυτού, ούτω και ώρισμένοι πυρήνες κατά την περιστροφή των δημιουργούν το πυρηνικό spin I , το όποιον λαμβάνει τās τιμές 0, 1/2, 1 ... εἰς μονάδας $h/2\pi$. Ἡ στροφική ὁρμή του πυρήνος P λόγω του spin αυτού δίδεται υπό της σχέσεως:

$$P = \frac{h}{2\pi} \sqrt{I(I+1)}$$

Ἀφ' ἑτέρου το μηχανικό spin, λόγω του φορτίου του πυρήνος, δημιουργεί μαγνητικό δίπολο, το μέγεθος του οποίου εκφράζεται ὡς πυρηνική μαγνητική ροπή μ και ή οποία συνδέεται μετά του γυρομαγνητικού λόγου γ του πυρήνος διά της σχέσεως:

$$\mu = \gamma \hbar I \quad (\hbar = \frac{h}{2\pi})$$

Ἡ μαγνητική ροπή του πρωτονίου εἶναι 1840 φορές μικρότερα της μαγνητικής ροπής του ηλεκτρονίου (μαγνητόνη Bohr), διότι ὑφίσταται ἀντίστροφος ἀναλογία μεταξύ μαγνητικής ροπής και μάζης του σωματιδίου

Πυρήνες με άρτιο ατομικό αριθμό και άρτιο μαζικό αριθμό $^{12}_6\text{C}$ $^{16}_8\text{O}$ έχουν $I=0$

Πυρήνες με περιττό μαζικό αριθμό έχουν ημιπεριττό I $^1_1\text{H } 1/2$ $^{13}_6\text{C } 1/2$ $^{11}_5\text{B } 3/2$ $^{15}_7\text{N } 1/2$ $^{19}_9\text{F } 1/2$

Πυρήνες με περιττό ατομικό αριθμό και άρτιο μαζικό έχουν I ακέραιο αριθμό $^2_1\text{H } 1$, $^{14}_7\text{N } 1$.

Μαγνητικό πεδίο

H_0

$\Rightarrow 2I+1$ στεροχικούς προσανατολισμούς ως προς το H_0

Εκτός πεδίου υπάρχει μόνο μία στάθμη ενέργειας, εντός μαγνητικού πεδίου κάθε προσανατολισμός έχει τη δική του ενέργεια

Η κατανομή των πληθυσμών μεταξύ δύο στρωτικών προσανατολισμών ορίζεται από ειδική σχέση. Για το υδρογόνο η κατανομή των δύο πληθυσμών είναι $0.99999/1.00001$ εάν το $H_0 = 10.000 \text{ gauss}$.

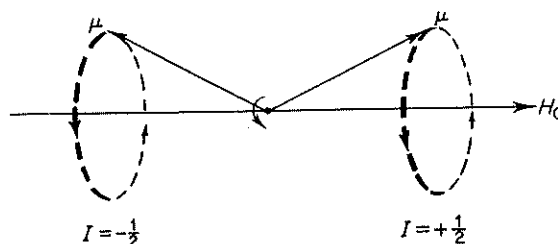


Fig. 5.1. Precession of the axis of the magnetic moment of a nucleus about the lines of an applied magnetic field.

nucleus is given by Eq. (5.1)

$$\Delta E = h\nu = \frac{\mu\beta_N B_0}{I} \quad (5.1)$$

where h is Planck's constant, ν is the frequency of the exciting radiation, μ is the magnetic moment of the nucleus expressed in multiples of the nuclear magneton¹ (see Table 5.1), and β_N is a constant called the nuclear magneton constant. For nuclei with more than two spin states, radiation-induced spin transitions are allowed only between adjacent spin states, the energies between any two spin states being equal (see later discussion).

Because various nuclei differ in their value of μ and I , they will undergo nuclear spin transitions at different frequencies in the same applied magnetic field. Table 5.1 lists several of the more common nuclei with their nuclear spin quantum number I , μ , resonance frequency in a 10,000 gauss field, and natural abundance. Since the frequency and field strength are directly proportional, the data given in Table 5.1 can be scaled up or down to correspond to other applied field strengths. It should also be pointed out at this time that the sensitivity, or response, of an equal number of different nuclei will vary (see Eq. (5.2)) as a function of the angular momentum m

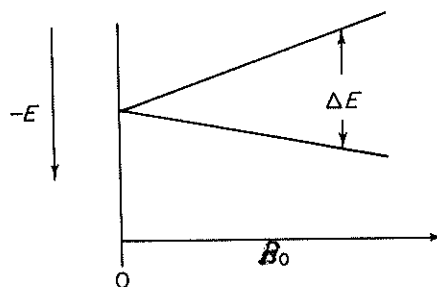


Fig. 5.2. Spin energy level separation for a nucleus with I of $\frac{1}{2}$ as a function of the applied field H_0 .

¹The magnetic moment μ may possess either a + or - sign and is due to the fact that the I and μ vectors may be parallel or antiparallel ($\mu = cI$).

$$\begin{aligned} &= \phi \alpha \sigma \mu \alpha \text{ } ^1\text{H} \text{ } \sigma \alpha \text{ } 60 \text{ MHz} \Rightarrow B_0 \text{ } 14.000 \text{ gauss} \\ &\text{ } // \text{ } // \text{ } // \text{ } 100 \text{ MHz} \Rightarrow B_0 \text{ } 23.500 \text{ gauss} \end{aligned}$$

ce, $\Delta X_B =$
 erse or per-
 the sym-
 instances
 data, and

s involving
 atics. The
 will be dis-
 rpter.

) or an in-

n A in Eq.

(5.6)

der of the
 ous nuclei
 e molecule.
 in different
 change in
 position is
 ave an ex-
 us nuclei in

CAL SHIFT

y ν and the
 one of these
 required for
 of 10^6 Hz.
 t are of the
 control and
 measurable
 io frequency
 ing a high-
 ntrolled by a
 he sample is
 uency is im-
 sweep coils,

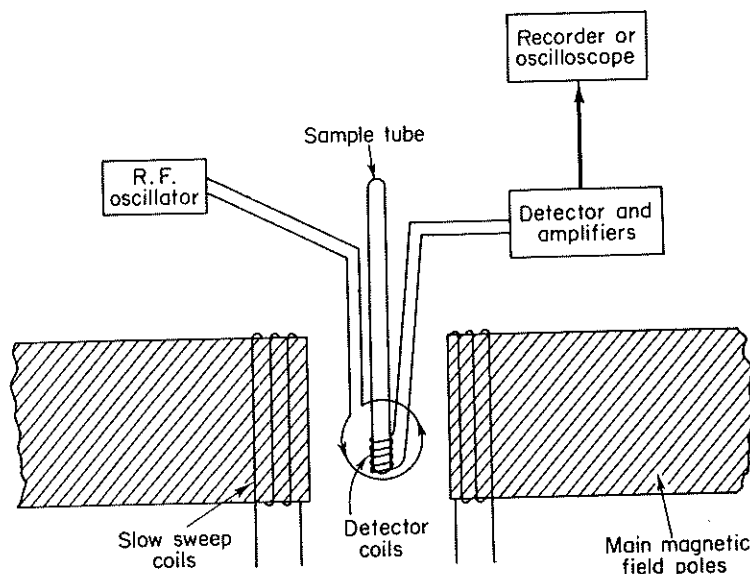


Fig. 5.3. Nuclear induction system of a nuclear magnetic resonance spectrometer.

the magnetic field changes until the correct conditions for resonance occur with the absorption of radio-frequency energy. The reorientation of the spin angular momenta of the nuclei undergoing spin excitation induces a signal in the receiver coils (the plane of the receiver coil is maintained at a right angle with respect to the plane of the radio-frequency coil), which is amplified and sent to a recorder, giving rise to an induction spectrum. Such a setup is referred to as a *double-coil* system and is used only for high-resolution nuclear magnetic resonance spectroscopy. Another experimental arrangement involves the use of only a single coil for the radio-frequency coil and receiver coil; this is referred to as a *single-coil* system. Single-coil systems give rise to true absorption spectra and are used for both low- and high-resolution nuclear magnetic resonance spectroscopy.

At present, there are two basically different instrument designs for recording nuclear magnetic resonance spectra. One involves recording the absorption or induced signal vs. a variable—field strength, time, or chart speed; the two quantities are essentially independent of one another. Spectra recorded on such instruments do not provide direct indications of the resonance positions. Examples of such instruments include the Varian Associates HR-40, HR-60, and HR-100, in which the number following the HR indicates the basic spectrometer frequency. To accurately pinpoint the peak positions, an internal standard is added to the sample; the position of absorption of the reference standard is used as a reference field strength. The peak positions are then determined by extrapolation or interpolation techniques, using a side band from the standard impressed at a known

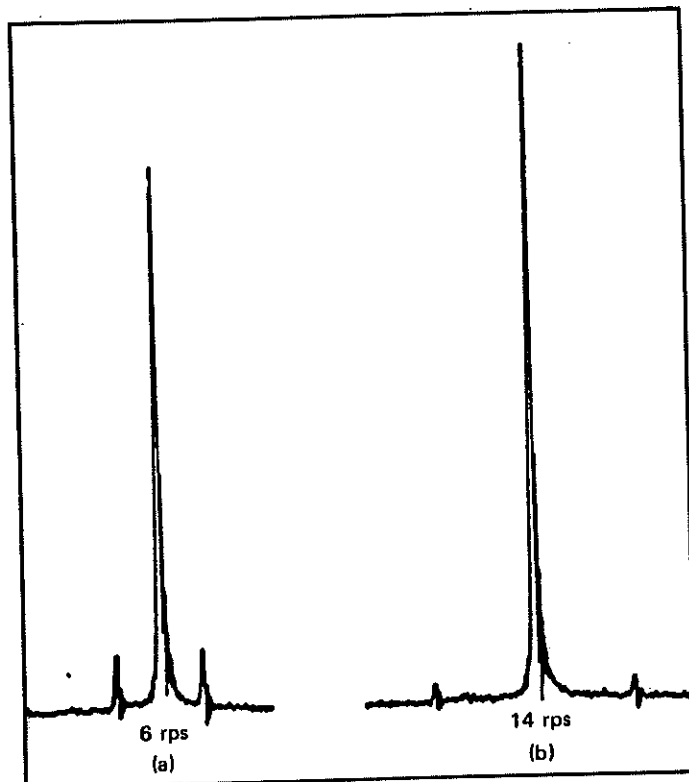


Fig. 6. Signal of neat chloroform with spinning side bands produced by spinning rate of (a) 6 rps and (b) 14 rps. (From F. A. Bovey, NMR Spectrometry, copyright 1969, Academic Press.)

III. CHEMICAL SHIFT

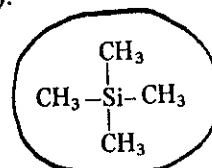
Thus far, we have obtained a single peak from the interaction of radio frequency and a strong magnetic field on a proton in accordance with the basic NMR equation in which γ , the magnetogyric ratio, is an intrinsic property of the nucleus. The peak area (measured by the integrator) is proportional to the number of protons it represents. Fortunately, the situation is not quite so simple. The nucleus is shielded to a small extent by its electron cloud whose density varies with the environment. This variation gives rise to different absorption positions within the range of about 1000 Hz or so in a magnetic field corresponding to 60 MHz or about 1700 Hz in a field corresponding to 100 MHz. The ability to discriminate among the individual absorptions describes high resolution NMR spectrometry.

Electrons under the influence of a magnetic field will circulate, and, in circulating, will generate their own magnetic field opposing the applied field; hence, the shielding effect (Figure 9). This effect accounts for the diamagnetism exhibited by all organic materials. In the case of materials with an unpaired electron, the paramagnetism

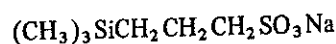
associated with the net electron spin far overrides the diamagnetism of the circulating, paired electrons.

The degree of shielding depends on the density of the circulating electrons, and as a first, very rough approximation, the degree of shielding of a proton on a carbon atom will depend on the inductive effect of other groups attached to the carbon atom. These are small effects; as we pointed out, we are talking about shifts of parts per million (i.e., Hz in a 60- or 100-MHz field) in relation to a standard reference. The difference in the absorption position of a particular proton from the absorption position of a reference proton is called the *chemical shift* of the particular proton.

The most generally useful reference compound is tetramethylsilane (TMS).



It has several advantages: it is chemically inert, magnetically isotropic, volatile (b.p. 27°), and soluble in most organic solvents; it gives a single sharp absorption peak, and absorbs at higher field than almost all organic protons. When water or deuterium oxide is the solvent, TMS can be used as an "external reference," i.e., sealed in a capillary immersed in the solution. The methyl protons of sodium 2,2-dimethyl-2-silapentane-5-sulfonate (DSS):



are sometimes used as an internal reference in aqueous solution. Since only enough is used to give a small methyl peak, the diffuse pattern of the CH_2 peaks barely shows on the base line. Unless hydrogen-bonding effects are involved, a proton peak referenced to TMS in deuteriochloroform will be within 0.01 to 0.03 ppm of the same peak referenced to DSS in water or deuterium oxide. Acetonitrile and dioxane are also used as references in aqueous solution.

Let us set up an NMR scale (Figure 10) and set the TMS peak at 0 Hz at the right-hand edge. The magnetic field increases toward the right. When chemical shifts are given in Hz (designated ν), the applied frequency must be specified. Chemical shifts can be expressed in dimensionless units (δ), independent of the applied frequency, by dividing ν by the applied frequency and multiplying by 10^6 . Thus a peak at 60 Hz (ν 60) from TMS at an applied frequency of 60 MHz would be at δ 1.00 or 1.00 ppm.

$$\left\langle \delta \text{ or ppm} = \frac{60}{60 \times 10^6} \times 10^6 = 1.00 \right\rangle$$

Since δ units are expressed in parts per million, the expression ppm is often used. The same peak at an applied frequency of 100 MHz would be at ν 100, but would still be at δ 1.00.

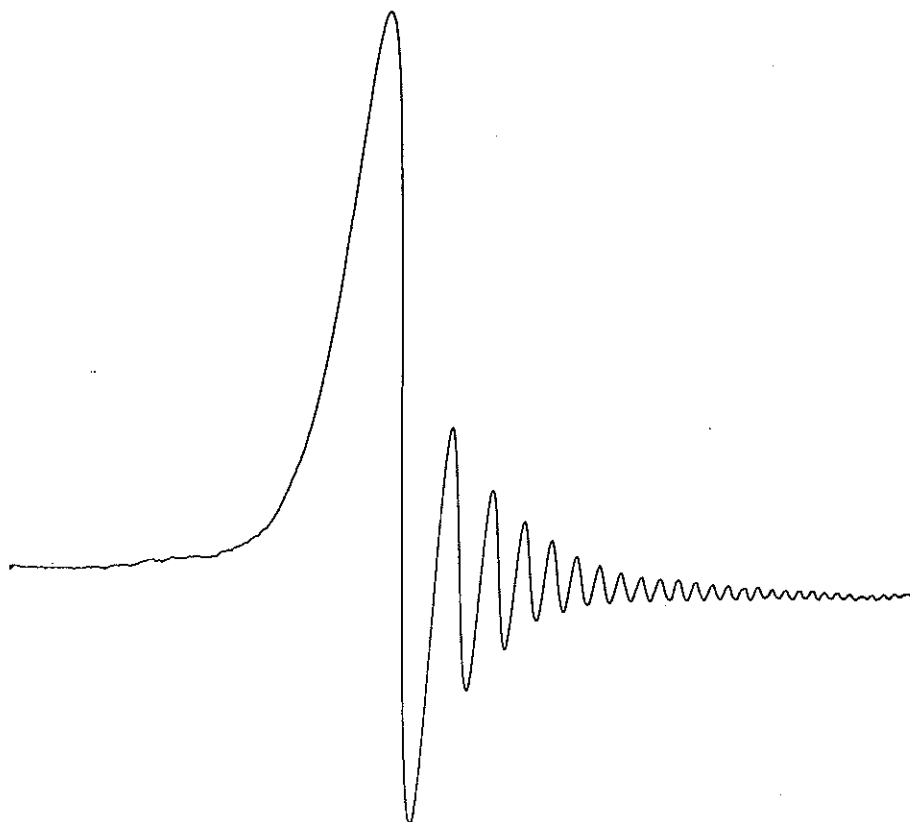


Fig. 7.
Ringing (or "wiggles") seen after passage through resonance. Direction of scan from left to right. (From E. C. Becker, High Resolution NMR, copyright 1969, Academic Press.)

$$\delta \text{ or ppm} = \frac{100}{100 \times 10^6} \times 10^6 = 1.00$$

This scheme has been criticized because δ values increase in the downfield direction; the rejoinder is that these are really negative numbers. The other commonly used system assigns a value of 10.00 for tetramethylsilane, and describes chemical shifts in terms of τ values.

$$\tau = 10.00 - \delta$$

It should be noted that δ is treated as a positive number. We shall make our assignments in both δ and τ values. Shifts at higher field than TMS (δ 0.00, τ 10.00) will be encountered very rarely; δ values are then shown with a negative sign, and τ values merely increase numerically.

It is important to realize that the chemical shift in Hz is directly proportional to the strength of the applied field H_0 , and therefore to the applied frequency. This is understandable because the chemical shift is dependent on the diamagnetic shielding induced by H_0 . The strongest magnetic field consistent with field homogeneity should be used to spread out the chemical shifts. This is made clear in

= σχετική ηλεκτραρρητικότητα =



(Hammett SIND)

Figure 11 in which increased applied magnetic field in the NMR spectrum of acrylonitrile means increased separation of signals.

The concept of electronegativity is a dependable guide, up to a point, to chemical shifts. It tells us that the electron density around the protons of TMS is high (silicon is electropositive relative to carbon), and these protons will therefore be highly shielded and their peak will be found at high field. We could make a number of good estimates as to chemical shifts, using concepts of electronegativity and proton acidity. For example, the following values are reasonable on these grounds:

	δ	τ
$(\text{CH}_3)_2\text{O}$	3.27	6.73
CH_3F	4.30	5.70
RCOOH	10.8 (approx.)	-0.8

ιονικό

But finding the protons of acetylene at δ 2.35, τ 7.65, that is more shielded than ethylene protons (δ 4.60, τ 5.40), is

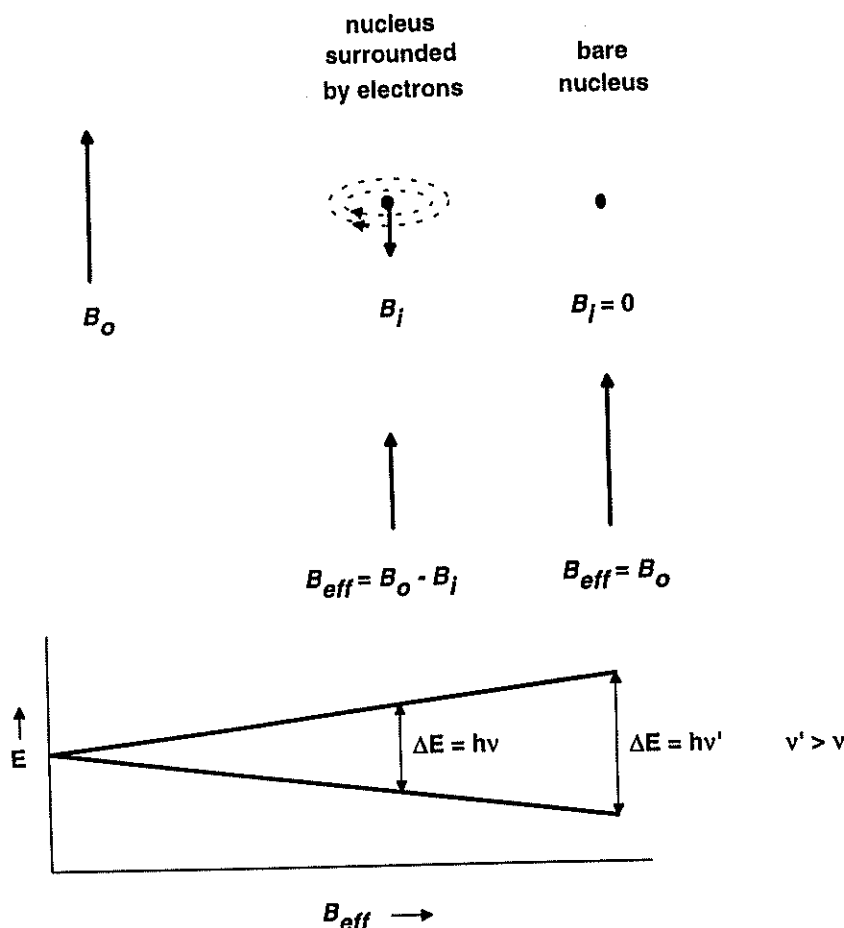


Figure 6.1. Effect of diamagnetic shielding. The dotted ellipses represent motion of electrons in their orbitals under the influence of B_0 .

$$\nu_{\text{precession}} = \frac{\gamma(1 - \sigma) B_0}{2\pi} \quad (6.4)$$

Thus, the greater the shielding of the nucleus (the larger the value of σ), the lower will be its resonance frequency and the farther to the right it will appear in an NMR spectrum. Conversely, nuclei from which electron density has been withdrawn (resulting in a smaller σ) are said to be *deshielded* and appear toward the left of the spectrum (higher frequency).

From an earlier chemistry course you may recall the concept of **electronegativity**, the tendency of an atom *in a molecule* to attract bonding electrons toward itself. The electronegativity of an atom is a consequence of a high kernel charge (nuclear charge minus subvalence electrons) coupled with a small atomic radius. The more electronegative an atom, the lower the energy of its valence orbitals and the higher its ionization energy. Table 6.1 lists the Pauling electronegativity values for some of the common main-group elements. Note that fluorine is the most electronegative element, and electronegativity decreases as you move down or to the left within

the periodic table (Appendix 2). It should come as no surprise that, in general, the more electronegative an atom or group of atoms, the greater its deshielding effect on neighboring atoms in the same molecule. The polarization (unequal sharing) of bonding electrons by virtue of differences in electronegativity among atoms is an example of **inductive effects**.

■ **EXAMPLE 6.1** (a) Arrange the following atoms from most electronegative to least: H, Li, C, Si. (b) Arrange the following underlined hydrogens from most deshielded to least: H₃C–H, H₃C–Li, H₃C–C, H₃C–Si.

TABLE 6.1 Pauling Electronegativities

H (2.1)							
Li (1.0)	Be (1.5)	B (2.0)	C (2.5)	N (3.0)	O (3.5)	F (4.0)	
Na (0.9)	Mg (1.2)	Al (1.5)	Si (1.8)	P (2.1)	S (2.5)	Cl (3.0)	
						Br (2.8)	
						I (2.5)	

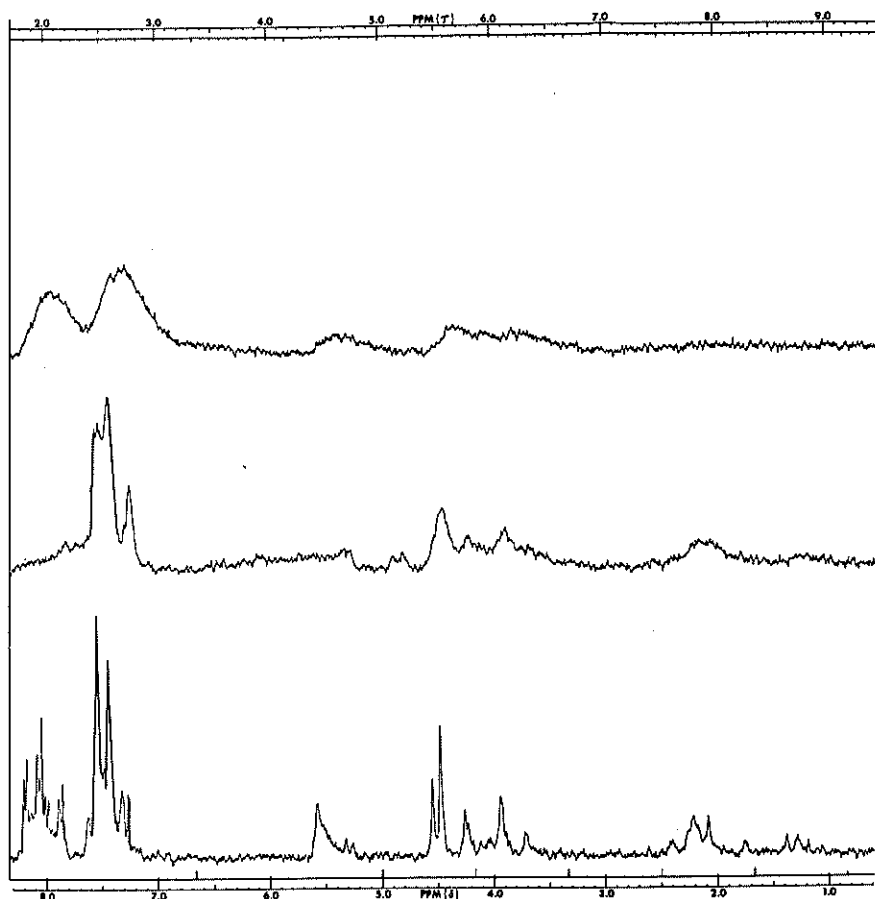


Fig. 8.
The effect of a tiny ferromagnetic particle on the proton resonance spectrum of a benzoylated sugar. The top and middle curves are repeat runs with the particle present; the bottom curve is the spectrum with the particle removed. (From E. C. Becker, *High Resolution NMR*, copyright 1969, Academic Press.)

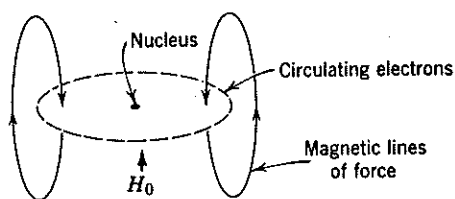


Fig. 9.
Diamagnetic shielding of nucleus by circulating electrons.

unsettling. And finding the aldehydic proton of acetaldehyde at δ 9.97, τ 0.03 definitely calls for some augmentation of the electronegativity concept. We shall use diamagnetic anisotropy to explain these and other apparent anomalies, such as the unexpectedly large deshielding effect of the benzene ring (benzene protons δ 7.27, τ 2.73).

Let us begin with acetylene. The molecule is linear, and the triple bond is symmetrical about the axis. If this axis is aligned with the applied magnetic field, the π -electrons of the bond can circulate at right angles to the applied field, thus inducing their own magnetic field opposing the applied field. Since the protons lie along the magnetic axis, the magnetic lines of force induced by the circulating electrons act to shield the protons (Figure 12) and the NMR peak is found further upfield than electronegativity would predict. Of course, only a small number of the rapidly tumbling molecules are aligned with the magnetic field, but the overall average shift is affected by the aligned molecules.

This effect depends upon diamagnetic anisotropy, which means that shielding and deshielding depend on the orientation of the molecule with respect to the applied magnetic field. Similar arguments can be adduced to rationalize the unexpected low field position of the aldehydic proton. In this case, the effect of the applied

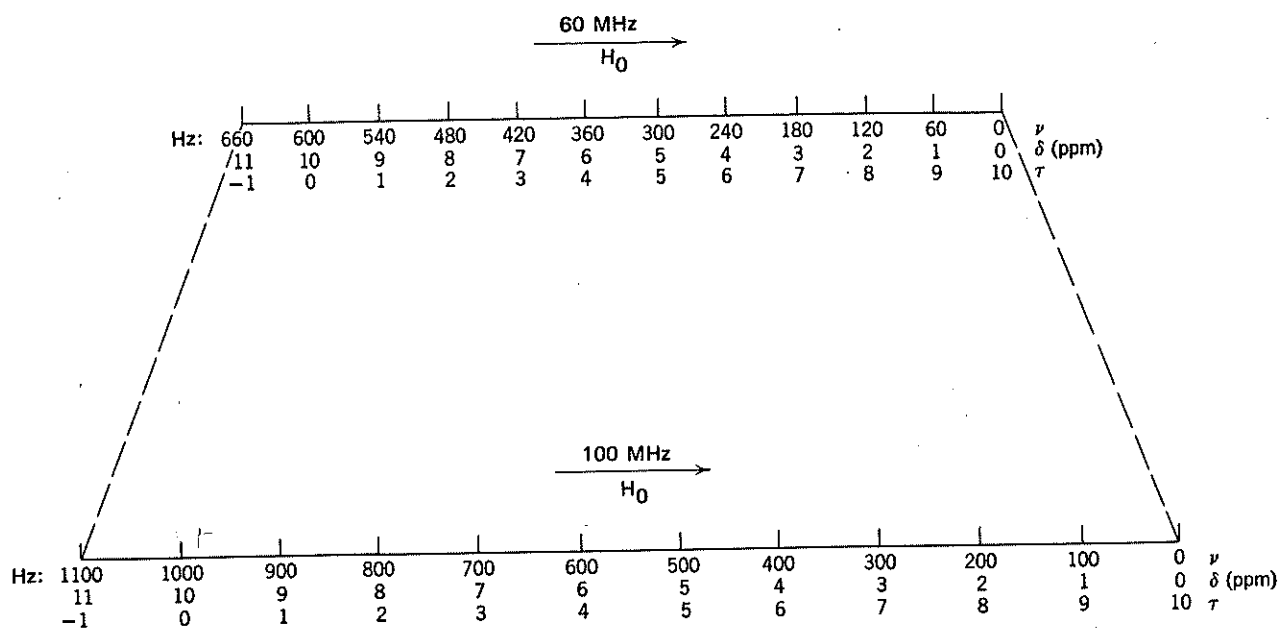


Fig. 10.
NMR Scale at 60 MHz and 100 MHz.

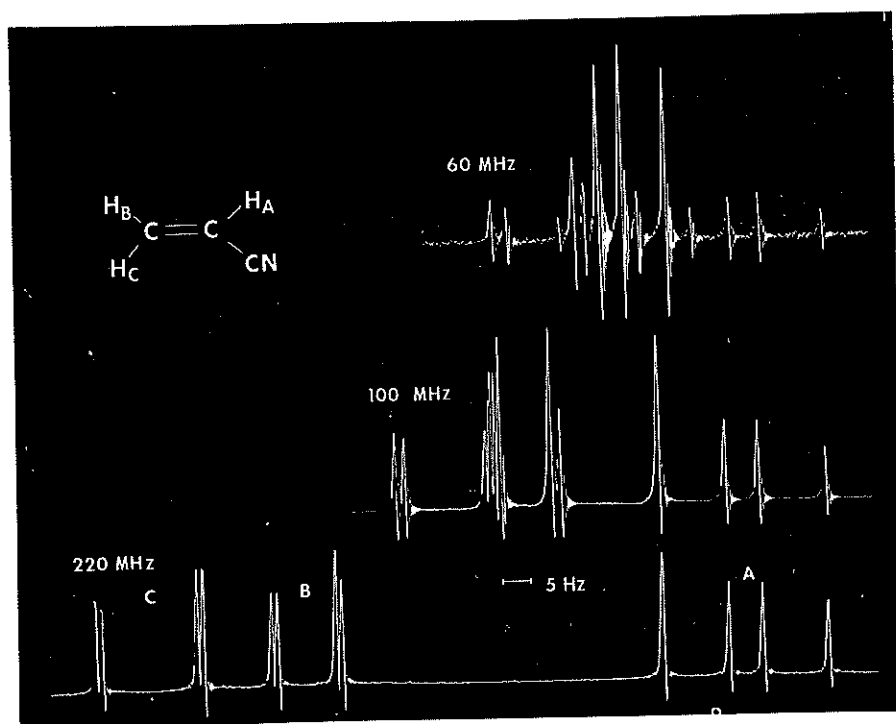


Fig. 11.
60-, 100-, and 220-MHz spectra of acrylonitrile. (Reprinted from Anal. Chem. Copyright 1971 by the American Chemical Society. Reprinted by permission of the copyright owner.)

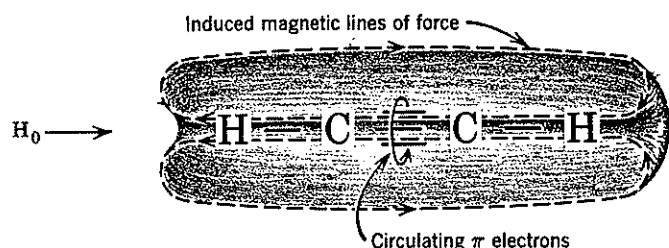


Fig. 12.
Shielding of acetylenic protons.

magnetic field is greatest along the transverse axis of the C=O bond (i.e., in the plane of the page in Figure 13). The geometry is such that the aldehydic proton, which lies in front of the page, is in the deshielding portion of the induced magnetic field. The same argument can be used to account for at least part of the rather large amount of deshielding of olefinic protons.

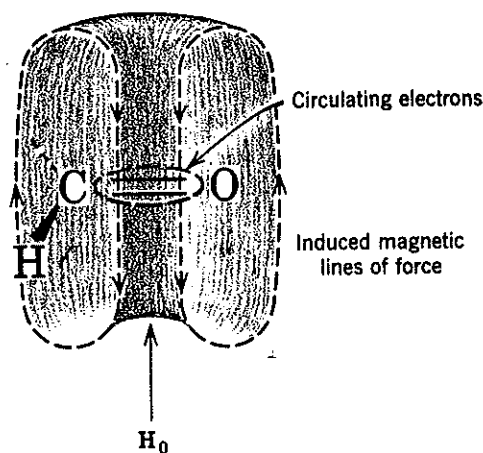


Fig. 13.
Deshielding of aldehydic protons.

The so-called "ring-current effect" is another example of diamagnetic anisotropy and accounts for the large deshielding of benzene ring protons. Figure 14 shows this effect. It also indicates that a proton held directly above or below the ring should be shielded. This has actually been found to be the case for some of the methylene protons in 1,4-polymethylenebenzenes.

All the ring protons of acetophenone are found downfield because of the ring current effect. Moreover, the ortho protons are shifted slightly further downfield (meta, para $\delta \sim 7.40$, τ 2.60; ortho $\delta \sim 7.85$, τ 2.15) because of the additional deshielding effect of the carbonyl group. In Figure 15 the carbonyl bond and the benzene ring are

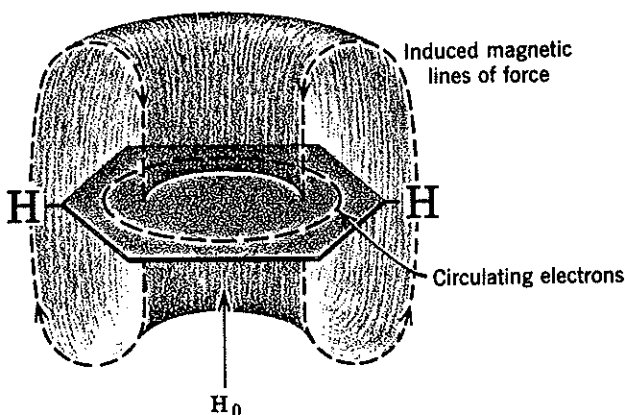
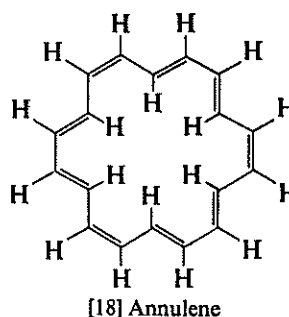


Fig. 14.
Ring current effects in benzene.

coplanar. If the molecule is oriented so that the applied magnetic field H_0 is perpendicular to the plane of the molecule, the circulating π electrons of the C=O bond shield the conical zones above and below them, and deshield the lateral zones in which the ortho proton is located. Both ortho protons are equally deshielded since another, equally populated, conformation can be written in which the "lefthand" ortho proton is more proximate to the anisotropy cone.

A spectacular example of shielding and deshielding by ring currents is furnished by some of the annulenes.¹⁷ The protons outside the ring of [18] annulene are strongly deshielded (δ 8.9, τ 1.1), and those inside are strongly shielded (δ - 1.8, τ 11.8).



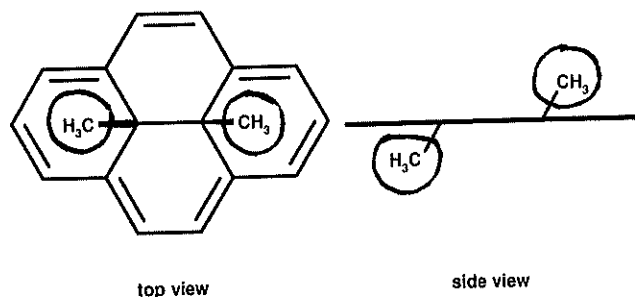
Demonstration of such a ring current is probably the best evidence available for aromaticity.

In contrast with the striking anisotropic effects of circulating π electrons, the σ electrons of a C—C bond produce a small effect. The axis of the C—C bond is the axis of the deshielding cone (Figure 16).

This figure accounts for the deshielding effect of successive alkyl substituents on a proton attached to a carbon atom. Thus the protons are found progressively downfield in the sequence $\underline{RCH_3}$, $\underline{R_2CH_2}$, and $\underline{R_3CH}$. The

The predicted chemical shift of these aromatic hydrogens is $\delta 7.27 + 0.58 + 0.21 = 8.06$. Note the close similarity of its spectrum to the one described in Example 6.17. \square

■ **EXAMPLE 6.20** Explain why the two equivalent methyl groups in structure 6-4 appear at $\delta -4.25$,⁵ far upfield of TMS:



6-4

□ **Solution:** The alternating single and double bonds around the periphery of the 14-membered ring give rise to an aromatic 14π electron cloud, with its associated ring current. The methyl groups lie directly above and below the plane of the ring, in the strongly shielding region of the induced field. \square

Not all cyclic molecules with alternating single and double bonds are aromatic, only those with $4n + 2\pi$ electrons. Furthermore, not all aromatic rings are six membered (**benzenoid aromatics**); some are five membered with a π system that includes an unshared pair of electrons donated by a **heteroatom** (an atom other than carbon). For example, the structures 6-5 through 6-9 all exhibit aromatic properties, and hydrogens attached to the rings fall in the aromatic region. The chemical shift of each set of equivalent hydrogens is given in parentheses. Compounds such as 6-5, 6-6, and 6-7 are called **het-**

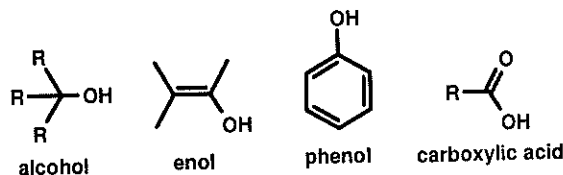
eroaromatic compounds because their rings contain atoms other than carbon. Compounds 6-8 and 6-9 are examples of **polycyclic aromatic hydrocarbons (PAH)**:

6.6 HYDROGEN ATTACHED TO ELEMENTS OTHER THAN CARBON

With more than 100 elements besides carbon in the periodic table (Appendix 2), you might fear that the number of ^1H chemical shift correlations is endless. However, except for a few specialized applications, the most important heteroatoms to which hydrogen finds itself bonded are oxygen and nitrogen. But before we discuss these two specific cases, here is a useful generalization: As the electronegativity (Table 6.1) of X increases, both the acidity and chemical shift of a hydrogen bonded directly to X increase.

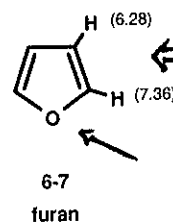
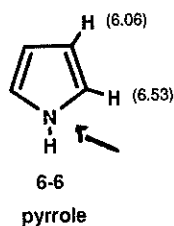
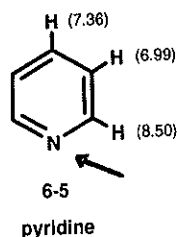
6.6.1 Hydrogens Attached to Oxygen

A hydrogen attached to an oxygen (O-H) constitutes a **hydroxyl group**. Hydroxyl groups appear in several classes of organic molecules, including **alcohols** (where the carbon bearing the O-H is tetrahedral), **enols** (where the O-H group is directly bonded to a vinyl carbon), **phenols** (where the O-H group is bonded directly to an aromatic ring), and **carboxylic acids** (where the O-H group is directly bonded to a carbonyl carbon):



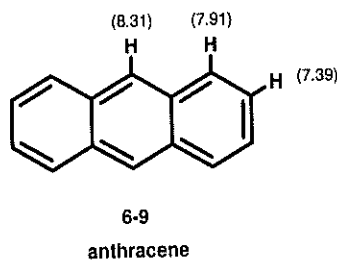
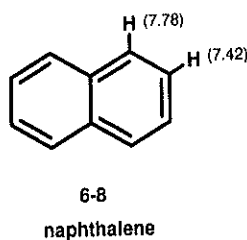
The order of acidity of these four classes of compounds is alcohols < enols < phenols < carboxylic acids. Therefore, it

Ετεροαρωματικά



electronegative
effect of
eteroatom

Πολυκυκλικά



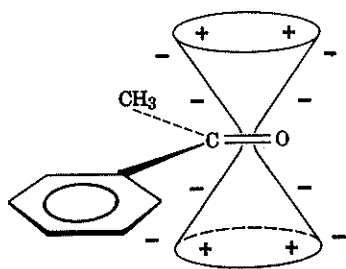


Fig. 15.
Shielding (+) and deshielding (-) zones of acetophenone.

observation that an equatorial proton is consistently found further downfield by 0.1–0.7 ppm than the axial proton on the same carbon atom in a rigid six-membered ring can also be rationalized (Figure 17). The axial and equatorial proton on C_1 are oriented similarly with respect to C_1-C_2 and C_1-C_6 , but the equatorial proton is within the deshielding cone of the C_2-C_3 bond (and C_5-C_6).

Chemical shifts of protons bound to carbon and near a single functional group are shown in chart form in Appendix B. Values assigned (δ and τ) are rough averages designed to indicate a region rather than an exact number. Except where otherwise specified, the shifts shown are for

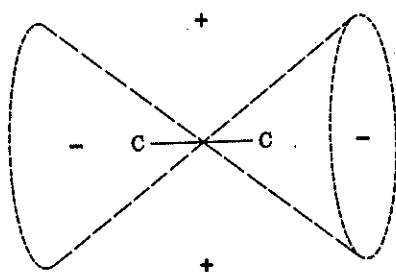


Fig. 16.
Shielding (+) and deshielding (-) zones of C—C.

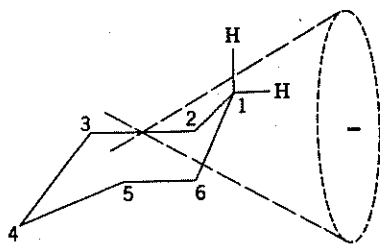


Fig. 17.
Deshielding of equatorial proton of a rigid six-membered ring.

aliphatic compounds in deuteriochloroform or carbon tetrachloride. Variations due to changes in concentration are usually small in the absence of hydrogen bonding effects. Solvent changes often cause appreciable changes in shift position. A separate value is given for methyl, methylene, and methine protons. Inspection of these charts gives the very useful general impression that chemical shifts of protons in organic compounds fall roughly into eight regions as summarized in Figure 18.

Appendix C gives shift positions for methylene protons carrying two functional groups. The calculated values were obtained from the set of Shoolery's constants,¹⁸ also presented in Appendix C. Appendix D lists shift ranges for protons subject to hydrogen bonding effects, and Appendix E has data useful for predicting olefinic proton chemical shifts.

IV. SIMPLE SPIN-SPIN COUPLING

We have obtained a series of absorption peaks representing protons in different chemical environments: each absorption area is proportional to the number of protons it represents. This achievement alone furnishes considerable information. We have now to consider one further refinement, spin-spin coupling. This can be described as the indirect coupling of proton spins through the intervening bonding electrons. Very briefly, it occurs because there is some tendency for a bonding electron to pair its spin with the spin of the nearest proton; the spin of a bonding electron, having been thus influenced, the electron will affect the spin of the other bonding electron and so on through to the next proton. Coupling is ordinarily not important beyond three bonds unless there is ring strain as in small rings or bridged systems, or bond delocalization as in aromatic or unsaturated systems.

Suppose two protons are in very different chemical environments from one another as in the compound

$$\begin{array}{c} \text{OR} \quad \text{CR}_3 \\ | \quad | \\ \text{RO}-\text{CH}-\text{CH}-\text{CR}_3 \end{array}$$
 Each proton will give rise to an absorption, and the absorptions will be quite widely separated. But the spin of each proton is affected slightly by the two orientations of the other proton through the intervening electrons so that each absorption appears as a doublet (Figure 19). The distance between the component peaks of a doublet is proportional to the effectiveness of the coupling, and is denoted by a coupling constant J , which is independent of the applied magnetic field H_0 . Whereas chemical shifts can range over about 1700 Hz at 100 MHz, coupling constants between protons rarely exceed 20 Hz (see Appendix F). So long as the chemical shift difference in Hz is much larger than the coupling

λογισα Η,
ανταλλαγή
με D₂O

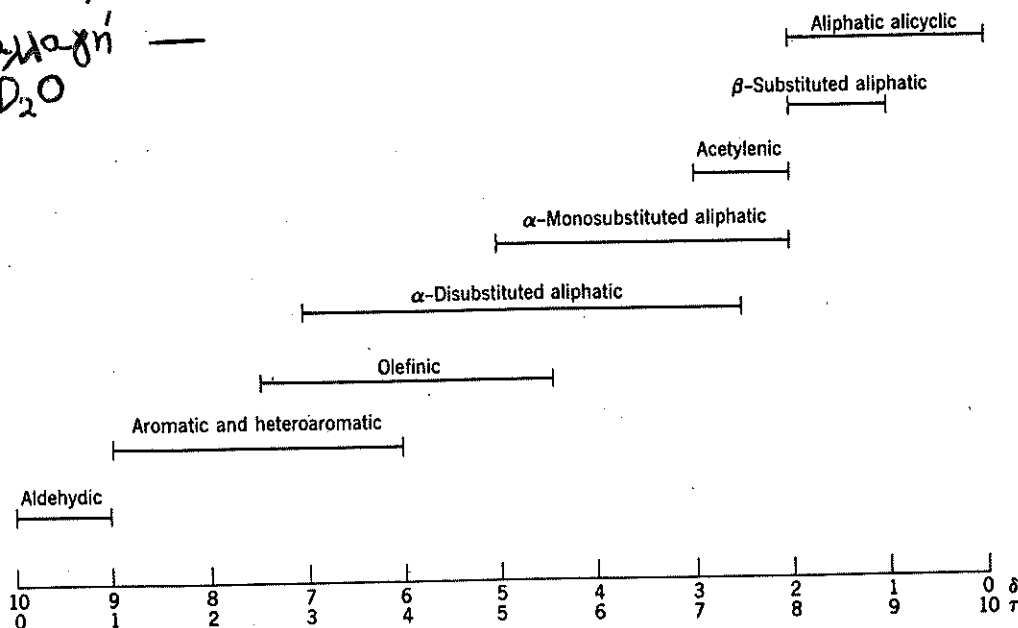


Fig. 18.
General regions of chemical shifts.

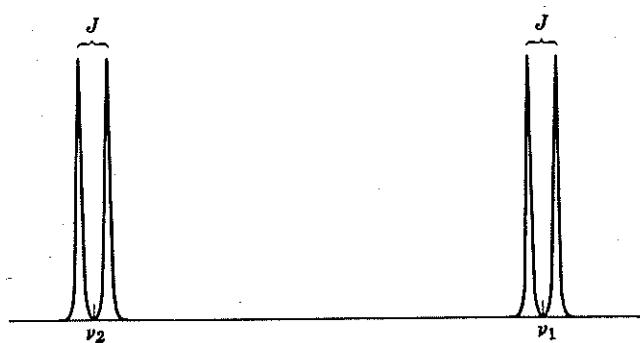


Fig. 19.
Spin-spin coupling between two protons with very different chemical shifts.

constant ($\Delta\nu/J$ is greater than about 10), the simple pattern of two doublets appears. As $\Delta\nu/J$ becomes smaller, the doublets approach one another, the inner two peaks increase in intensity, and the outer two peaks decrease (Figure 20). The shift position of each proton is no longer midway between its two peaks as was the case in Figure 19 but is at the "center of gravity" (Figure 21); it can be estimated with fair accuracy by inspection, or determined precisely by the following formula in which the peak positions (1, 2, 3, and 4 from left to right) are given in Hz from the reference.

$$(1-3) = (2-4) = \sqrt{(\Delta\nu)^2 + J^2}$$

The shift position of each proton is $\frac{\Delta\nu}{2}$ from the midpoint of the pattern. When $\Delta\nu = J\sqrt{3}$, the two pairs resemble a quartet resulting from splitting by three equivalent vicinal protons. Failure to note the small outer peaks (i.e., 1 and 4) may lead to mistaking the two large inner peaks for a doublet. When the chemical shift difference becomes zero, the middle peaks coalesce to give a single peak and the end peaks vanish—that is, the protons are equivalent. (Equivalent protons do spin-spin couple with one another, but splitting is not observed). A further point to be noted is the obvious one that the spacing between the peaks of two coupled multiplets is the same.

The dependence of chemical shift on the applied magnetic field and the independence of the spin-spin coupling afford a method of distinguishing between them. The spectrum is merely run at two different applied magnetic fields. Chemical shifts are also solvent dependent, but J values are usually only slightly affected by change of solvent, at least to a lesser degree than are chemical shifts. The chemical shift of the methyl and acetylenic protons of methylacetylene are (fortuitously) coincident (δ 1.80, γ 8.20) when the spectrum is obtained in a CDCl_3 solvent; the spectrum of a neat sample of this alkyne shows the acetylenic proton at δ 1.80 (γ 8.20) and the methyl protons at δ 1.76 (γ 8.24). Fig. 22 illustrates the chemical shift dependence of the protons of biacetyl on solvent. The change from a chlorinated solvent (e.g. CDCl_3) to an aromatic solvent (e.g. C_6D_6) often drastically influences the position and appearance of NMR signals.⁴



AX
↓

58

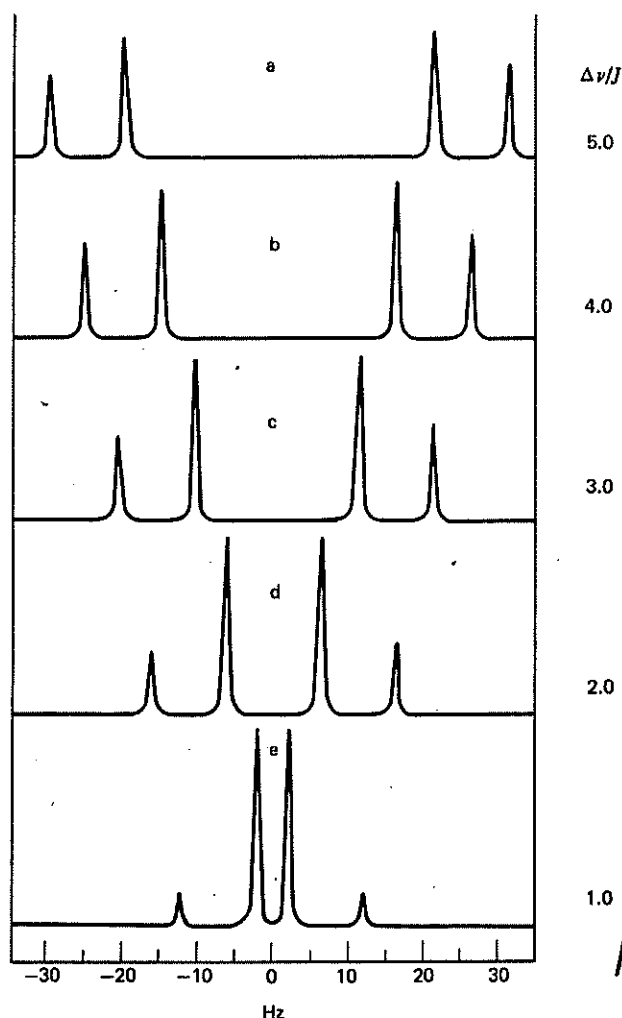


Fig. 20.
Change in an AX system spin coupling with a decreasing difference in chemical shifts and a large J value (10 Hz); the AX notation is explained in the text.

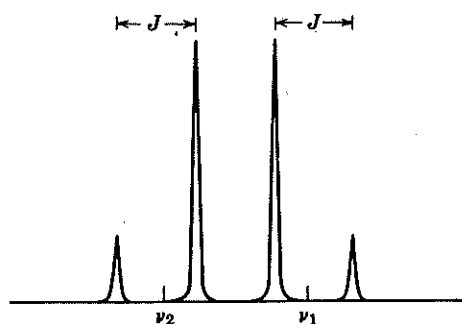


Fig. 21.
"Center of gravity," instead of linear midpoints, for shift position location (due to "low" $\Delta\nu/J$ ratio).

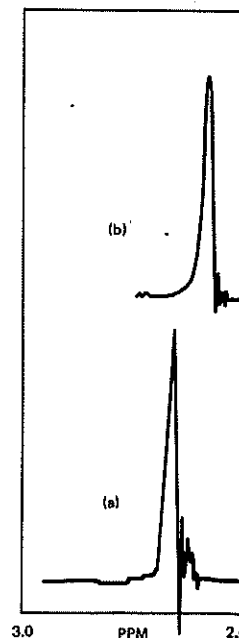


Fig. 22.
The NMR spectrum of biacetyl (2,3-butanedione): (a) CDCl_3 ; (b) C_6D_{12} .

AB

Look at the next stage in complexity of spin-spin coupling (Figure 23). Consider the system $-\text{HC}-\text{CH}_2-$ in

OR

the compound $\text{RO}-\text{CH}-\text{CH}_2-\text{CR}_3$ in which the single methine proton is in a very different chemical environment from the two methylene protons. As before, we see two sets of absorptions widely separated, and now the absorption areas are in the ratio of 1:2. The methine proton couples with the methylene protons and splits the methylene proton absorption into a symmetrical doublet, as explained above. The two methylene protons split the methine proton absorption into a triplet because three combinations of proton spins exist in the two methylene protons (a and b) of Figure 24. Since there are two equivalent combinations of spin (pairs 2 and 3) that do not produce any net opposing or concerted field relative to the applied field, there is an absorption of relative intensity two at the center of the multiplet. Since there are single pairs (1 and 4) respectively opposed and in concert with the applied field, there are equally spaced (J) lines of relative intensity one upfield and one downfield from the center line. In summary, the intensities of the peaks in the triplet are in the ratio 1:2:1.

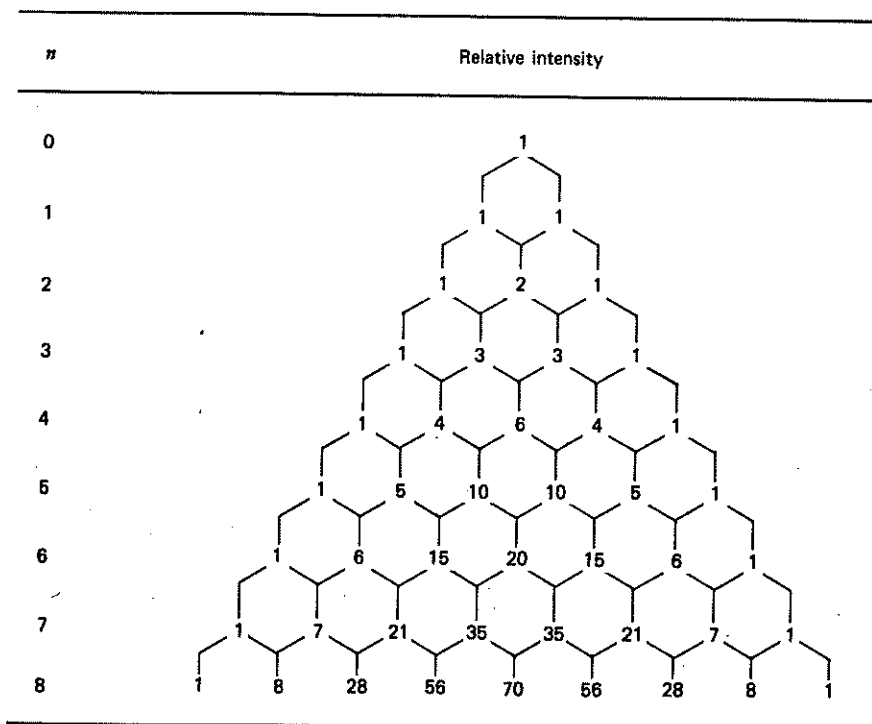


Fig. 25. Pascal's triangle.

Relative intensities of first-order multiplets from coupling with n nuclei of spin $1/2$ (e.g., protons).

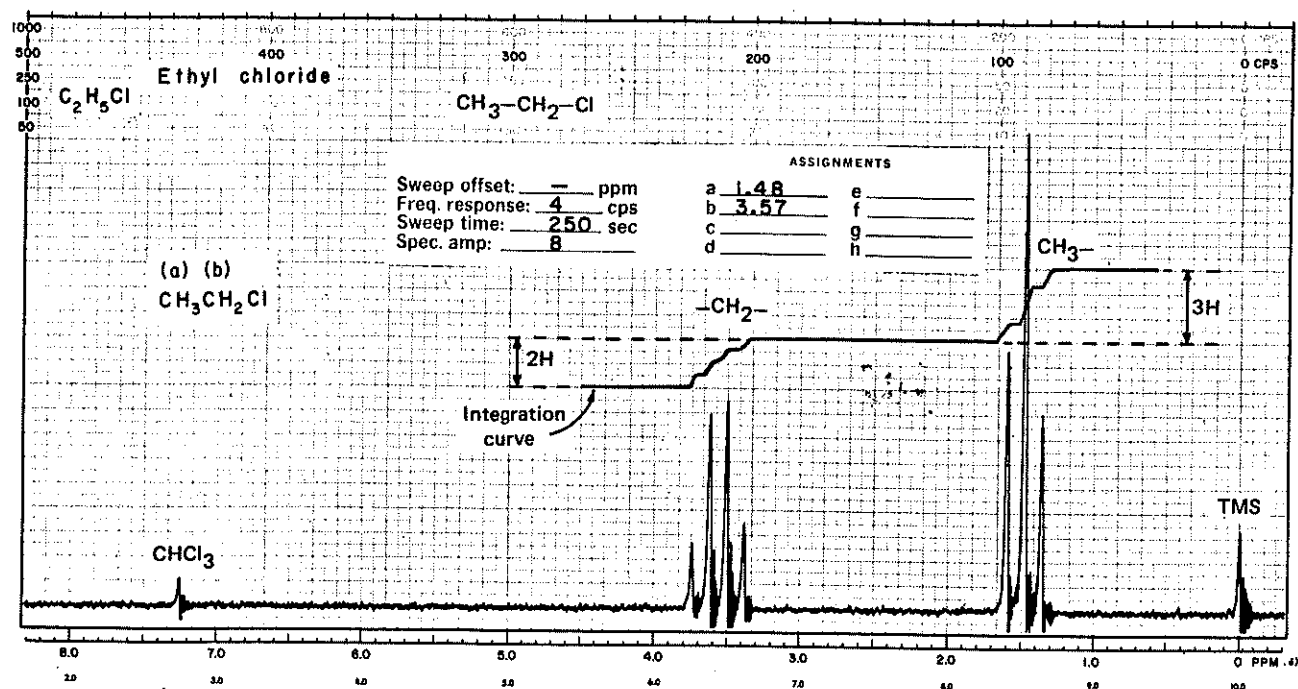
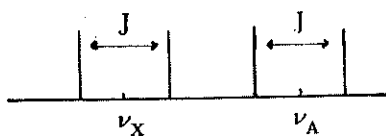


Fig. 26.

Ethyl chloride in CDCl_3 at 60 MHz. (Courtesy of Varian Associates, Palo Alto, Calif.)

Συνεπώς έχομεν συνολικώς 4 δυνατάς διεγέρσεις: $1 \rightarrow 3$ και $2 \rightarrow 4$ διὰ τὸν πυρῆνα Α και $1 \rightarrow 2'$ και $3 \rightarrow 4$ διὰ τὸν πυρῆνα Χ, ἥτοι συνολικώς 4 φασματικές γραμμές (σχ. 41).



Σχ. 41. Φάσμα τύπου ΑΧ.

Εἰς τὸν πίνακα 17 δίδονται αἱ σταθεραὶ συζεύξεως J μεταξύ πρωτονίων διαφόρων ομάδων. Εἰς τὰς κεκορεσμένας ενώσεις πρωτόνια, εὑρισκόμενα εἰς 1,3 - ἢ πλέον ἀπομεμακρυσμένας θέσεις, δὲν σχάζονται.

ΠΙΝΑΞ 17

Σταθεραὶ συζεύξεως μεταξύ διαφόρων πρωτονίων.

	J 0 - 20 Hz
	εἰς πλαγίαν - διαμόρφωσιν J 2 - 5 Hz εἰς ἀντι - διαμόρφωσιν J 5 - 12 Hz
	cis - J 6 - 14 Hz
	trans - J 12 - 18 Hz
	ο - J 6 - 9 Hz μ - J 1 - 3 Hz π - J 0 - 1 Hz
	$J \sim 0$ Hz

the methylene group is downfield (lower τ , higher δ) from the methyl by 2.09 ppm. or about 125 Hz. Since the coupling is about 9 Hz, $\Delta\nu/J$ is about 14, a large enough ratio for first order analysis. The system is A_3X_2 and the first order rules correctly predict a triplet and a quartet with relative intensities (see integration curves) of three to two corresponding to the number of protons causing the absorptions. Note that even at $\Delta\nu/J = 14$ that there is a "leaning" of the two interacting signals toward each other; i.e., the intensity of the upfield lines of the methylene signal and the downfield lines of the methyl signal are somewhat larger than they would be if these signals were perfectly symmetrical. This fact, together with the same spacing in both multiplets, is valuable in identifying interacting proton signals in more complex spectra.

Consider the NMR spectrum of cumene in Figure 27. The five aromatic protons, δ 7.25, (τ 2.75), although actually not chemical shift equivalent (see Section VII) are coincidentally equivalent and occur as a single absorption downfield from the remaining absorptions (because of the benzene ring current, Figure 14). The side chain is treated as an A_6X system. The six methyl protons occur as a doublet at δ 1.25 (τ 8.75), the methine proton as a 1:6:15:20:15:6:1 septet at δ 2.90 (τ 7.10). Note that this signal is completely seen only when the sample is run at high gain (upper lines). Outer lines of complex multiplets may be overlooked, especially when these lines are part of a

single proton absorption and when base line noise is substantial.

V. PROTONS ON HETEROATOMS

Protons on a heteroatom differ from protons on a carbon atom in that: (1) they are exchangeable, (2) they are subject to hydrogen-bonding, and (3) they are subject to partial or complete decoupling by electrical quadrupole effects of some heteroatoms. Shift ranges for protons on heteroatoms are given in Appendix D.

PROTONS ON OXYGEN

Alcohols

Unless special precautions are taken (see below) the spectrum of neat ethanol usually shows the hydroxylic proton as a sharp peak at δ 5.35, τ 4.65. At the commonly used concentration of about 5 to 20% in a nonpolar solvent (e.g., carbon tetrachloride or deuteriochloroform), the hydroxylic peak is found between δ 2, τ 8, and δ 4, τ 6. On

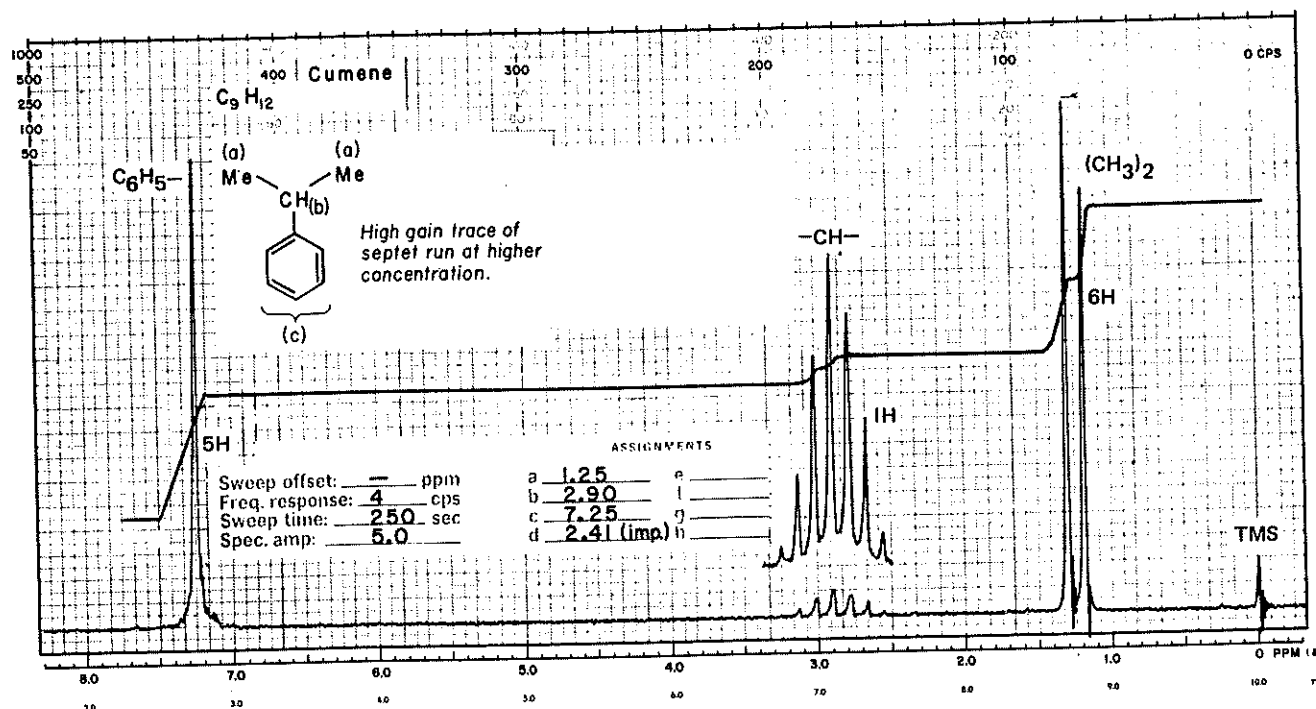
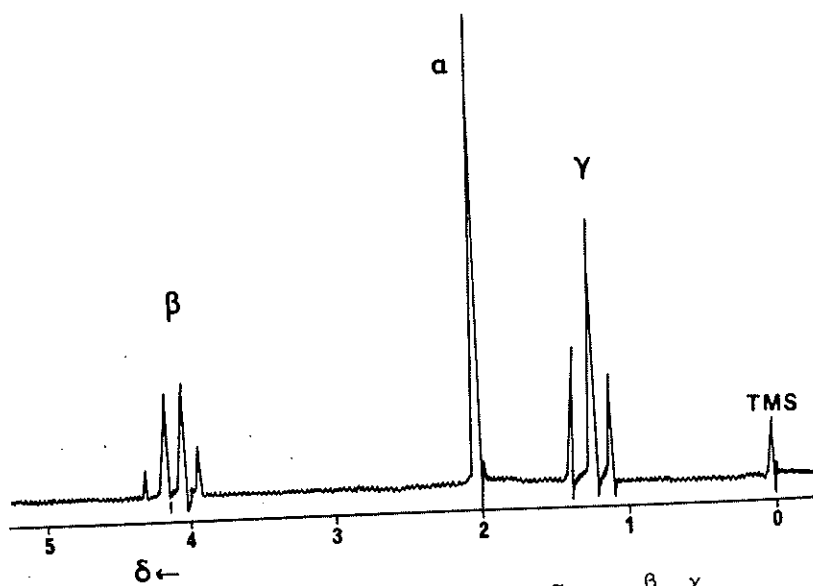
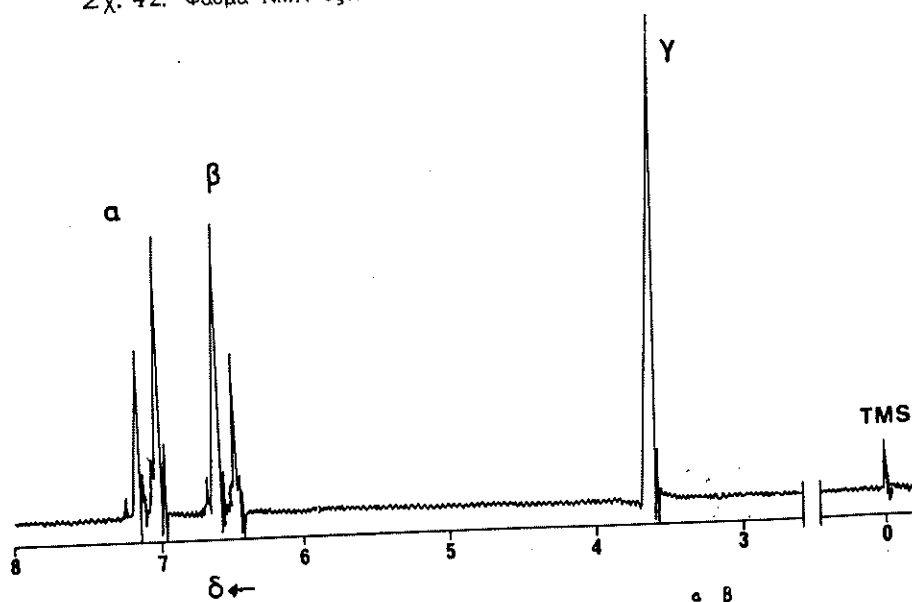


Fig. 27.
Cumene in $CDCl_3$ at 60 MHz. (Courtesy of Varian Associates, Palo Alto, Calif.)



Σχ. 42. Φάσμα NMR όξινοϋ αίθυλεστέροσ ($\text{CH}_3\text{COOCH}_2\text{CH}_3$).



Σχ. 43. Φάσμα NMR π-χλωροανιλίνης $\left(\text{Cl}-\text{C}_6\text{H}_4-\text{NH}_2 \right)$.

= ΠΡΟΤΟΝΙΑ ΣΕ ΕΤΕΡΟΑΤΟΜΑ =

- Επίδραση ηλεκτροαρνητικότητας ετεροατόμου = ^{σύγκριση} αλκοόλης = αλκυλικής αμιν
- Ανταλλάσσονται εύκολα = τί σημαίνει; =
- Υφίστανται δεσμοί υδρογόνου = Επίδραση στο δ = (παράδειγμα)
- περιπτώσεις όπου γίνεται μερική ή ολική αποσύζευξη = τί σημαίνει; =

= Αλκοόλες =

αύξηση δ
αύξηση οξύτητας

- Σε συνηθισμένους διαλύτες και συγκεντρώσεις δ: 2-4
- Ανταλλάσσονται με μεγάλη ταχύτητα και συνήθως είναι οξείες απλές κορυφές = εξαίρεση =
- Ανταλλάσσονται με D₂O

= Ενόλες = - Όπως αλκοόλες -

= Φαινόλες =

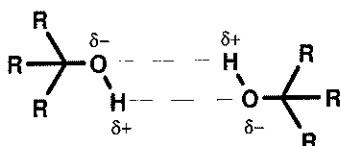
- Όπως αλκοόλες, δ: 4.0-7.5 (αποπροστασία)

= Καρβοξυλικά οξέα =

- δ: ~10-14 (αποπροστασία)
- οξείες ή ευρείες
- Ανταλλαγή με D₂O

should not surprise us that the chemical shifts (in CDCl_3 solvent) follow pretty much the same order: alcohols (δ 1–4) < phenols (δ 4.0–7.5) < enols (δ 6–7 for enols of cyclic α -diketones, δ 14.5–16.5 for enols of β -dicarbonyls) < carboxylic acids (δ 10–14). In fact, carboxylic acid hydrogens and β -dicarbonyl enol hydrogens are among the most deshielded of all hydrogens, thereby defining the high-frequency (low-field) limit of the ^1H spectral width.

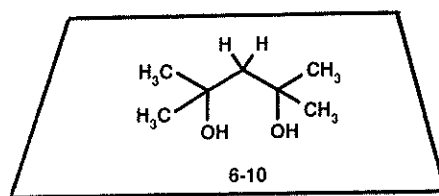
However, hydroxyl proton NMR signals have several additional characteristics of which you should be aware. To describe these, we need to know a little about an important property of acidic hydrogens. Unlike most hydrogens attached to carbon, those attached to oxygen and nitrogen are subject to **hydrogen bonding** and **exchange**. Hydrogen bonding is a special type of charge dipole–dipole interaction involving a relatively acidic, partially positively charged hydrogen still bonded to X ($\text{X}-\text{H}^{\delta+}$) but also attracted to another electronegative atom, $\text{Y}^{\delta-}$ ($\delta+$ and $\delta-$ represent partial charges). This is usually written $\text{X}-\text{H}\cdots\text{Y}$ or $\text{X}-\text{H}\cdots\text{Y}$. Thus, two hydrogen-bonded alcohol molecules might look something like this:



Under certain conditions (such as the presence of a small amount of acid or base catalyst), the hydrogens can actually be traded (i.e., exchanged) between the two hydroxyl groups. Such exchange processes can be very rapid, occurring at rates comparable to the NMR time scale (Section 1.4). The results of hydrogen bonding and exchange are that hydroxyl proton signals are often broader (larger halfwidth, Section 3.5.1) than C–H proton signals, and their chemical shifts are quite dependent on temperature, concentration, and the nature of the solvent (Section 3.5.2) because all three of these variables affect the rate of hydrogen exchange and the strength of the hydrogen bonds. The upshot of all this is that hydroxyl proton chemical shifts are quite variable, and it is difficult to be as accurate in our predictions of their chemical shifts as we were with hydrogens attached to carbon.

Finally, it is important to recognize that hydrogen bonding can be either intermolecular ($\text{X}-\text{H}$ and Y are part of separate molecules) or intramolecular ($\text{X}-\text{H}$ and Y are part of the same molecule).

■ **EXAMPLE 6.21** Examine the 250-MHz ^1H NMR spectrum (Figure 6.6) of 2,4-dimethyl-2,4-pentanediol, **6-10**:



- (a) Give the chemical shift and integration of each signal. (b) Assign each signal to specific hydrogens in the molecule, and compare the observed chemical shifts with predicted values. (c) Account for the halfwidth of the signal at δ 4.29.

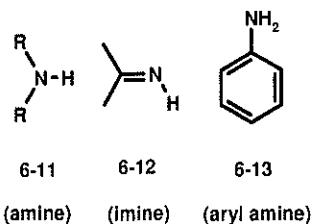
□ **Solution:** (a) δ 1.32 (12H), 1.72 (2H), and 4.29 (2H). (b) The 12H signal must be due to the four equivalent methyl groups, whose predicted chemical shift is δ 1.22 [$0.23 + 0.62 (\alpha\text{-R}) + 2(0.01, \beta\text{-R}) + 0.35 (\beta\text{-OH})$]. The methylene hydrogens are predicted to appear at δ 1.99 [$0.9[0.23 + 2(0.62) + 4(0.01) + 2(0.35)]$], and this corresponds to the signal observed at δ 1.72. The alcoholic OH signal should appear in the range δ 1–4, consistent with the signal observed at δ 4.29. (c) This signal, being due to the OH groups, is broadened by hydrogen bonding and exchange. □

■ **EXAMPLE 6.22** A dilute solution of CH_3OH in CDCl_3 exhibits its O–H signal at δ 1.43 ppm. When a slight excess of D_2O (deuterated water) is added to the sample, the hydroxyl signal disappears and is replaced by a signal at δ 4.75.¹ Explain.

□ **Solution:** Remember that deuterium (^2H , Table 2.1) does not show up in a ^1H spectrum. But *chemically* deuterium acts just like hydrogen. So there is exchange between the OH hydrogens of the alcohol and the deuteria of D_2O , thereby generating CH_3OD (which exhibits only a methyl signal) and $\text{H}-\text{O}-\text{D}$. The latter gives rise to the δ 4.75 signal. This **deuterium exchange** technique is a useful way of confirming the presence of a readily exchangeable hydrogen. □

6.6.2 Hydrogens Attached to Nitrogen

Hydrogens directly bonded to nitrogen occurs in several classes of compounds, as shown in structures **6-11** through **6-15**. Compare these structures with those of alcohols, enols, phenols, and acids:



■ **EXAMPLE 6.21** Examine the 250-MHz ^1H NMR spectrum (Figure 6.6) of 2,4-dimethyl-2,4-pentanediol, **6-10**:

the methylene group is downfield (lower τ , higher δ) from the methyl by 2.09 ppm. or about 125 Hz. Since the coupling is about 9 Hz, $\Delta\nu/J$ is about 14, a large enough ratio for first order analysis. The system is A_3X_2 and the first order rules correctly predict a triplet and a quartet with relative intensities (see integration curves) of three to two corresponding to the number of protons causing the absorptions. Note that even at $\Delta\nu/J = 14$ that there is a "leaning" of the two interacting signals toward each other; i.e., the intensity of the upfield lines of the methylene signal and the downfield lines of the methyl signal are somewhat larger than they would be if these signals were perfectly symmetrical. This fact, together with the same spacing in both multiplets, is valuable in identifying interacting proton signals in more complex spectra.

Consider the NMR spectrum of cumene in Figure 27. The five aromatic protons, δ 7.25, (τ 2.75), although actually not chemical shift equivalent (see Section VII) are coincidentally equivalent and occur as a single absorption downfield from the remaining absorptions (because of the benzene ring current, Figure 14). The side chain is treated as an A_6X system. The six methyl protons occur as a doublet at δ 1.25 (τ 8.75), the methine proton as a 1:6:15:20:15:6:1 septet at δ 2.90 (τ 7.10). Note that this signal is completely seen only when the sample is run at high gain (upper lines). Outer lines of complex multiplets may be overlooked, especially when these lines are part of a

single proton absorption and when base line noise is substantial.

V. PROTONS ON HETEROATOMS

Protons on a heteroatom differ from protons on a carbon atom in that: (1) they are exchangeable, (2) they are subject to hydrogen-bonding, and (3) they are subject to partial or complete decoupling by electrical quadrupole effects of some heteroatoms. Shift ranges for protons on heteroatoms are given in Appendix D.

PROTONS ON OXYGEN

Alcohols

Unless special precautions are taken (see below) the spectrum of neat ethanol usually shows the hydroxylic proton as a sharp peak at δ 5.35, τ 4.65. At the commonly used concentration of about 5 to 20% in a nonpolar solvent (e.g., carbon tetrachloride or deuteriochloroform), the hydroxylic peak is found between δ 2, τ 8, and δ 4, τ 6. On

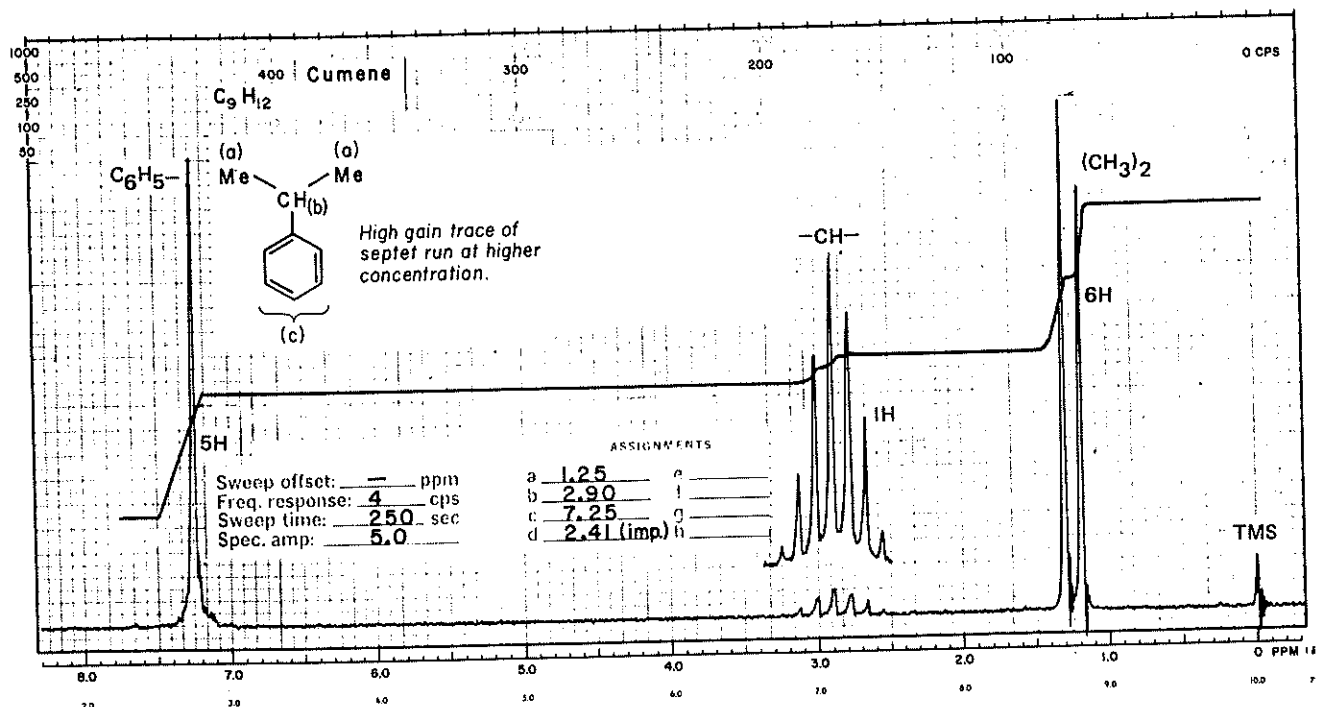


Fig. 27.

Cumene in $CDCl_3$ at 60 MHz. (Courtesy of Varian Associates, Palo Alto, Calif.)

extrapolation to infinite dilution or in the vapor phase, the peak is near δ 0.5, τ 9.5. A change in solvent or temperature will also shift the hydroxylic peak.

Hydrogen bonding explains why the shift position of the hydroxylic proton depends on concentration, temperature, and solvent. Hydrogen bonding decreases the electron density around the proton and thus moves the proton absorption to lower field. The extent of intermolecular hydrogen bonding is decreased by dilution with a nonpolar solvent and with increased temperature. Polar solvents introduce the additional complication of hydrogen bonding between the hydroxylic proton and the solvent. Intramolecular hydrogen bonds are less affected by their environment than intermolecular bonds; in fact the enolic hydroxylic absorption of β -diketones, for example, is hardly affected by change of concentration or solvent, though it can be shifted upfield somewhat by warming. NMR spectrometry is a powerful tool for studying such effects as hydrogen bonding and keto-enol tautomerism.

Exchangeability explains why the hydroxylic peak of ethanol is usually seen as a sharp singlet. Under ordinary conditions, enough acidic impurities are present in solution to catalyze rapid exchange of the hydroxylic proton. The proton is not on the oxygen atom long enough for it to "see" the three states of the methylene protons, and there is no coupling. The rate of exchange can be decreased by treating the solution or the solvent with anhydrous sodium carbonate, alumina, or molecular sieves immediately before obtaining the spectrum.^{19,20} Purified deuterated dimethyl sulfoxide or acetone, in addition to allowing a slower rate of exchange, shifts the hydroxylic proton to lower field, even in dilute solution, by hydrogen-bonding between solute and solvent.^{21,22} Since the hydroxylic proton can now "see" the protons on the α -carbon, a primary alcohol will show a triplet, a secondary alcohol a doublet, and a tertiary alcohol a singlet. This is illustrated in Figure 28^{11d} and a list of successful applications is given in Table I. Exceptions have been reported;²³ these may be due to the sensitive concentration dependence of this phenomenon.^{23a} At intermediate rates of exchange, the multiplet merges into a broad absorption band; at this point, the exchange rate in Hz is equal to $\pi J/\sqrt{2}$.

A dihydroxy alcohol may show separate absorption peaks for each hydroxylic proton; in this case, the rate of exchange in Hz is much less than the difference in Hz between the separate absorptions. As the rate increases, the two absorption peaks broaden, then merge to form a single broad peak; at this point, the exchange rate in Hz is equal to the original separation in Hz. The relative position of each peak depends on the extent of hydrogen bonding of each hydroxylic proton; steric hindrance to hydrogen bonding frequently accounts for a relative upfield absorption.

Table I²² Hydroxyl Proton Resonances in Dimethyl Sulfoxide (purified)

Compound ^a	Chemical Shift, τ	Multiplicity ^b
Methanol	5.92	q
Ethanol	5.65	t
Isopropyl alcohol	5.65	d
<i>t</i> -Butyl alcohol	5.84	s
<i>t</i> -Amyl alcohol	6.01	s
Propylene glycol, 1-OH	5.55	t
2-OH	5.62	d
Cyclohexanol	5.62	d
<i>cis</i> -4- <i>t</i> -Butylcyclohexyl alcohol	5.89	d
<i>trans</i> -4- <i>t</i> -Butylcyclohexyl alcohol	5.55	d
Benzyl alcohol	4.84	t
Phenol	0.75	s
β -L-Arabinopyranose, O-C-OH ^c	4.02	d
α -D-Glucopyranose, O-C-OH ^c	3.34	d
α -D-Fructopyranose, O-C-OH ^c	4.88	s

^aAll spectra were taken of dimethyl sulfoxide solutions with concentrations 10 mole % or less.

^bq = quartet, t = triplet, d = doublet, s = singlet. All splittings fall within the range 3.5–5.0 Hz.

^cOther hydroxyl protons (τ 5.0–5.9) show splitting but overlap to such an extent that specific assignments are not possible.

The spectrum of a compound containing exchangeable protons can be simplified, and the exchangeable proton absorption removed, simply by shaking the solution with excess deuterium oxide or by obtaining a spectrum in deuterium oxide solution if the compound is soluble. A peak due to HOD will appear, generally between δ 5, τ 5, and δ 4.5, τ 5.5 in nonpolar solvents, and near δ 3.3, τ 6.7 in dimethyl sulfoxide (see Appendix D).

Acetylation or benzylation of a hydroxyl group moves the α protons of a primary alcohol downfield about 0.5 ppm, and that of a secondary alcohol about 1.0–1.2 ppm.

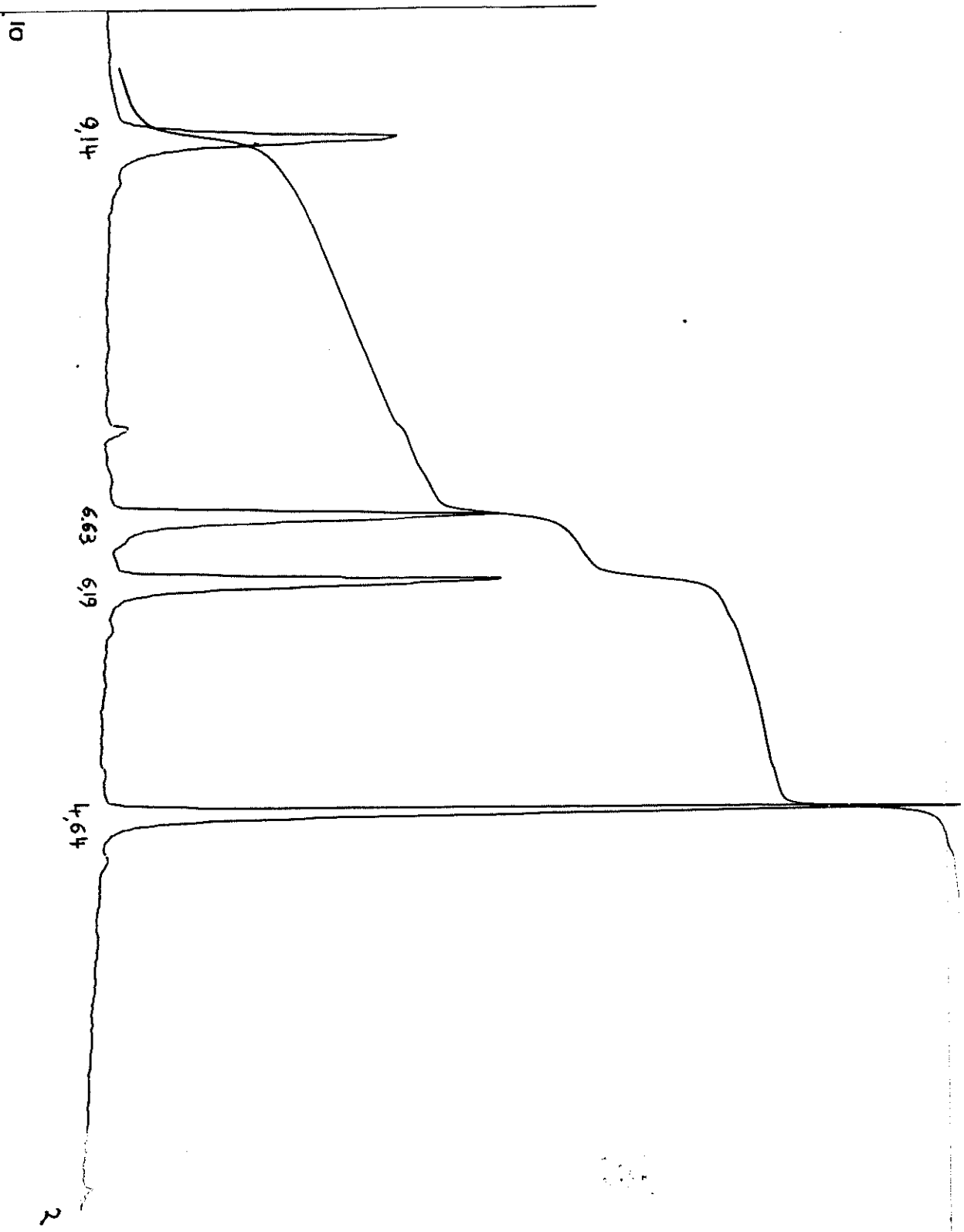
Phenols

The behavior of a phenolic proton resembles that of an alcoholic proton. The phenolic proton peak is usually a sharp singlet (rapid exchange, no coupling) and its range, depending on concentration, solvent and temperature, is generally downfield ($\delta \sim 7.5$, τ 2.5 to $\delta \sim 4.0$, τ 6.0) compared with the alcoholic proton. This is illustrated in Figure 29. Note the concentration dependence of the OH peak. A carbonyl group in the ortho position shifts the phenolic proton absorption downfield to the range of about δ 12.0, $\tau - 2.0$ to δ 10.0, τ 0.0 because of intramolecular hydrogen bonding. Thus *o*-hydroxyacetophenone shows a

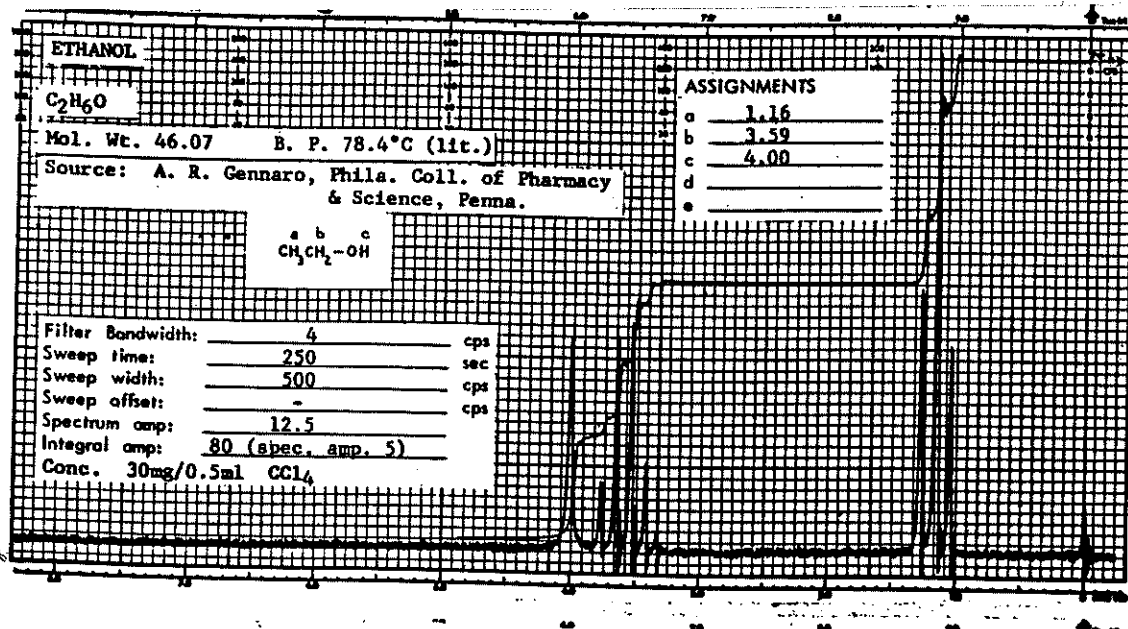


BD-1-8/6/92

CDCl₃

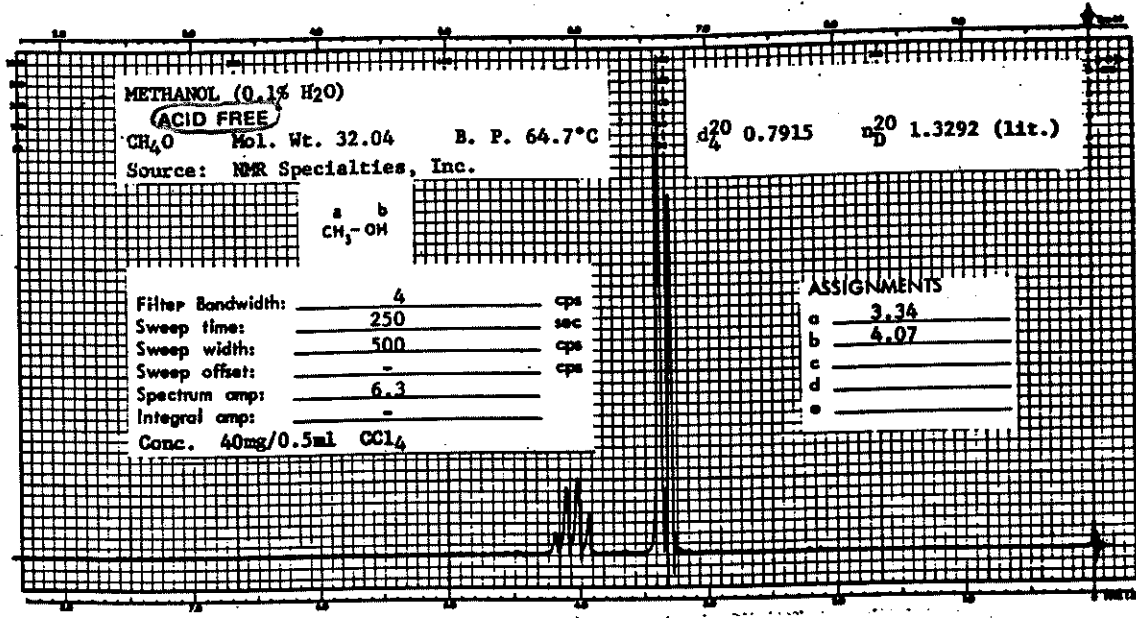


No. 12

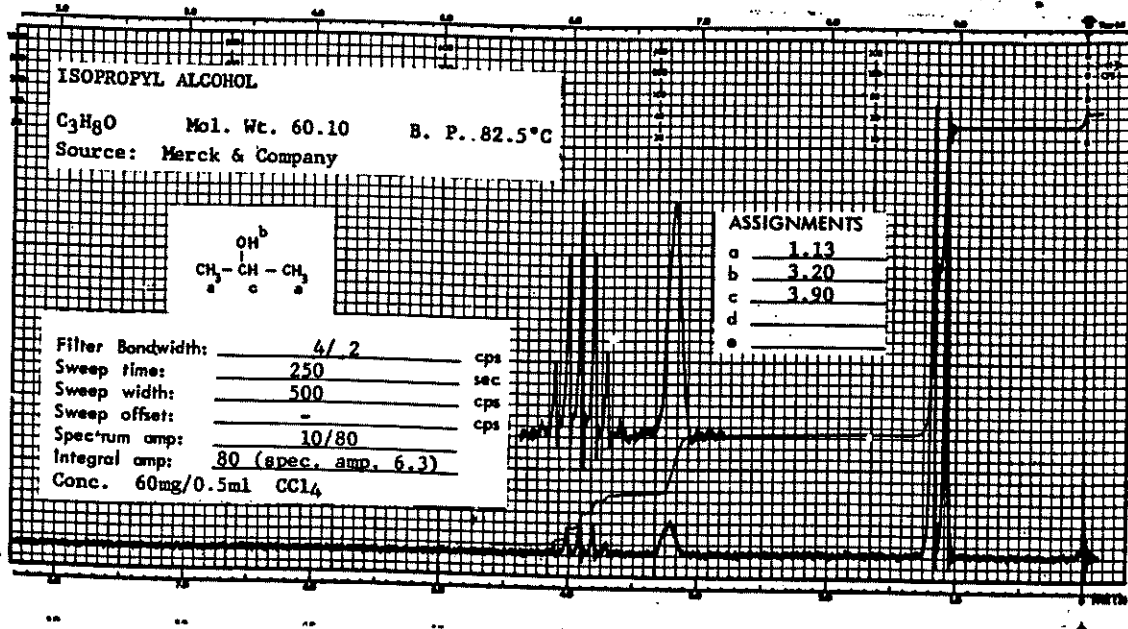


No. 18

Egapeon



No. 15



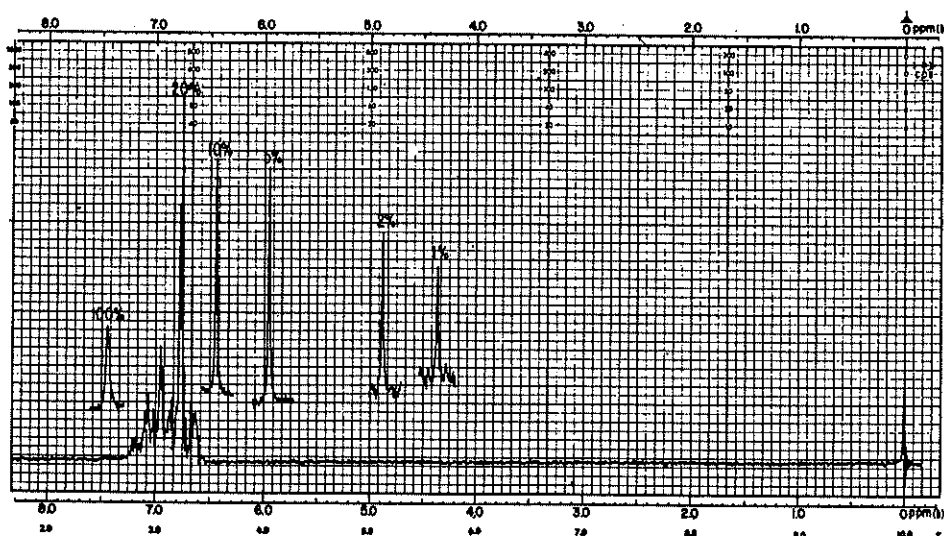


Fig. 29.
Phenol, in CCl_4 , at various w/v %, at 60 MHz. Complete sweep is at 20%; single absorptions represent the OH proton at the indicated w/v %. (From J. R. Dyer, *Applications of Absorption Spectroscopy of Organic Compounds*, copyright 1965, p. 90. Reprinted by permission of Prentice-Hall, Inc., Englewood Cliffs, N.J.)

peak at about δ 12.05, τ - 2.05 almost completely invariant with concentration. The much weaker intramolecular hydrogen bonding in *o*-chlorophenol explains its shift range ($\delta \sim 6.3$, τ 3.7 at 1 molar concentration to $\delta \sim 5.6$, τ 4.4 at infinite dilution) which is broad compared with that of *o*-hydroxyacetophenone, but narrow compared with that of phenol.

Enols

Enols are usually stabilized by intramolecular hydrogen-bonding, which varies from very strong in aliphatic β -diketones to weak in cyclic α -diketones. The enolic proton is downfield relative to alcohol protons and, in the case of the enolic form of some β -diketones, may be found as far downfield as δ 16.6, τ - 6.6 (the enolic proton of acetylacetone absorbs at δ 15.0, τ - 5.0, and that of dibenzoylmethane at δ 16.6, τ - 6.6). The enolic proton peak is frequently broad at room temperature because of slow exchange. Furthermore, the keto-enol conversion is slow enough so that absorption peaks of both forms can be observed, and the equilibrium measured.

When strong intramolecular bonding is not involved, the enolic proton absorbs in about the same range as the phenolic proton.

Carboxylic Acids

Carboxylic acids exist as stable hydrogen-bonded dimers in nonpolar solvents even at high dilution. The carboxylic proton therefore absorbs in a characteristically narrow

range, $\delta \sim 13.2$, τ - 3.2 to $\delta \sim 10.0$, τ 0.0, and is affected only slightly by concentration. Polar solvents partially disrupt the dimer and shift the peak accordingly.

The peak width at room temperature ranges from sharp to broad, depending on the exchange rate of the particular acid. The carboxylic proton exchanges quite rapidly with protons of water and alcohols (or hydroxy groups of hydroxyacids) to give a single peak whose position depends on concentration. Sulfhydryl or enolic protons do not exchange rapidly with carboxylic protons, and individual peaks are observed.

PROTONS ON NITROGEN

The ^{14}N nucleus has a spin number $I = 1$ and, in accordance with the formula $2I + 1$, should cause a proton attached to it and a proton on an adjacent carbon atom to show three equally intense peaks. There are two factors, however, that complicate the picture: the rate of exchange of the proton on the nitrogen atom, and the electrical quadrupole moment of the ^{14}N nucleus.

The proton on a nitrogen atom may undergo rapid, intermediate, or slow exchange. If the exchange is rapid, the NH proton(s) is decoupled from the N atom and from protons on adjacent carbon atoms. The NH peak is therefore a sharp singlet, and the adjacent CH protons are not split by NH. Such is the case for most aliphatic amines.* At an intermediate rate of exchange, the NH proton is

H-C-N-H coupling in several amines has been observed^{24a} following rigorous removal (with Na-K alloy) of traces of water. This effectively stops proton exchange on the NMR time scale.

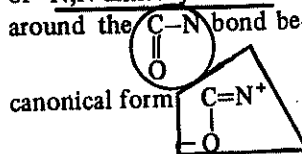
All nuclei with $I = \frac{1}{2}$ have a spherical (symmetrical) distribution of spinning charge, so the electric and magnetic fields surrounding such nuclei are spherical, homogeneous, and isotropic in all directions. By contrast, nuclei with $I > \frac{1}{2}$ have a nonspherical distribution of spinning charge, resulting in nonsymmetrical electric and magnetic fields. This imparts an electric quadrupole (Q) to the nucleus, a property that can complicate their NMR behavior. As a result, the most commonly studied nuclei are those with a nuclear spin of $\frac{1}{2}$.

partially decoupled, and a broad NH peak results. The adjacent CH protons are not split by the NH proton. Such is the case for *N*-methyl-*p*-nitroaniline. If the NH exchange rate is slow, the NH peak is still broad because the electrical quadrupole moment of the nitrogen nucleus induces a moderately efficient spin relaxation and thus an intermediate lifetime for the spin states of the nitrogen nucleus. The proton thus sees three spin states of the nitrogen nucleus (spin number = 1) which are changing at a moderate rate, and the proton responds by giving a broad peak. In this case, coupling of the NH proton to the adjacent protons is observed. Such is the case for pyrroles, indoles, secondary and primary amides and carbamates (Figure 30). Note that H-N-C-H coupling takes place through the C-H, C-N, and N-H bonds, but coupling between nitrogen and protons on adjacent carbons is negligible. The coupling is observed in the signal due to hydrogen on carbon; the N-H proton signal is severely broadened by the quadrupolar interaction with nitrogen. In the spectrum of ethyl *N*-methyl carbamate (Figure 30) $\text{CH}_3\text{NHCOCH}_2\text{CH}_3$,

the NH proton shows a broad absorption centered about δ 5.16, τ 4.84, and the N-CH₃ absorption at δ 2.78, τ 7.22 is split into a doublet ($J \sim 5$ Hz) by the NH proton. The ethoxy protons are represented by the triplet at δ 1.23, τ

8.77, and the quartet at δ 4.14, τ 5.86. The small peak at δ 2.67, τ 7.33 is an impurity.

Aliphatic and cyclic amine NH protons absorb from $\delta \sim 3.0$, τ 7.0 to $\delta \sim 0.5$, τ 9.5; aromatic amines absorb from $\delta \sim 5.0$, τ 5.0 to $\delta \sim 3.0$, τ 7.0. Because amines are subject to hydrogen bonding, the shift position depends on concentration, solvent, and temperature. Amides, pyrroles, and indoles absorb from $\delta \sim 8.5$, τ 1.5 to $\delta \sim 5.0$, τ 5.0; the effect on the absorption position of concentration, solvent, and temperature is generally smaller than in the case of amines. The nonequivalence of the protons on the nitrogen atom of a primary amide and of the methyl groups of *N,N*-dimethylamides is caused by hindered rotation around the C-N bond because of the contribution of the



Protons on the nitrogen atom of an amine salt exchange at a slow rate; they are seen as a broad peak downfield ($\delta \sim 8.5$, τ 1.5 to $\delta \sim 6.0$, τ 4.0), and they are coupled to protons on adjacent carbon atoms ($J \sim 7$ Hz); the α -protons are recognized by their downfield position in the salt compared with that in the free amine. The use of trifluoroacetic acid as both a protonating agent and a solvent frequently allows classification of amines as pri-

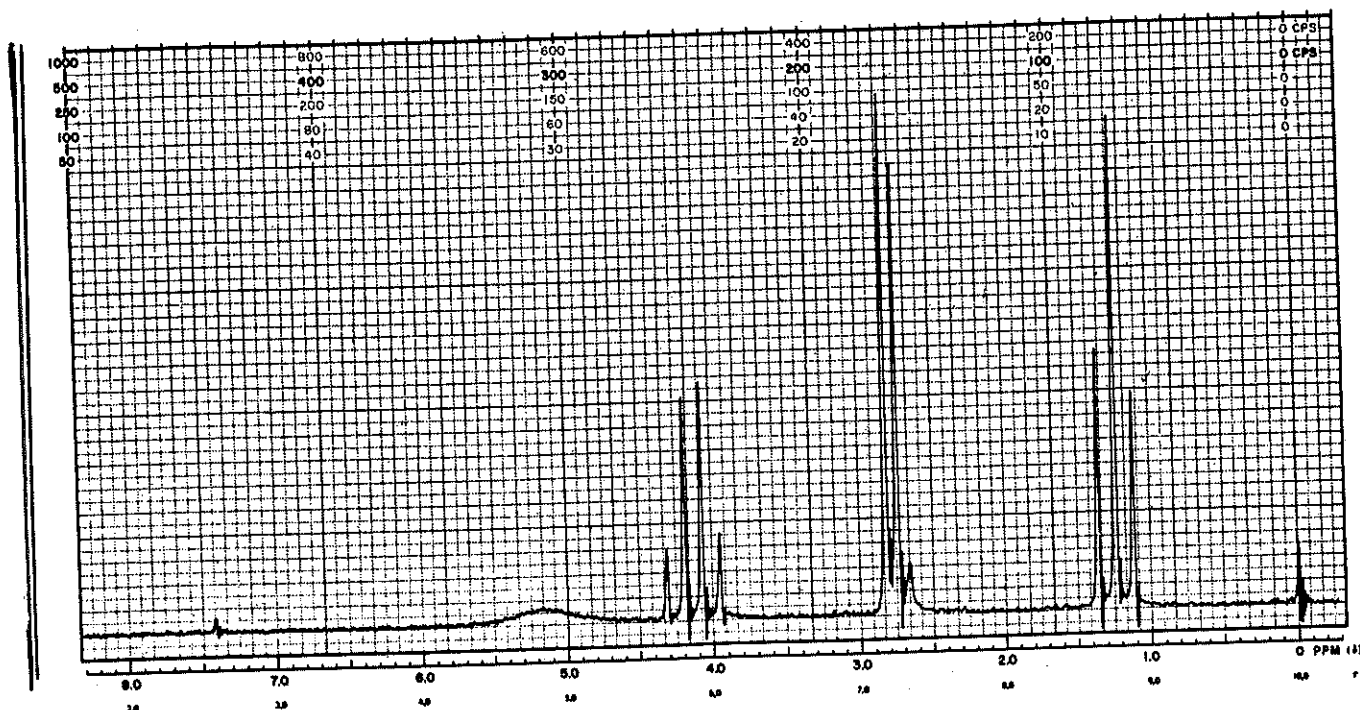
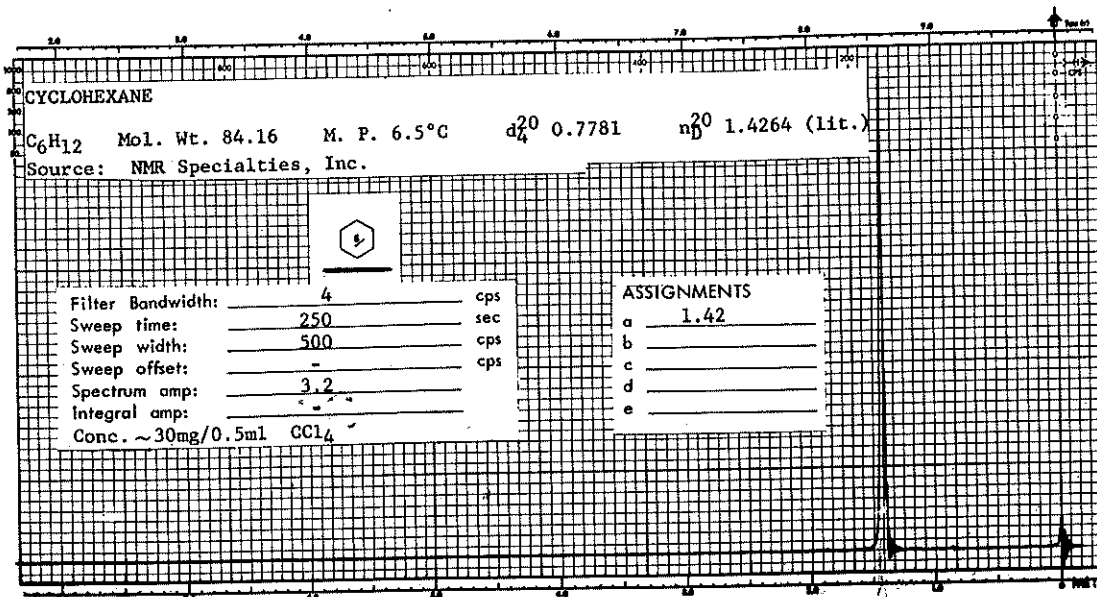
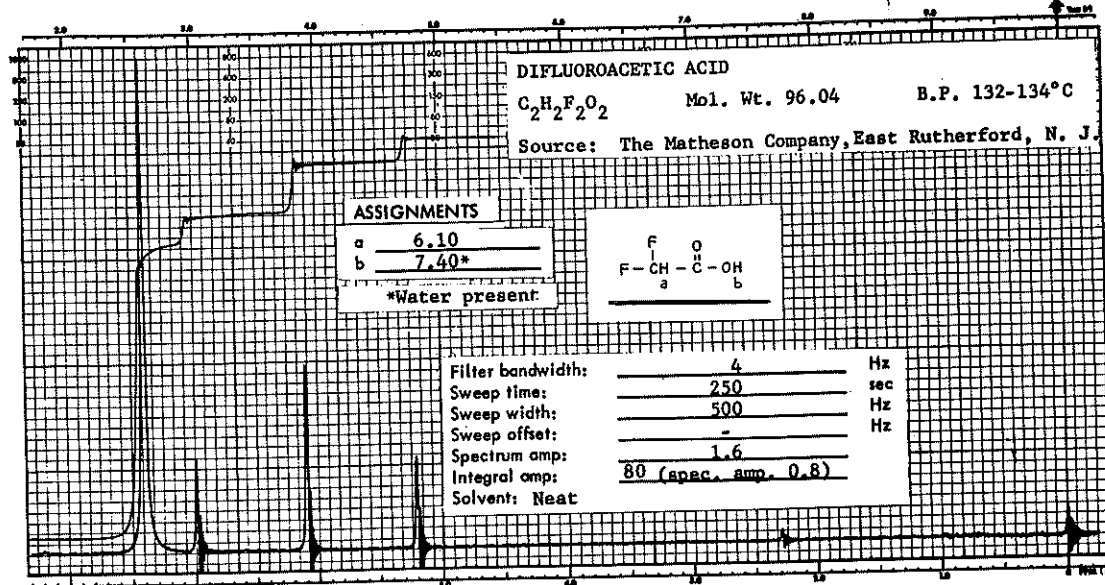


Fig. 30.
Ethyl *N*-methyl carbamate $\text{CH}_3\text{NHCOCH}_2\text{CH}_3$, 60 MHz.

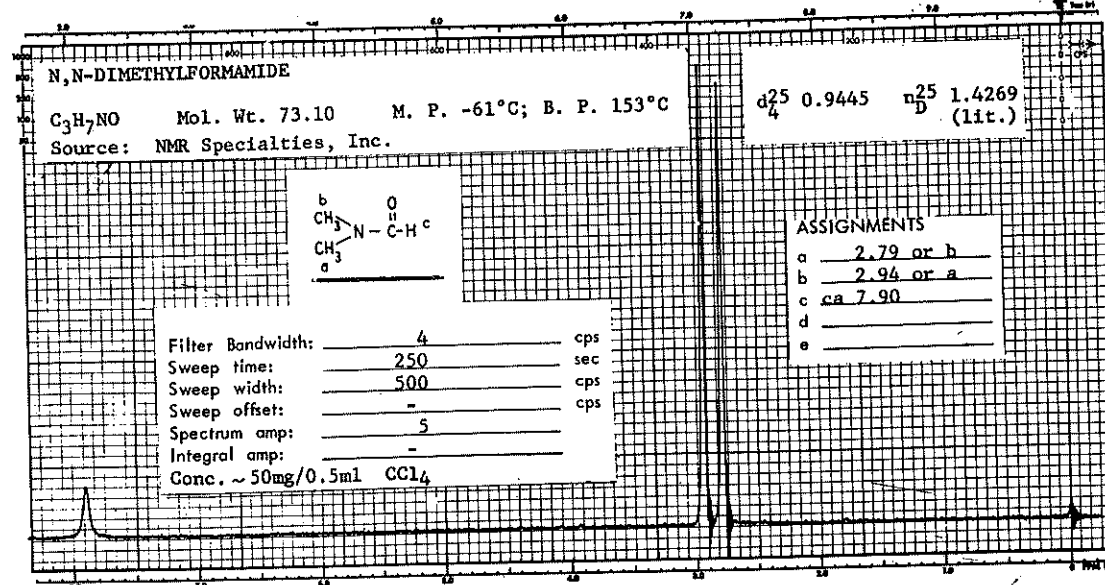
No. 6

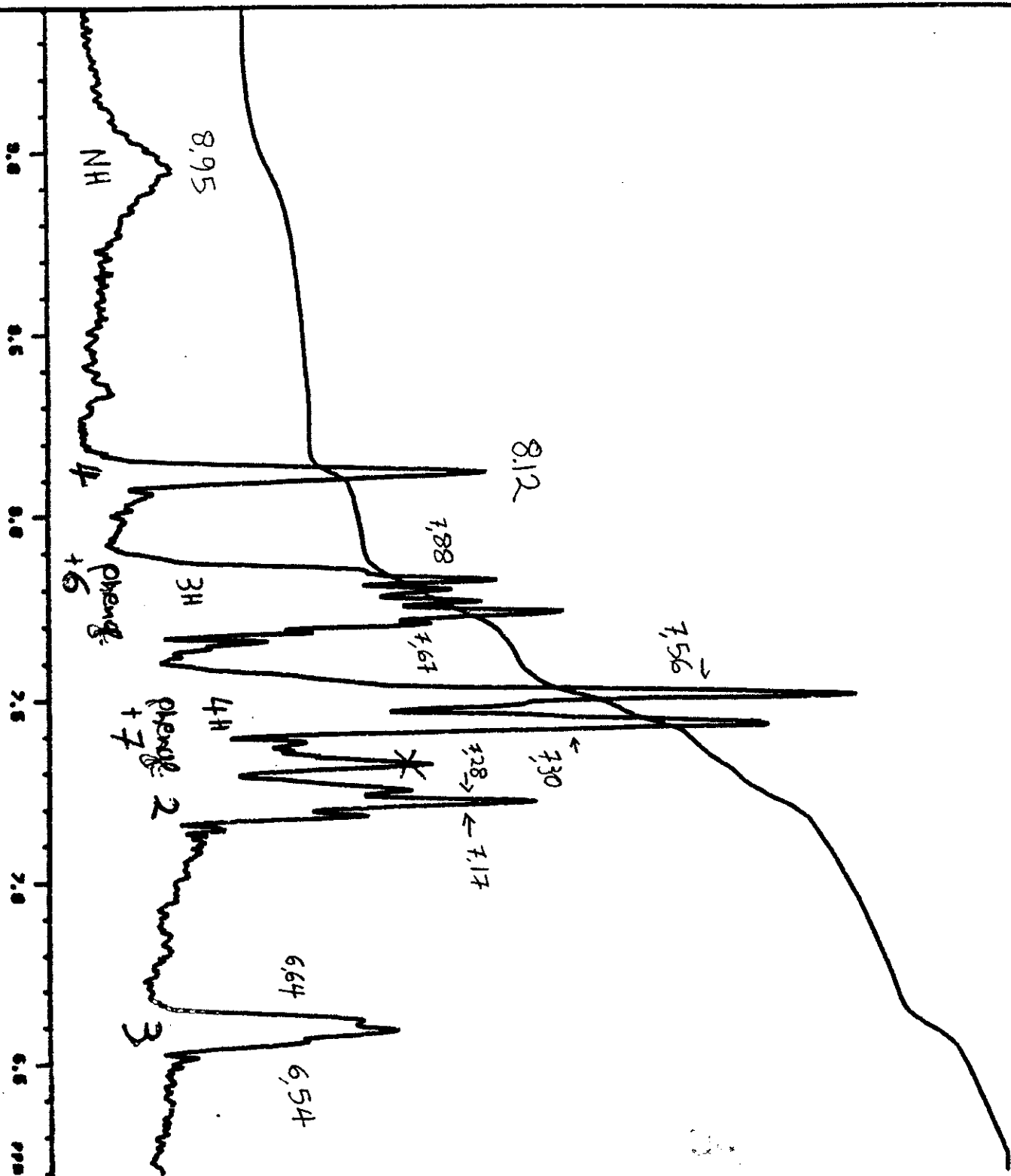
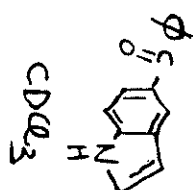


No. 7



No. 8





SOLVENT: AC-80

DATE: 00-14-57

SPECTRUM:

TIME: 100.0 SEC

POWER: 35.0 DB

GAIN: 40.0 DB

LINE BROAD: 0.152 HZ

SCANS: 1

LOC: 12.01 HZ/CN

POWER: 42.0 DB

GAIN: 30.1 DB


 $\text{CDCl}_3 + \text{D}_2\text{O}$

BRUKER AM-80

DATE 06-14-82

SPECTRUM:

TIME 100.0 SEC
 POWER 35.0 DB
 GAIN 43.0 DB
 LINE BROAD 0.153 HZ
 SCANS 1

LOCK: 43.0 DB
 POWER 25.3 DB
 GAIN

13.01 HZ/CM

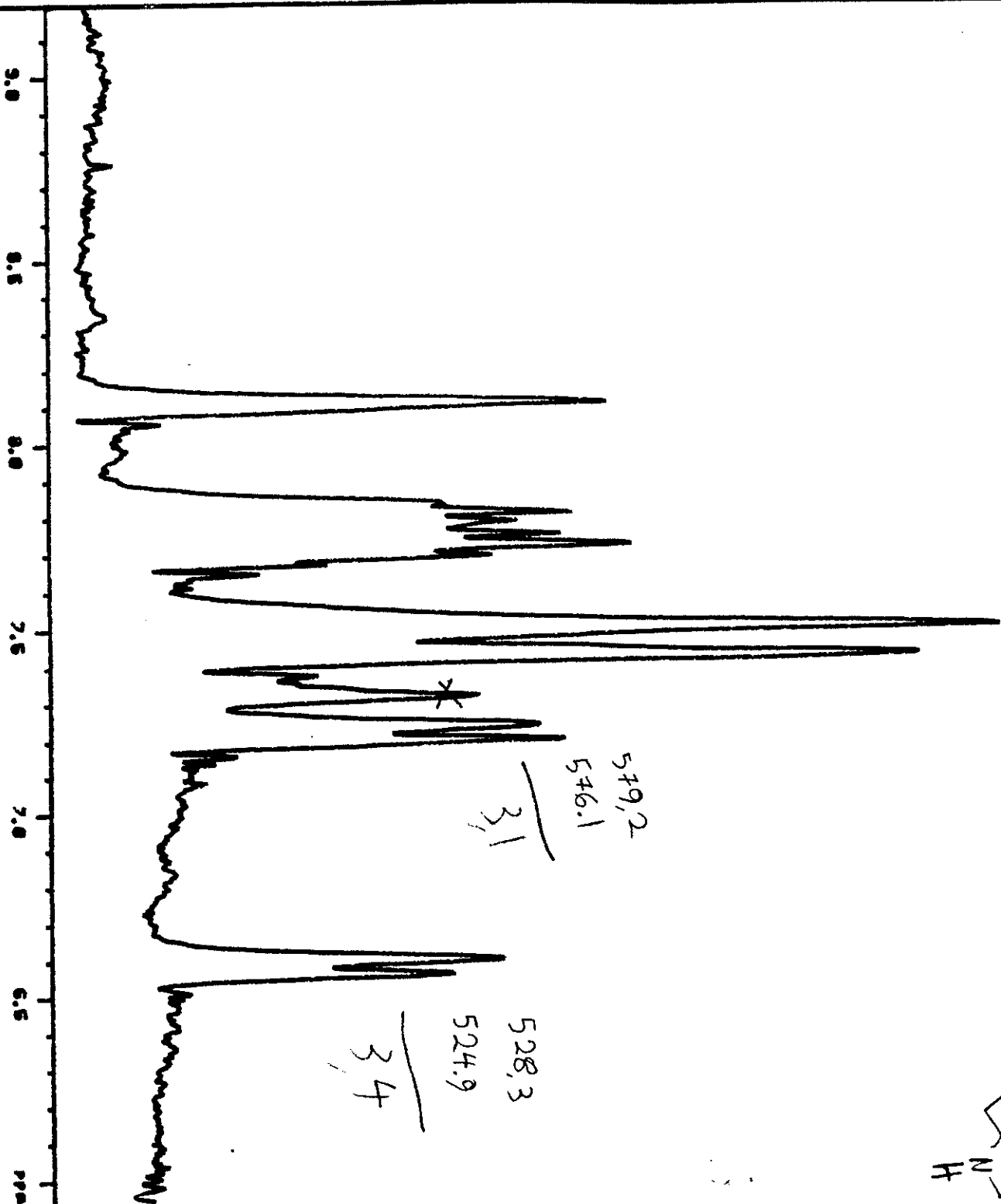


Table II Classification of Amines by NMR of Ammonium Salts in Trifluoroacetic Acid²⁴

Amine Precursor Class	Ammonium Salt Structure	Multiplicity of Methylene Unit
Primary	$C_6H_5CH_2NH_3^+$	Quartet (Figure 31)
Secondary	$C_6H_5CH_2NH_2R^+$	Triplet
Tertiary	$C_6H_5CH_2NHR_2^+$	Doublet

mary, secondary, or tertiary.²⁴ This is illustrated in Table II in which the number of protons on nitrogen determines the multiplicity of the methylene unit in the salt (Figure 31). Sometimes the broad ^+NH , $^+NH_2$, or $^+NH_3$ absorption can be seen to consist of three broad humps. These humps represent splitting by the nitrogen nucleus ($J \sim 50$ Hz). With good resolution, it is sometimes possible to observe splitting of each of the humps by the protons on adjacent carbon atoms ($J \sim 7$ Hz).

PROTONS ON SULFUR

Sulphydryl protons usually exchange at a slow rate so that at room temperature they are coupled to protons on adjacent carbons ($J \sim 8$ Hz). Nor do they exchange rapidly with hydroxylic, carboxylic, or enolic protons on the same or on other molecules; thus separate peaks are seen.

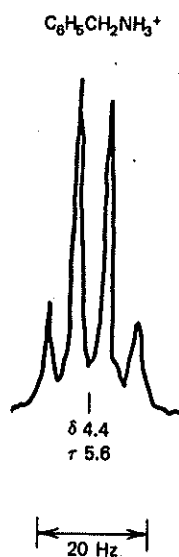


Fig. 31.
NMR spectrum of α methylene unit of a primary amine in CF_3CO_2H ; corresponds to Table II, first line.

However, exchange is rapid enough so that shaking for a few minutes with deuterium oxide replaces sulphydryl protons with deuterium. The absorption range for aliphatic sulphydryl protons is $\delta \sim 1.6$, τ 8.4, to $\delta \sim 1.2$, τ 8.8; for aromatic sulphydryl protons, $\delta \sim 3.6$, τ 6.4 to $\delta \sim 2.8$, τ 7.2. Concentration, solvent, and temperature affect the position within these ranges.

PROTONS ON HALOGENS

Chlorine, bromine, and iodine nuclei are completely decoupled from protons directly attached, or on adjacent carbon atoms, because of strong electrical quadrupole moments. The absorption positions for protons of halogen acids vary over a wide range as a function of concentration, solvent, and temperature (in the vapor phase, for example HF absorbs at δ 2.7, τ 7.3, and HI absorbs at δ -13, τ 23).

The ^{19}F atom has a spin number of $1/2$ and couples strongly with protons (see Appendix G). The rules for coupling of protons with fluorine are the same as proton-proton coupling; in general, the proton-fluorine coupling constants are somewhat larger, and long-range effects are frequently found. The ^{19}F nucleus can be observed at 56.4 MHz at 14,092 gauss. Of course, its spin is split by proton and fluorine spins, and the multiplicity rules are the same as those observed in proton spectra.

VI. COUPLING OF PROTONS TO OTHER NUCLEI

The organic chemist may encounter proton coupling with such other nuclei (besides 1H , ^{19}F , and ^{14}N) as ^{31}P , ^{13}C , 2H , and ^{29}Si . Three factors must be considered: natural abundance, spin number, and electrical quadrupole moment; the nuclear magnetic moment and relative sensitivity are important when a spectrum of the particular nucleus is considered. These properties are listed for a number of nuclei in Appendices G and H.

The magnetogyric ratio, γ , describes the combined effect of the magnetic moment and spin number of a given type of nucleus. The ratio of the magnetogyric ratios of one type of nucleus to that of another type of nucleus is a measure of the relative coupling constants of those two nuclei to a given reference nucleus^{11e}. Consider the relative magnitudes of coupling of hydrogen and of deuterium to a particular nucleus, X : Since

$$\frac{J_{HX}}{J_{DX}} = \sim \frac{\gamma_H}{\gamma_D} \quad D = ^2H$$

But then, why have we not seen couplings between ^1H and ^{13}C in all the ^1H spectra we have examined so far? The answer is that the natural abundance of ^{13}C is only 1% of all carbon (Table 2.1). So only 1% of the hydrogens bonded to carbon are attached to a ^{13}C nucleus, and this small fraction of coupled hydrogens can normally be neglected. Nonetheless, in some cases you *can* see the effect of $^{13}\text{C}-\text{H}$ coupling in ^1H spectra. Look at the highly amplified singlet in the ^1H spectrum of TMS (Figure 8.10) or any other sharp ^1H singlet for that matter. The two small satellite peaks (sidebands) flanking the singlet (each integrating to 0.5% of the main singlet) are not spinning sidebands (Section 3.3.3) because changing the sample spinning rate does not affect their position. In fact, the satellites are due to one-bond $^{13}\text{C}-\text{H}$ coupling. One percent of the methyl groups in a collection of TMS molecules possess a ^{13}C atom. This atom splits the methyl hydrogen signal (the one we use as our reference signal) into a doublet,

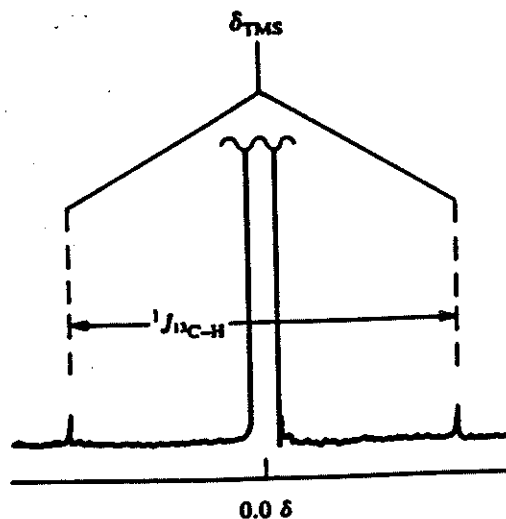


Figure 8.10. The ^{13}C satellite peaks flanking a greatly amplified TMS singlet.

with line spacing $^1J_{\text{CH}}$. Of course, you will see these satellites only if you greatly increase the signal amplification (gain). But they *are* there, and the magnitude of $^1J_{\text{CH}}$ is approximately 125 Hz, independent of sample spin rate or instrument operating frequency.

VII. MORE COMPLEX SPIN-SPIN COUPLING

As was pointed out in Section IV, A_aX_x and $A_aM_mX_x$ systems are first order. The deviations from a first order spectrum as an AX pattern moves through an AB to an A_2 pattern were traced; the AB pattern could still be analyzed by inspection. But more complex changes occur as an A_2X becomes an A_2B pattern, and a complete analysis by inspection is no longer possible; the ratios of peak intensities are not those predicted by first order calculation, additional splitting occurs, and the spacings are not necessarily equal to the coupling constants. Most spectra encountered are not first order spectra. On the other hand, the resemblance of many spectra to first order spectra can be recognized because there is a gradual transition from A_aX_x to A_aB_b types; Wiberg's collection of calculated spectra^{25a} can be used for matching fairly complex splitting patterns.

DEFINITIONS

To develop more complex cases, let us list the pertinent definitions here (some of which have been alluded to in Section IV).

1. A spin system consists of sets of nuclei that "interact (spin couple) among each other but do not interact with any nuclei outside the spin system. It is not necessary for all nuclei within a spin system to be coupled to all the other nuclei"⁴ in the spin system. The spin system definition requires that spin systems be "insulated" from one another: e.g., the ethyl protons in ethyl isopropyl ether constitute one system, and the isopropyl protons another.
2. A set of nuclei consists of chemical shift equivalent nuclei:
3. If nuclei are interchangeable by a symmetry operation or a rapid mechanism, they are chemical shift equivalent; that is, they have exactly the same chemical shift under all achiral conditions. The interchange by a symmetry operation may occur in any reasonable conformation of the molecule. A rapid mechanism means one that occurs faster than once in about 10^{-3} seconds.
4. Nuclei are magnetically equivalent if they couple to all other nuclei in the spin system in exactly the same way. Chemical shift equivalence is presupposed.

CHEMICAL SHIFT EQUIVALENCE

The symmetry operations are: rotation about a symmetry axis (C_n), reflection at a center of symmetry (i), reflection at a plane of symmetry (σ), or higher orders of rotation about an axis followed by reflection in a plane normal to

this axis (S_n). The symmetry element (axis, center, or plane) must be a symmetry element for the entire molecule. The term "interchange" will be clarified by the examples below. Chemical shift equivalent protons are given the same letter of the alphabet in the Pople notation (i.e., placed in a set as described above) and if magnetically nonequivalent are distinguished by primes such as A, A', A'', \dots , etc.

Protons a and b in *trans*-1,2-dichlorocyclopropane are chemical shift equivalent, as are the protons c and d (Figure 32). The molecule has an axis of symmetry passing through C_1 and bisecting the C_1-C_2 bond. Rotation of the molecule by 180° around the axis of symmetry interchanges proton H_a for H_b and H_c for H_d . If the protons were not labeled, it would not be possible to tell if the symmetry operation had been performed merely by inspecting the molecule before and after the operation.

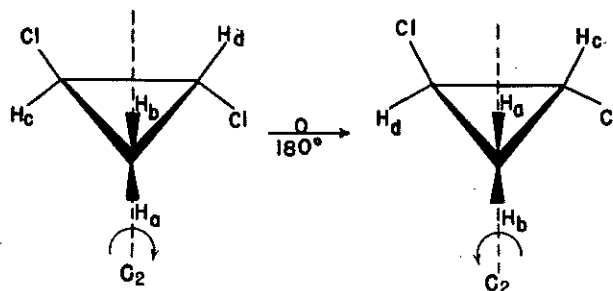


Fig. 32.
Trans-1,2-Dichlorocyclopropane showing axis of symmetry and effect of rotation around the axis.

An interesting situation occurs in a molecule such as 1,3-dibromo-1,3-diphenylpropane which has a methylene group between two centers of optical activity (Figure 33). There are two sets of protons in the molecule, H_a, H_b and H_c, H_d . In (1*R*,3*R*)-1,3-dibromo-1,3-diphenylpropane (one of a *dl* pair), H_a and H_b are chemical shift equivalent and so are H_c and H_d , because of an axis of symmetry (C_2) in the molecule. Rotation around that axis interchanges H_a with H_b and H_c with H_d . On the other hand, in (1*S*,3*R*)-1,3-dibromo-1,3-diphenylpropane (a *meso* compound), H_c and H_d are not chemical shift equivalent: they cannot be interchanged by a symmetry operation. (1*S*,3*R*)-1,3-dibromo-1,3-diphenylpropane does have a plane of symmetry (σ), but both H_c and H_d are in that plane. H_a and H_b are chemical shift equivalent because they can be interchanged by reflection through the plane of symmetry shown in Figure 33.

Although it is of no consequence unless a chiral solvent is used, note that only those protons that are interchangeable through an axis of rotation are completely identical

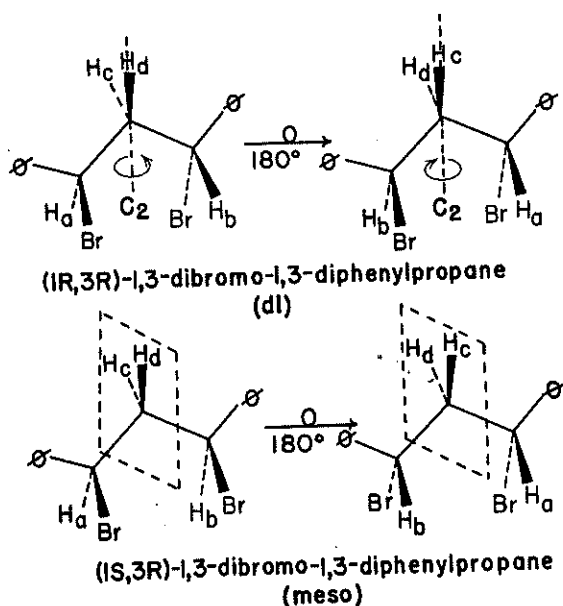


Fig. 33.

Two isomers of 1,3-dibromo-1,3-diphenylpropane. In the (1R, 3R) isomer, H_a and H_b are chemical shift equivalent, as are H_c and H_d . In the (1S, 3R) isomer, H_a and H_b are chemical shift equivalent, but H_c and H_d are not.

protons, whereas those that are interchangeable through other symmetry operations are enantiotopic, i.e., nonsuperimposable mirror images. Noninterchangeable protons are termed diastereotopic. Identical protons are chemical shift equivalent in any environment, chiral or achiral. Enantiotopic protons are chemical shift nonequivalent only in a chiral solvent. Diastereotopic protons are not chemical shift equivalent in any environment, although they may fortuitously absorb at the same position.

The concept of exchange through a rapid mechanism can be illustrated by the rapidly exchanging protons on some heteroatoms and by protons in molecules that are rapidly changing conformations. If the exchange is rapid enough, a single peak will result from, say, the carboxylic acid proton and the hydroxylic proton of a hydroxycarboxylic acid. Chemical shift equivalence of protons on a CH_3 group results from rapid rotation around a carbon-carbon single bond even in the absence of a symmetry element. Figure 34 shows Newman projections of the three staggered and three eclipsed conformers of a molecule containing a methyl group attached to another sp^3 carbon atom having three different substituents, i.e., an optically active center. In any single conformation, protons H_a, H_b, H_c are not chemical shift equivalent because the protons cannot be interchanged by a symmetry operation. However, the protons are rapidly changing position. The time spent in any one conformation

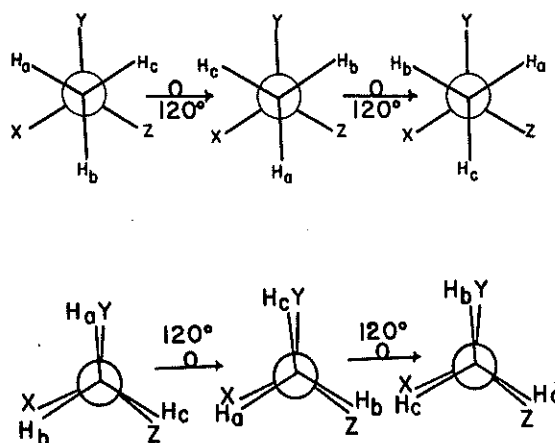


Fig. 34.

Newman projections of staggered and eclipsed conformers of a molecule with a methyl group attached to an optically active sp^3 carbon atom.

is short ($\sim 10^{-6}$ second), because the energy barrier for rotation around a C-C single bond is small. The chemical shift of the methyl group is an average of the shifts of each of the three protons. In other words, each proton can be interchanged with the others by a rapid rotational operation. Thus without the a, b, c labels the various staggered and eclipsed conformations, within each type, are indistinguishable.

Consider, in contrast with the methyl group, a methylene group next to a center of optical activity, as in 1-bromo-1,2-dichloroethane (Figure 35). Protons H_a and H_b are not chemical shift equivalent, since they cannot be interchanged by a symmetry operation in any conformation. In fact the molecule has no axis, plane, center, or

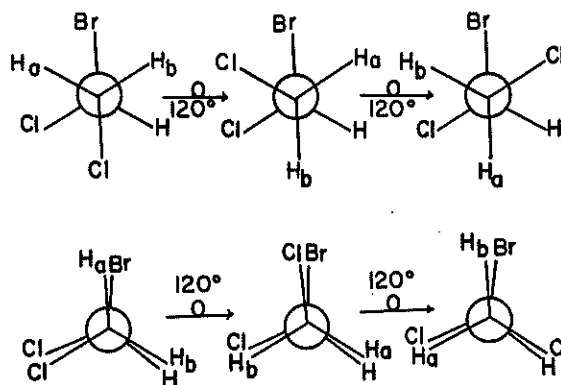


Fig. 35.

Newman projection of 1-bromo-1,2-dichloroethane. H_a and H_b cannot be interchanged by rotation nor by a symmetry operation.

reflection axis of symmetry. Although there is a rapid rotation around the carbon-carbon single bond, the protons are not interchangeable by a rotational operation. An observer can detect the difference before and after rotating the methylene group; the molecules are not superimposable.

The chemical shift of cyclohexane protons is an average of the shifts of the axial and the equatorial protons. The chemical shift equivalence of the cyclohexane protons results from rapid interchange of axial and equatorial protons as the molecule flips between chair forms. Since the planar conformation of cyclohexane is not a reasonable one, the chemical equivalence of its protons is not a consequence of achieving a planar conformation.

MAGNETIC EQUIVALENCE

Magnetic equivalence presupposes chemical shift equivalence. To determine whether chemical shift equivalent nuclei are magnetically equivalent, one determines whether they are coupled equally to each nucleus (probe nucleus) in every other set in the spin system. This is done by examining geometrical relationships. If the bond distances and angles from each nucleus in relation to the probe nucleus are identical, the nuclei in question are magnetically equivalent. Magnetically nonequivalent nuclei in a set are designated by primes (e.g., AA').

Consider the protons a, b and c, d in *p*-fluoronitrobenzene (Figure 36). Protons a and b are chemical shift equivalent by interchange through an axis or plane of symmetry. Protons a and b are coupled to nucleus F through the same bond distances and angles. However, protons a and b are coupled to proton c (or d) with different geometry. Thus, protons a and b fail the test for magnetic equivalence. Protons c and d are treated in the same way and are also found not to be magnetically equivalent. The system is $AA'BB'X$.

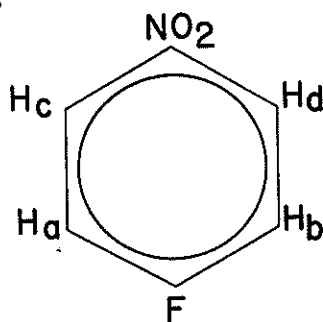
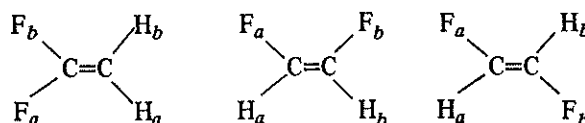


Fig. 36.
p-Fluoronitrobenzene.

We propose a somewhat more practical definition and test for magnetic equivalence: two chemical shift equivalent protons are magnetically equivalent if they are symmetrically disposed with respect to each nucleus (probe) in any other set in the spin system. This means that the two protons under consideration can be interchanged through a reflection plane passing through the probe nucleus and perpendicular to a line joining the chemical shift equivalent protons. Note first that this plane is not necessarily a molecular plane of symmetry. Note also that the test is valid in any reasonable molecular conformation.

The three isomeric difluoroethylenes furnish additional examples of chemical shift equivalent nuclei that are not magnetically equivalent.



In each case, the protons H_a and H_b and fluorines F_a and F_b comprise sets (of chemical shift equivalent nuclei) that are not magnetically equivalent.

Note that in the 1R,3R-compound of Figure 33, H_a and H_b are not magnetically equivalent (since they do not identically couple to H_c); H_c and H_d also are not magnetically equivalent since $J_{cb} \neq J_{da}$ and $J_{da} \neq J_{ca}$. Observe also that in the 1S,3R compound of Figure 33, $J_{ad} = J_{bd}$ and $J_{ac} = J_{bc}$; thus, in this molecule H_aH_b are magnetically equivalent.

The question of magnetic equivalence in freely rotating methylene groups of aliphatic compounds becomes complex. The following assignments illustrate the nuances involved (if substituents Y and Z cause large chemical shift differences, the AMX designation is used instead of ABC):

CH_3CH_2Y	A_3B_2
ZCH_2CH_2Y	$AA'BB'$
$YCH_2CH_2CH_2Y$	$AA'BB'AA'$
$CH_3CH_2CH_2Y$	$A_3BB'CC'$
$ZCH_2CH_2CH_2Y$	$AA'BB'CC'$
$YCH_2CH_2CH_2CH_2Y$	$AA'BB'B''B'''A''A'''$
$ZCH_2CH_2CH_2CH_2Y$	$AA'BB'CC'DD'$

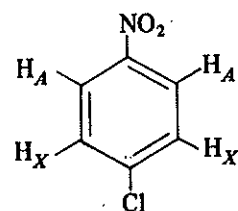
Methyl protons are magnetically equivalent by rotational averaging of the couplings to an adjacent methylene group whose protons are also magnetically equivalent if there is no other coupling involved. Averaging by rotation is valid since the rotational conformers are equivalent, thus equally populated. In ZCH_2CH_2Y , however, the population of the anti conformer is probably different from those of the enantiomeric gauche conformers, and rotational averaging is not valid. As pointed out by Ault¹²: "True A_2X_2 systems are quite rare (examples include difluoromethane, 1,1-difluoroallene, and 1,1,3,3-tetrachloropropane), and most

systems which are described as A_2X_2 systems should really be classified as $AA'XX'$ systems."

$AA'XX'$ systems often give deceptively simple A_2X_2 spectra; the spectrum of 2-dimethylaminoethyl acetate (Figure 37a) is a case in point. Figure 37 shows the progressive distortions as $AA'XX' \rightarrow AA'BB'$ (i.e., $\Delta\nu/J$ decreases) in compounds of type ZCH_2CH_2Y . As the absorptions move closer together, the inner peaks increase in intensity, additional splitting occurs, and some of the outer peaks disappear in the baseline noise. The general appearance of symmetry throughout aids recognition of the type of spin system involved. At the extreme, the two methylene groups become chemical shift equivalent and a single A_4 peak results.

Although 1,3-dichloropropane is properly described as an $XX'AA'XX'$ system, it also presents a deceptively simple spectrum (Figure 40) that resembles an A_2X_4 system (triplet and quintet). A discussion of conditions leading to these types of deceptively simple spectra is given by Ault^{11g}.

In *p*-chloronitrobenzene,



the protons ortho to the nitro group (H_A and $H_{A'}$) are chemical shift equivalent to each other, and the protons ortho to the chlorine group (H_X and $H_{X'}$) are chemical shift equivalent to each other. J_{AX} and $J_{A'X'}$ are the same, approximately 7 to 10 Hz, and $J_{A'X}$ and $J_{AX'}$ are also the same but much smaller, approximately 0 to 1 Hz. Since H_A and $H_{A'}$ couple differently to another specific proton, they are not magnetically equivalent, and first-order rules do not apply. (Similarly, H_X is not magnetically equivalent to $H_{X'}$). In fact for calculations, H_A and $H_{A'}$, and H_X and

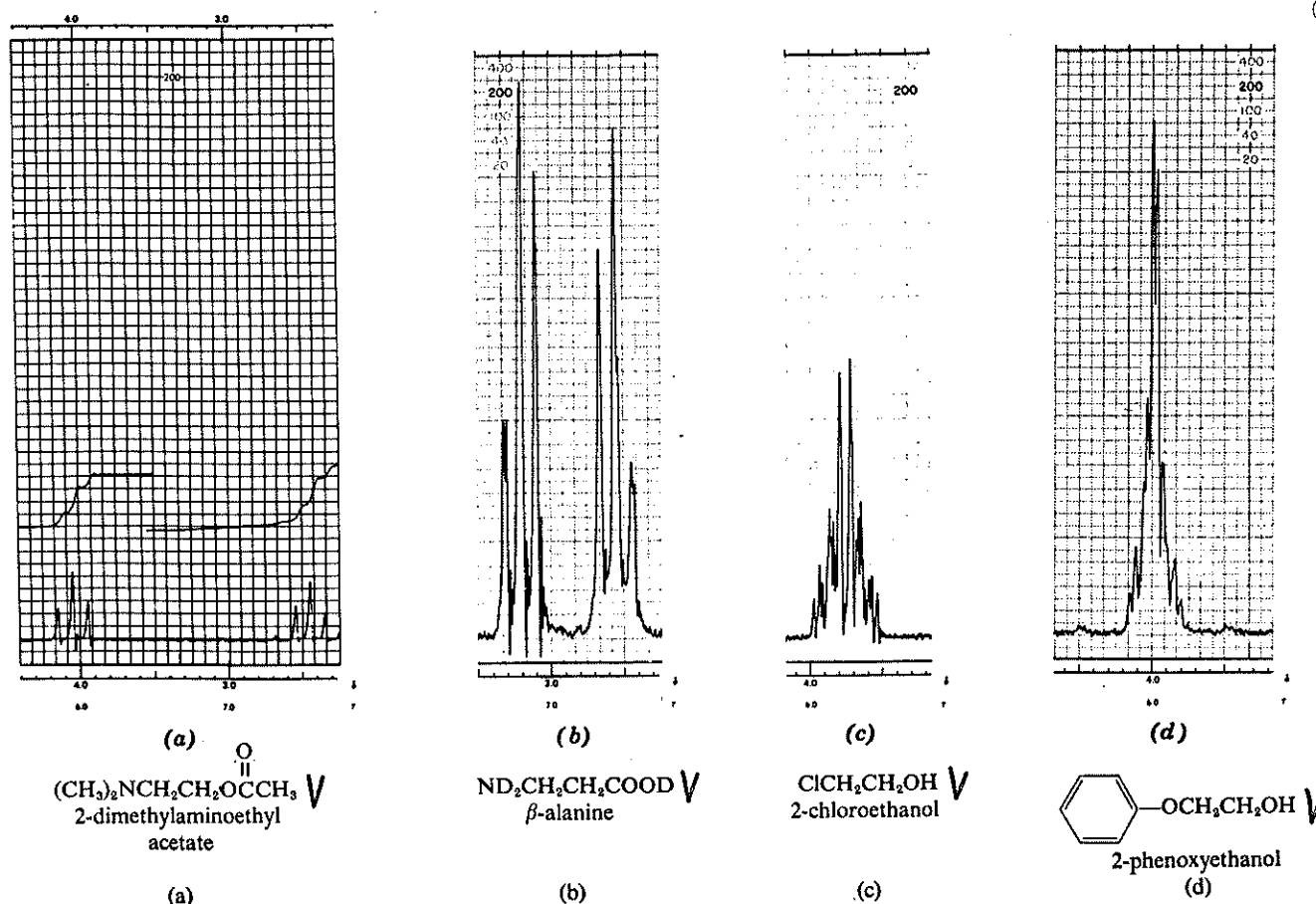


Fig. 37.

Progressive distortions as $AA'XX' \rightarrow AA'BB'$ in the configuration $Z-CH_2-CH_2Y$. 60 MHz.

that can readily be related to an AMX pattern. The following analysis, though not rigorous, is useful.

characteristic: the *trans* coupling is larger than the *cis*, and the geminal coupling is very small.

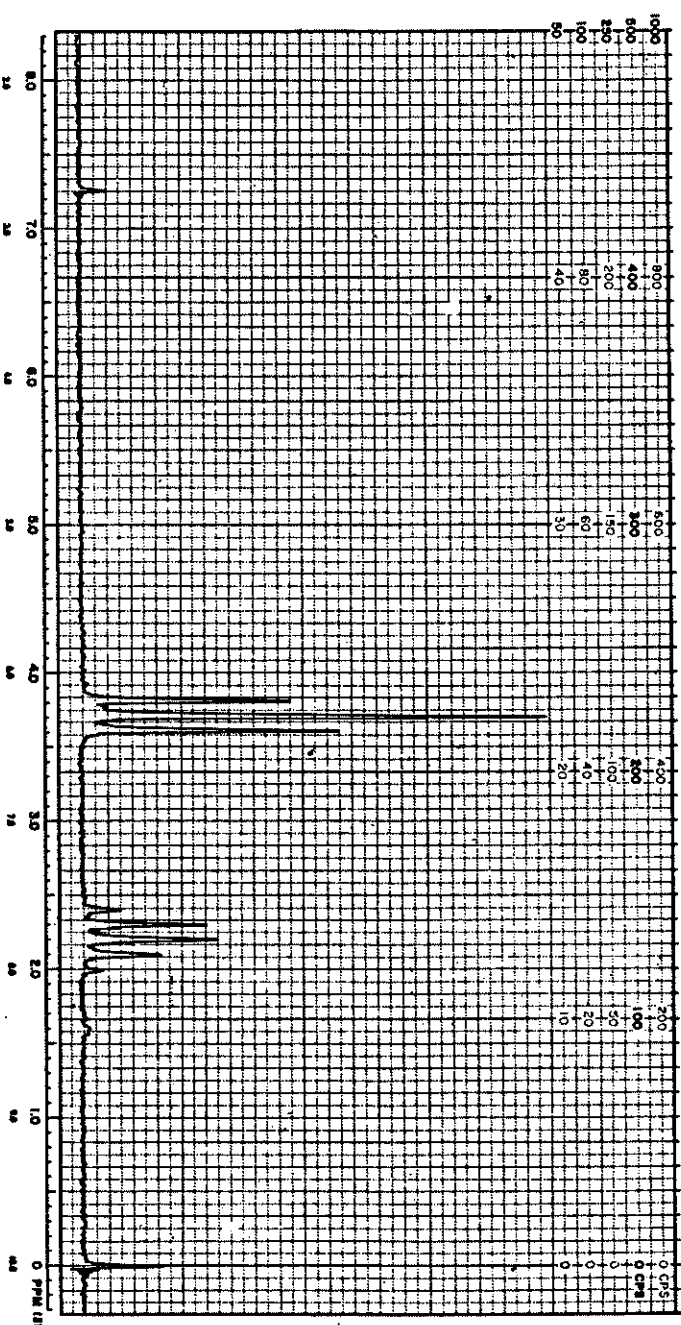


Fig. 40.
1,3-Dichloropropane in $CDCl_3$. 60 MHz. $XX'AA'XX'$ system.

The preceding analysis lacks splittings in proton X do not and J_{AX} , although this is a good greater than about 10 for information obtainable from spread between the outside lines. The distortions in peak intensities obvious. The pattern of two can be confused with the quartet of three equivalent protons.

As the shift positions of protons other so that $\Delta\nu$ becomes deviations from a first-order spectrum and B patterns overlap, and pattern merge. In the extreme J_{BX} , protons A and B are spectrum is simply A_2X and triplet. Note that a very similar A pair were chemically, but i.e., an $AA'X$ system. As the approaches the A and B absorbers to a very complex ABC

$H_{X'}$ are also coupled ($J \sim 3$ Hz). The system is described as $AA'XX'$, and the spectrum is actually very complex. Fortunately, the pattern is readily recognized because of its symmetry and *apparent* simplicity; under ordinary resolution it resembles an AB pattern of two distorted doublets. (Closer inspection reveals many additional splittings, Figure 38.) As the para substituents become more similar to each other (in their shielding properties), the system tends toward $AA'BB'$; even these absorptions resemble AB patterns until they overlap.

The aromatic protons of symmetrically *o*-disubstituted benzenes also give $AA'BB'$ spectra. An example is *o*-dichlorobenzene (Figure 39).

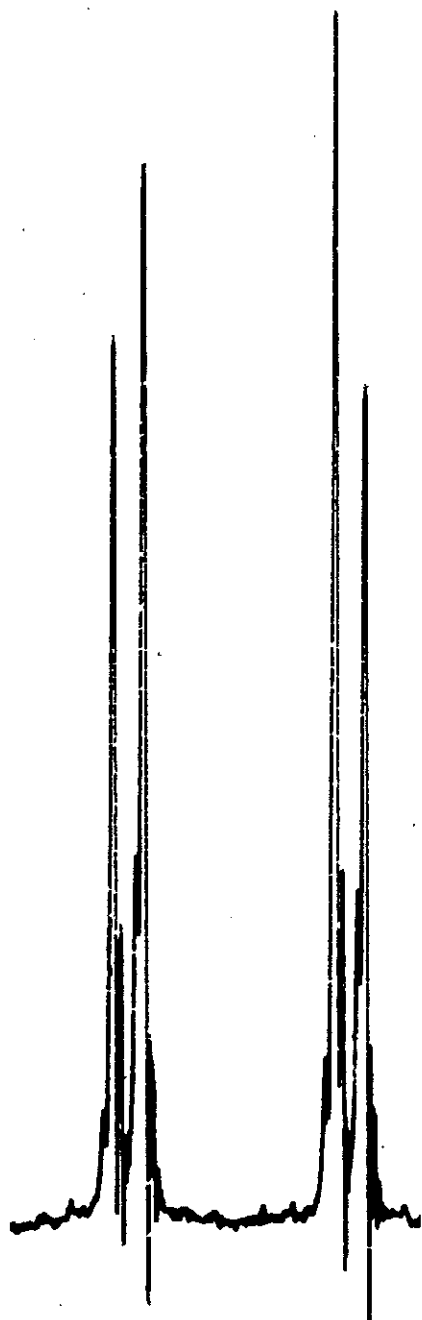
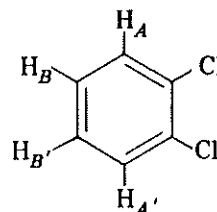


Fig. 38.
p-Chloronitrobenzene, 100 MHz CCl_4

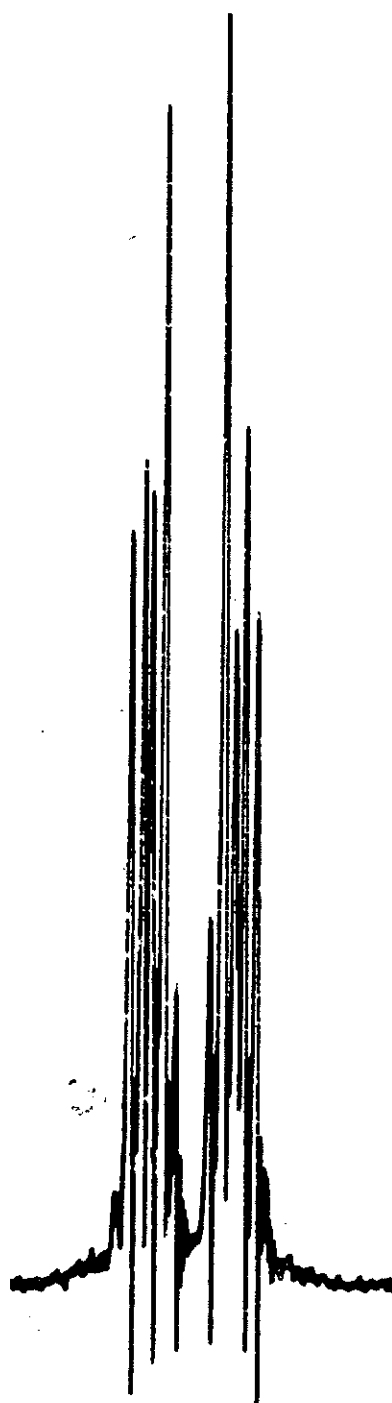
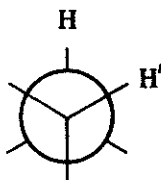


Fig. 39.
o-Dichlorobenzene, 100 MHz CCl_4 .

X. VICINAL AND GEMINAL COUPLING IN RIGID SYSTEMS

Coupling between protons on vicinal carbon atoms in rigid systems depends primarily on the dihedral angle ϕ between the H-C-C' and the C-C'-H' planes. This angle can be visualized by an end-on view of the bond between the



vicinal carbon atoms and by the perspective in Figure 46 in which the calculated relationship between dihedral angle and vicinal coupling constant²⁸ is graphed. Karplus emphasized²⁹ that his calculations are approximations and do not take into account such factors as electronegative substituents, the bond angles θ (\angle H-C-C' and \angle C-C'-H'), and bond lengths. Deductions of dihedral angles from measured coupling constants are safely made only by comparison with closely related compounds. The correlation has been very useful in cyclopentanes, cyclohexanes, carbohydrates, and bridged polycyclic systems. In cyclopentanes, the observed values of about 8 Hz for vicinal *cis* protons and about 0 Hz for vicinal *trans* protons are in accord with the corresponding angles of about 0° and about 90° , respectively. In substituted or fused cyclohexane rings, the following relations obtain:

	Calc. J	Observed J (Hz)
axial-axial	9	8-14 (usually 8-10)
axial-equatorial	1.8	1-7 (usually 2-3)
equatorial-equatorial	1.8	1-7 (usually 2-3)

A modified Karplus equation³⁰ can be applied to vicinal coupling in olefins. The prediction of a larger *trans* coupling ($\phi = 180^\circ$) than *cis* coupling ($\phi = 0^\circ$) is borne out. The *cis* coupling in unsaturated rings decreases with (increasing bond angle θ) decreasing ring size as follows: cyclohexenes $J = 8.8$ to 10.5 , cyclopentenenes $J = 5.1$ to 7.0 , cyclobutenenes $J = 2.5$ to 4.0 , and cyclopropenes $J = 0.5$ to 2.0 .³¹

The calculated relationship³² between the H-C-H angle of geminal protons is shown in Figure 47. This relationship is quite susceptible to other influences and should be used with due caution. However, it is useful for characterizing methylene groups in a fused cyclohexane ring (approximately tetrahedral, $J \sim 12$ to 18), methylene groups of a cyclopropane ring ($J \sim 5$), or a terminal methylene group ($J \sim 0$ to 3). Geminal coupling constants are actually negative numbers, but this can be ignored except for calculations.

In view of the fact that influence of substituents on the coupling constants is not taken into account in the Karplus equation, the application of this equation to the determination of dihedral angles in substituted cyclohexanes is not reliable.

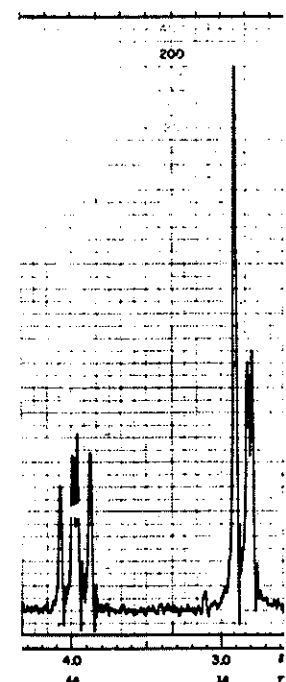
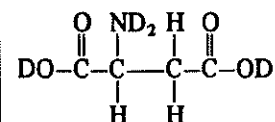
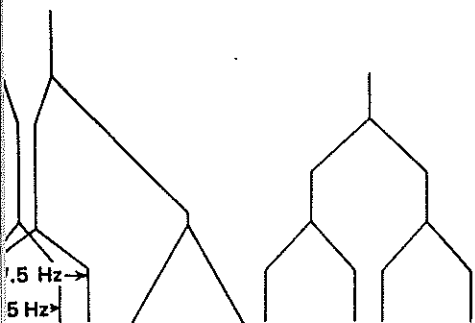


Fig. 45.
Aspartic acid in D_2O , 60 MHz.

The protons in aspartic acid (Figure 45) are equivalent, and the shift difference between the methylene protons is compared with the geminal coupling constant. The shift difference from the geminal coupling



and the inner peaks are strong, the outer peaks are weak. The methylene proton is also split by the methine proton with coupling constants of ~ 7.5 Hz and ~ 1.5 Hz. Two of the peaks coincide, the end of the baseline noise, and the net result is a multiplet consisting of two



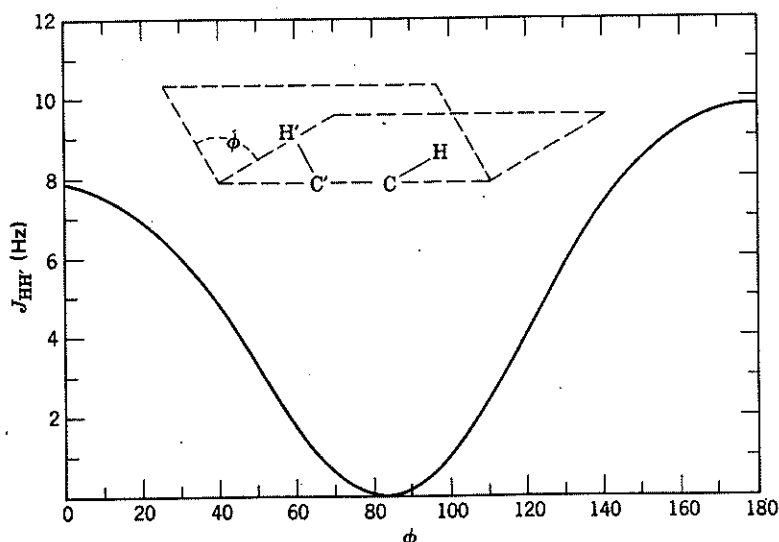


Fig. 46.
The vicinal Karplus correlation. Relationship between dihedral angle and coupling constant for vicinal protons.

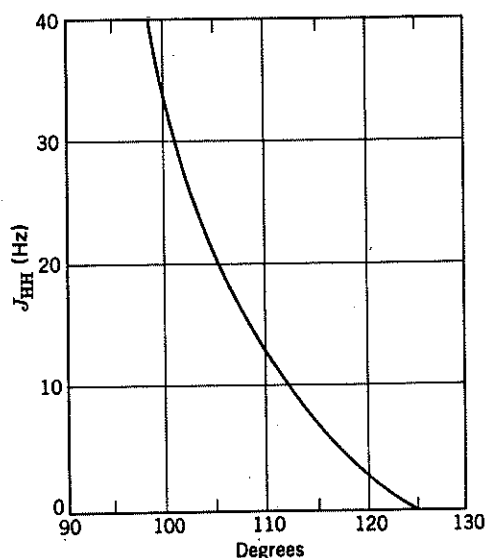


Fig. 47.
The geminal Karplus correlation. J_{HH} for CH_2 groups as function of $\angle H-C-H$.

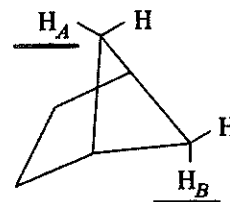
In view of the many factors other than angle dependence that influence coupling constants, it is not surprising that there have been "uses and abuses" of the Karplus correlation.⁴ Direct "reading off" of the angle from the magnitude of the J value is a very dangerous practice. The safest application of the relationships is to structure determinations in which molecular geometries have provided the

extrema of the high and low expected J values and for which the 0° and 90° or 90° and 180° structures are known for a given system. A more detailed description of the limitations of the Karplus correlations has been provided in Jackman and Sternhell.⁴

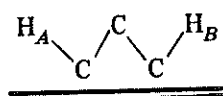
XI. LONG-RANGE COUPLING

Proton-proton coupling beyond three bonds may occur in olefins, acetylenes, aromatics, and heteroaromatics, and in strained ring systems (small or bridged rings). Allylic ($H-C-C=C-H$) coupling constants are about 0 to 3 Hz. Homoallylic ($H-C-C=C-CH$) couplings are usually negligible but may be as much as 1.6 Hz. Coupling through conjugated polyacetylenic chains may occur through as many as nine bonds. Meta coupling in a benzene ring is 1 to 3 Hz, and para, 0 to 1 Hz. In five-membered heteroaromatic rings, coupling between the 2, 4 protons is 0 to 2 Hz.

J_{AB} in the bicyclo [2.1.1] hexane system is about 7 Hz. This unusually high long-range coupling constant is attri-



buted to the "W-conformation"⁴ of the four sigma bonds between H_A and H_B :



7

CHEMICAL SHIFT CORRELATIONS FOR ^{13}C AND OTHER ELEMENTS7.1 ^{13}C CHEMICAL SHIFTS REVISITED

In Chapter 6 we developed an understanding of the relationships between the molecular environment of a hydrogen atom and the chemical shift of its nucleus. Now let us see if the same approach of base values plus substituent parameters [Eq. (6.5b)] will allow us to predict ^{13}C chemical shifts. Recall from Sections 2.1 and 2.2 that ^{13}C (like ^1H) has a nuclear spin of $\frac{1}{2}$ but undergoes resonance at a much lower frequency than ^1H because of the lower magnetogyric ratio of ^{13}C . Also, the low natural abundance and low relative sensitivity of ^{13}C (Table 2.1) require that the signal-averaged pulsed-mode technique (Section 3.4) be used for data collection. Remember that TMS (its carbon signal now) still defines the zero point of our chemical shift scale and that ^{13}C chemical shifts span a range of about 250 ppm. And finally, unless otherwise noted, all ^{13}C spectra discussed in this chapter are proton decoupled (Section 5.5).

7.2 TETRAHEDRAL (sp^3 HYBRIDIZED) CARBONS

Take a moment to review the ^{13}C spectra of toluene in Section 5.4. How would you go about predicting the ^{13}C chemical shift of the methyl group in toluene? The logical base value is the ^{13}C chemical shift of methane (which, it turns out, is δ -2.3, Table 7.1), to which we add the ^{13}C substituent parameter of a phenyl ring connected directly to the methyl carbon ($\Delta\delta = 23$, Table 7.2). The predicted value, therefore, is δ 20.7, in excellent agreement with the observed value of δ 21.4. Table 7.1 lists ^{13}C chemical shifts for a number of common alkanes and cycloalkanes, to be used as base values. Table 7.2 gives the substituent parameters for many common substituent groups as a function of their proximity to the carbon of interest (α = one-bond separation, β = two-bond separation, γ = three-bond separation). Notice once again that the

(de)shielding effect of a substituent tends to decrease as the number of intervening bonds increases. In fact, most groups exert a modest shielding effect (shown by the negative value of $\Delta\delta$) on the γ carbon.

■ **EXAMPLE 7.1** Why does butane (Table 7.1) exhibit only two ^{13}C signals rather than four?

□ **Solution:** By symmetry, the two methyl groups are equivalent (δ 13.4), as are the two methylenes (δ 25.2). □

TABLE 7.1 ^{13}C Chemical Shifts for Common Alkanes and Cycloalkanes^a

Name	Structure	C1 ^b	C2	C3
Methane	CH_4	-2.3		
Ethane	CH_3CH_3	5.7		
Propane	$\text{CH}_3\text{CH}_2\text{CH}_3$	15.8	16.3	
Butane	$\text{CH}_3\text{CH}_2\text{CH}_2\text{CH}_3$	13.4	25.2	
Pentane	$\text{CH}_3\text{CH}_2\text{CH}_2\text{CH}_2\text{CH}_3$	13.9	22.8	34.7
Hexane	$\text{CH}_3\text{CH}_2\text{CH}_2\text{CH}_2\text{CH}_2\text{CH}_3$	14.1	23.1	32.2
Cyclopropane	Cyclo-(CH_2) ₃	-3.5		
Cyclobutane	Cyclo-(CH_2) ₄	22.4		
Cyclopentane	Cyclo-(CH_2) ₅	25.6		
Cyclohexane	Cyclo-(CH_2) ₆	26.9		
Cycloheptane	Cyclo-(CH_2) ₇	28.4		
Cyclooctane	Cyclo-(CH_2) ₈	26.9		

^aData from ref. 1.

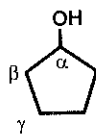
^bNumbering starts at a terminal carbon.

TABLE 7.2 ^{13}C Substituent Parameters ($\Delta\delta$, ppm)^a

X	Terminal X $\text{X}-\text{C}_\alpha-\text{C}_\beta-\text{C}_\gamma$			Internal X $\text{C}_\gamma-\text{C}_\beta-\text{C}_\alpha(\text{X})-\text{C}_\beta-\text{C}_\gamma$		
	α	β	γ	α	β	γ
-F	68	9	-4	63	6	-1
-NO ₂	63	4	—	57	4	—
-OR	58	8	-4	51	5	-4
-OC(=O)R	51	6	-3	45	5	-3
-OH	48	10	-5	41	8	-5
-NR ₂	42	6	-3	—	—	—
-NHR	37	8	-4	31	6	-4
-C(=O)Cl	33	—	—	28	2	—
-Cl	31	11	-4	32	10	-4
-C(=O)H	—	31	-2	0	—	-2
-C(=O)R	30	1	-2	24	1	-2
-NH ₂	29	11	-5	24	10	-5
-N ⁺ H ₃	26	8	-5	24	6	-5
-C(=O)O ⁻	25	5	-2	20	3	-2
-Phenyl	23	9	-2	17	7	-2
-C(=O)NH ₂	22	—	-0.5	2.5	—	-0.5
-C(=O)OH	21	3	-2	16	2	-2
-CH=CH ₂	20	6	-0.5	—	—	—
-C(=O)OR	20	3	-2	17	2	-2
-Br	20	11	-3	25	10	-3
-SR	20	7	-3	—	—	—
-SH	11	12	-4	11	11	-4
-CH ₃	9	10	-2	6	8	-2
-C≡C-H	4.5	5.5	-3.5	—	—	—
-C≡N	4	3	-3	1	3	-3
-I	-6	11	-1	4	12	-1

^aData from Wehrli, F.W., and Wirthlin, T., *Interpretation of Carbon-13 NMR Spectra*, 2nd Ed., Heyden, London, 1983, as quoted in ref. 1.

■ **EXAMPLE 7.2** Predict the chemical shift of each carbon in cyclopentanol (the C-H hydrogens are not shown in the structure below):



□ **Solution:** Using as a base value the chemical shift of cyclopentane (δ 25.6, Table 7.1) and the internal substituent parameters for the -OH group, we calculate:

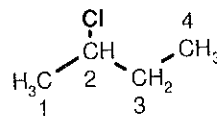
$$\delta_\alpha = 25.6 + 41 = 66.6$$

$$\delta_\beta = 25.6 + 8 = 33.6$$

$$\delta_\gamma = 25.6 + (-5) = 20.6$$

These are in reasonable agreement with the observed values of δ 73.3, 35.0, and 23.4.¹ □

■ **EXAMPLE 7.3** The ^{13}C spectrum of 2-chlorobutane (Figure 7.1) exhibits signals at δ 11.01, 24.85, 33.33, and 60.38. Assign each signal to a specific carbon in the structure by correlating the observed chemical shifts with the predicted values:



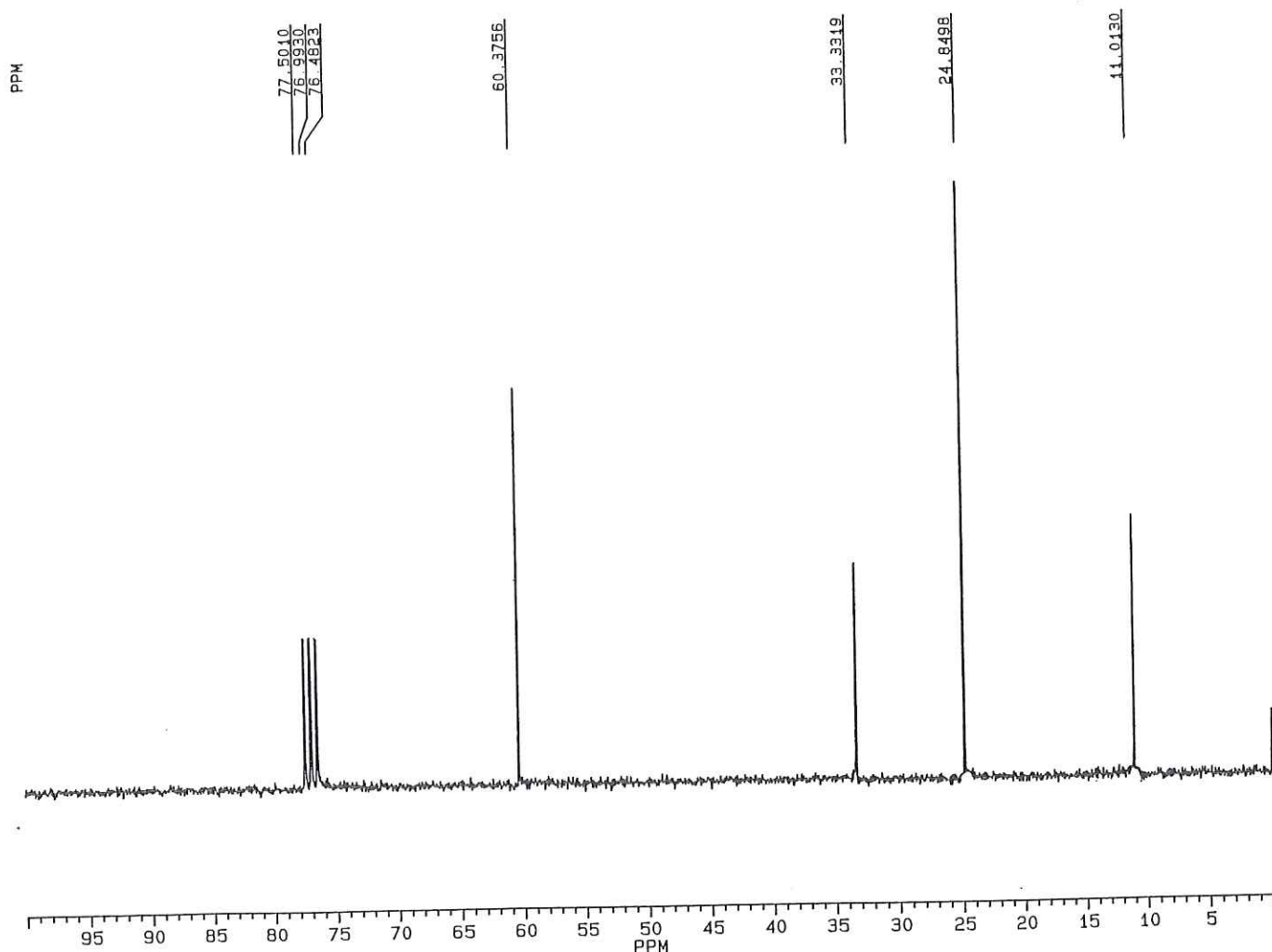


Figure 7.1. The 62.5 MHz ^{13}C spectrum of 2-chlorobutane.

- **Solution:** For carbon 1 we use the C1 base value for butane (δ 13.4 ppm, Table 7.1) and add the $\Delta\delta$ value for an internal β chlorine (10 ppm, Table 7.2). Thus,

$$\delta_1 = 13.4 + 10 = 23.4 \text{ ppm}$$

Similarly,

$$\delta_2 = 25.2 + 32 = 57.2 \text{ ppm}$$

$$\delta_3 = 25.2 + 10 = 35.2 \text{ ppm}$$

$$\delta_4 = 13.4 + (-4) = 9.4 \text{ ppm}$$

Clearly, δ_1 corresponds to the peak at δ 24.85, δ_2 to the peak at 60.38, δ_3 to the peak at 33.33, and δ_4 to the peak at 11.01. Note that ^{13}C chemical shifts can be ascertained

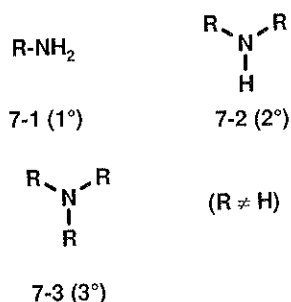
only to ± 1 ppm when determined visually from a plotted spectrum. These more precise values come from peak picking (the number plotted above each signal) or a computer listing that accompanies the spectrum. □

Did you notice the relative intensities of the lines in Figure 7.1? From Section 5.4 we know that ^{13}C signal intensities are not necessarily proportional to the numbers of carbons giving rise to the signal (as they are in the case of hydrogen signals) because of differences in relaxation times and NOE enhancements. Nonetheless, as is usually the case, the relative intensities of the four tetrahedral carbon signals in the spectrum of 2-chlorobutane vary according to the number of hydrogens directly attached to each carbon, that is, methyl > methylene > methine.

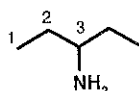
■ **EXAMPLE 7.4** Now let us try to identify an unknown. Suggest a structure for $\text{C}_5\text{H}_3\text{N}$, whose ^{13}C spectrum ² exhibits

signals at δ 10.4, 30.4, and 54.4. Assign each signal to a carbon in your structure; then calculate the expected chemical shift of each carbon in your structure.

- **Solution:** The IOU for this molecular formula is zero; therefore, it is saturated, with no rings or multiple bonds. The fact that there are only three signals for the five carbons indicates that the structure has some symmetry. The only substituent groups with a single nitrogen that give a signal in the δ 50–60 region are **primary** (1°), **secondary** (2°), or **tertiary** (3°) amines (structures 7-1 through 7-3):



The signal at δ 54.4 represents either one carbon or two or three *equivalent* carbons attached directly to nitrogen. A little thought should convince you that there is no way to distribute five carbons among two or three equivalent R groups to yield a secondary or tertiary amine unless there were *two* different signals in the δ 50–60 range. Therefore, we must be dealing with a primary amine with just *one* carbon attached to nitrogen. The four remaining carbons must be divided into two sets of two to account for the two remaining signals. The only structure that fulfills these criteria is 3-aminopentane:



To confirm our assignment, let us calculate the predicted chemical shifts using the base values for pentane (Table 7.1) and the $\Delta\delta$ values for an NH_2 substituent (Table 7.2):

$$\delta_1 = 13.9 + (-5) = 8.9$$

$$\delta_2 = 22.8 + 10 = 32.8$$

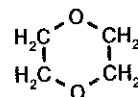
$$\delta_3 = 34.7 + 24 = 58.7$$

Once again, the agreement with the observed values is close enough to give us confidence in our structural assignment. □

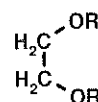
7.3 HETEROCYCLIC STRUCTURES

A cyclic molecule in which one or more of the ring atoms is a heteroatom is referred to as a **heterocyclic molecule**.

- **EXAMPLE 7.5** Predict the chemical shift of the carbons in the heterocyclic molecule below, known as dioxane:



- **Solution:** First, we recognize by symmetry that all four carbons are equivalent. We can think of the molecule as a derivative of ethane:

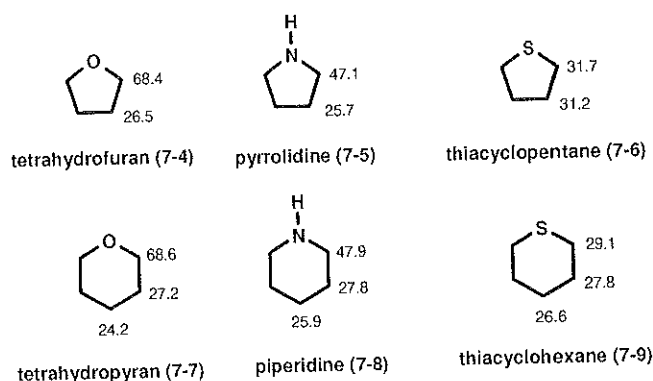


Thus, each carbon is α to one and β to another (equivalent) O–R group. Using the data in Tables 7.1 and 7.2, we calculate

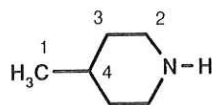
$$\begin{aligned} \delta &= \delta(\text{ethane}) + \Delta\delta(\text{OR}, \alpha) + \Delta\delta(\text{OR}, \beta) \\ &= 5.7 + 58 + 8 = 71.7 \end{aligned}$$

The observed value is 66.5.¹ □

When predicting chemical shifts for substituted heterocycles, you will find it preferable to use the chemical shifts of the parent heterocycle as base values. The ^{13}C chemical shifts for a few typical examples are shown in structures 7-4 through 7-9.^{1,3,4} Consult the references listed at the end of this chapter for additional examples:



- **EXAMPLE 7.6** Predict the chemical shift of each carbon in the structure below:



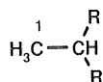
- **Solution:** Using the base values in structure 7-8 and the substituent parameters for an internal CH_3 group (Table 7.2), we predict the following for the ring carbons:

$$\delta_2 = \delta(\text{piperidine, C2}) + \Delta\delta(\text{CH}_3, \gamma) = 47.9 + (-2) = 45.9$$

$$\delta_3 = \delta(\text{piperidine, C3}) + \Delta\delta(\text{CH}_3, \beta) = 27.8 + 8 = 35.8$$

$$\delta_4 = \delta(\text{piperidine, C4}) + \Delta\delta(\text{CH}_3, \alpha) = 25.9 + 6 = 31.9$$

We can calculate the chemical shift of the methyl carbon by viewing the molecule as a substituted derivative of ethane (Table 7.2):



$$\delta_1 = \delta(\text{ethane}) + 2[\Delta\delta(\text{CH}_3, \beta)] = 5.7 + 2(10) = 25.7$$

These turn out to be very close to the observed values of δ 46.8, 35.7, 31.3, and 22.5, respectively. □

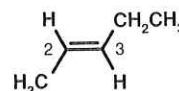
7.4 TRIGONAL CARBONS

You remember that the *aromatic* carbons of toluene (Section 5.4) appear far downfield of the methyl carbon. Just as with vinyl and aromatic hydrogens (Sections 6.3 and 6.5), sp^2 hybridized vinyl and aromatic carbons are deshielded in comparison to their sp^3 hybridized tetrahedral counterparts. For this reason, their signals usually fall in the region of δ 100–165.

7.4.1 Vinyl Carbons

We will treat molecules with vinyl carbons as derivatives of ethylene ($\text{H}_2\text{C}=\text{CH}_2$, Section 6.3), whose ^{13}C signal appears at δ 123.3.¹ To this base value, we will apply $\Delta\delta$ corrections (Table 7.3) for substituents according to their location with respect to the carbon of interest.

■ **EXAMPLE 7.7** Predict the chemical shift of the two vinyl carbons in *trans*-2-pentene:



- **Solution:** Carbon 2 has alkyl carbon substituents at positions α , a , and b . Therefore, $\delta_2 = \delta(\text{C}_2\text{H}_4) + \Delta\delta(\text{R}, \alpha) +$

TABLE 7.3 Vinyl Carbon Substituent Parameters ($\Delta\delta$, ppm)^{a,b}

X	α	β	γ	a	b	c
–R	10.6	7.2	–1.5	–7.9	–1.8	–1.5
–OR	29	2	—	–39	–1	—
–OC(=O)R	18	—	—	–27	—	—
–C(=O)R	15	—	—	6	—	—
–Phenyl	12	—	—	–11	—	—
–C(=O)OR	6	—	—	7	—	—
–C(=O)OH	4	—	—	9	—	—
–OH	—	6	—	—	–1	—
–Cl	3	–1	—	–6	2	—
–Br	–8	0	—	–1	2	—
–C \equiv N	–16	—	—	15	—	—
–I	–38	—	—	7	—	—

^aData from refs. 1 and 4. R = alkyl.

^bWhen a group is in the b (or β) position, X_a (or X_α) is assumed to be carbon; when a group is in the c (or γ) position, both X_a and X_b (or X_α and X_β) are assumed to be carbon.

$$\Delta\delta(R, a) + \Delta\delta(R, b) = 123.3 + 10.6 + (-7.9) + (-1.8) = 124.2$$

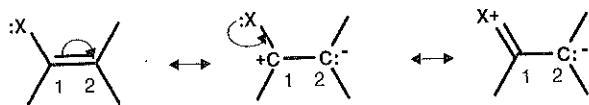
Similarly,

$$\begin{aligned}\delta_3 &= \delta(C_2H_4) + \Delta\delta(R, \alpha) + \Delta\delta(R, a) + \Delta\delta(R, \beta) \\ &= 123.3 + 10.6 + (-7.9) + 7.2 = 133.2\end{aligned}$$

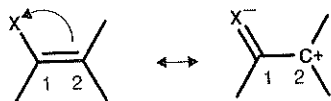
The observed values are δ 123.7 and 133.3, respectively. \square

Table 7.3 includes substituent parameters for several heteroatom-containing substituents. Notice that there is a very large difference between the $\Delta\delta$ value for a group located at the α position and the value for the same group at the a position. This is because the π electrons in the carbon-carbon double bond interact directly through **resonance** with many of these substituents, causing substantial shielding when at the α position and deshielding when at the a position, or vice versa.

For example, an atom X with an unshared pair of electrons (e.g., X = OR, NR₂, S, or halogen) can donate the pair to (i.e., share it with) the π system, as shown in the resonance structures below. This interaction increases the electron density at carbon 2 (thereby shielding it), while decreasing the electron density on carbon 1 and X (deshielding them):

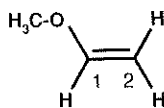


Conversely, if atom X has an empty p -type valence orbital (e.g., X = C=O, C \equiv N, NO₂), it can withdraw a pair of electrons from the π bond, significantly deshielding carbon 2 while shielding X:



Thus, the net effect of any such **polar** substituent is the sum of its resonance effects and its inductive (electronegativity) effects.

■ **EXAMPLE 7.8** Predict the chemical shifts for the vinyl carbons in the molecule below; then draw a resonance structure of the molecule that shows why one vinyl carbon is exceptionally shielded while the other is deshielded:

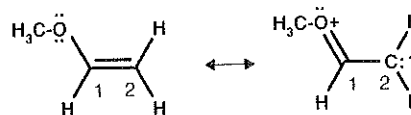


□ **Solution:** Using the data in Table 7.3,

$$\delta_1 = \delta(\text{ethylene}) + \Delta\delta(OR, \alpha) = 123.3 + 29 = 152.3$$

$$\delta_2 = \delta(\text{ethylene}) + \Delta\delta(OR, a) = 123.3 + (-39) = 84.3$$

Recall that a divalent oxygen has two unshared electron pairs, either of which can be donated to the π system:



The observed signals occur at δ 153.2 and 84.2, respectively.¹ Notice that carbon 1 is deshielded by the electronegative oxygen directly connected to it, while carbon 2 is shielded by resonance between the π bond and the unshared pair on oxygen.

Because of such resonance interactions, the best policy to follow when you are predicting chemical shifts of vinyl carbons with polar substituents directly connected is to find a model compound as similar in structure as possible to serve as the source of base values. \square

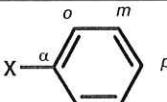
In organometallic complexes of alkenes, where a transition metal uses an empty d orbital to coordinate to the π bond of the alkene, the vinyl carbons move upfield to the range of δ 7–110, varying widely and depending on the exact structure of the complex.⁵ The reasons for this upfield shift include both shielding by the electron-rich electropositive metal, and a change in hybridization of the vinyl carbons toward less s character (i.e., more sp^3 like).

7.4.2 Aromatic Carbons

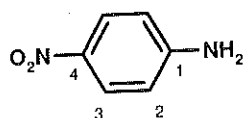
In the case of aromatic carbons, we will use as our base value the ¹³C chemical shift of benzene (Example 4.3), δ 128.5. Notice that aromatic carbons appear slightly downfield of vinyl carbons, just as aromatic hydrogens appear downfield of vinyl hydrogens (Sections 6.3 and 6.5). Table 7.4 lists substituent parameters for a number of aromatic substituents as a function of proximity to a given carbon. Observe how, for many of these groups, their effect alternates back and forth from deshielding to shielding as the number of intervening bonds increases. This is a consequence of the changing balance between competing inductive and resonance effects of the substituent as a function of location.

■ **EXAMPLE 7.9** Predict the chemical shifts of each aromatic carbon in *para*-nitroaniline:

TABLE 7.4 Aromatic Substituent Parameters ($\Delta\delta$, ppm)^a

				
X	α	<i>o</i> (Ortho)	<i>m</i> (Meta)	<i>p</i> (Para)
-F	35.1	-14.3	0.9	-4.5
-OCH ₃	31.4	-14.4	1.0	-7.7
-OPh	29.0	-9.4	1.6	-5.3
-OH	26.6	-12.7	1.6	-7.3
-OC(=O)CH ₃	22.4	-7.1	-0.4	-3.2
-N(CH ₃) ₂	22.4	-15.7	0.8	-11.8
-C(CH ₃) ₃	22.2	-3.4	-0.4	-3.1
-CH(CH ₃) ₂	20.1	-2.0	0	-2.5
-NO ₂	19.6	-5.3	0.9	6.0
-NH ₂	19.2	-12.4	1.3	-9.5
-CH ₂ CH ₃	15.6	-0.5	0.0	-2.6
-S(O) ₂ NH ₂	15.3	-2.9	0.4	3.3
-Si(CH ₃) ₃	13.4	4.4	-1.1	-1.1
-CH ₂ OH	13.3	-0.8	-0.6	-0.4
-phenyl	12.1	-1.8	-0.1	-1.6
-NHC(=O)CH ₃	11.1	-9.9	0.2	-5.6
-SCH ₃	10.2	-1.8	0.4	-3.6
-CH ₃	9.3	0.7	-0.1	-2.9
-CH=CH ₂	9.1	-2.4	0.2	-0.5
-C(=O)Ph	9.1	1.5	-0.2	3.8
-C(=O)H	8.2	1.2	0.6	5.8
-C(=O)CH ₃	7.8	-0.4	-0.4	2.8
-CH ₂ OC(=O)CH ₃	7.7	0	0	0
-Cl	6.4	0.2	1.0	-2.0
-N=C=O	5.7	-3.6	1.2	-2.8
-C(=O)Cl	4.6	2.9	0.6	7.0
-C(=O)OH	2.9	1.3	0.4	4.3
-CF ₃	2.6	-3.1	0.4	3.4
-SH	2.3	0.6	0.2	-3.3
-C(=O)OCH ₃	2.0	1.2	-0.1	4.8
-Br	-5.4	3.4	2.2	-1.0
-C(=O)CF ₃	-5.6	1.8	0.7	6.7
-C \equiv CH	-5.8	6.9	0.1	0.4
-C \equiv N	-16.0	3.6	0.6	4.3
-I	-32.2	9.9	2.6	-7.3

^aData abstracted from ref. 1.



□ **Solution:** By symmetry, the aromatic carbons are divided into four sets in the ratio of 1 : 2 : 2 : 1. Carbon 1 is α to an NH_2 group, and para to an NO_2 group. Therefore,

$$\begin{aligned}\delta_1 &= \delta(\text{benzene}) + \Delta\delta(\text{NH}_2, \alpha) + \Delta\delta(\text{NO}_2, p) \\ &= 128.5 + 19.2 + 6.0 = 153.7\end{aligned}$$

Likewise,

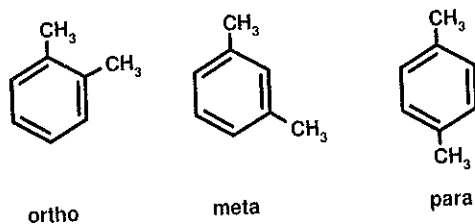
$$\begin{aligned}\delta_2 &= \delta(\text{benzene}) + \Delta\delta(\text{NH}_2, o) + \Delta\delta(\text{NO}_2, m) \\ &= 128.5 + (-12.4) + 0.9 = 117.0\end{aligned}$$

$$\begin{aligned}\delta_3 &= \delta(\text{benzene}) + \Delta\delta(\text{NH}_2, m) + \Delta\delta(\text{NO}_2, o) \\ &= 128.5 + 1.3 + (-5.3) = 124.5\end{aligned}$$

$$\begin{aligned}\delta_4 &= \delta(\text{benzene}) + \Delta\delta(\text{NH}_2, p) + \Delta\delta(\text{NO}_2, \alpha) \\ &= 128.5 + (-9.5) + 19.6 = 138.6\end{aligned}$$

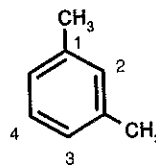
These predictions agree quite nicely with the observed values of δ 155.1, 112.8, 126.3, and 136.9, respectively. Notice how carbons 1 and 4 are deshielded (the former quite strongly) while carbons 2 and 3 are shielded, relative to benzene. □

■ **EXAMPLE 7.10** Which of the three isomers of xylene gives a ^{13}C spectrum with signals at δ 137.7, 130.0, 128.2, 126.2, and 21.3? To confirm your choice, predict the chemical shift of each carbon in your structure:



□ **Solution:** If you took more than 1 minute to pick out the correct answer, you have forgotten what you learned about symmetry in Chapter 4. In each of these three structures the two methyl groups are equivalent. But the number of aromatic carbon signals would vary: The ortho isomer would show three, the meta four, and the para only two. Since the first four ^{13}C signals are squarely in the aromatic

region, only the meta isomer fits the observed spectrum. To confirm our identification, let us predict chemical shifts:



$$\begin{aligned}\delta_1 &= \delta(\text{benzene}) + \Delta\delta(\text{CH}_3, \alpha) + \Delta\delta(\text{CH}_3, m) \\ &= 128.5 + 9.3 + (-0.1) = 137.7\end{aligned}$$

$$\begin{aligned}\delta_2 &= \delta(\text{benzene}) + 2[\Delta\delta(\text{CH}_3, o)] \\ &= 128.5 + 2(0.7) = 129.9\end{aligned}$$

$$\begin{aligned}\delta_3 &= \delta(\text{benzene}) + \Delta\delta(\text{CH}_3, o) + \Delta\delta(\text{CH}_3, p) \\ &= 128.5 + 0.7 + (-2.9) = 126.3\end{aligned}$$

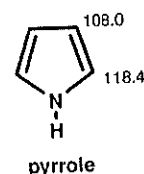
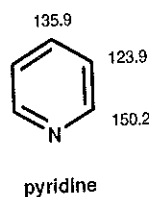
$$\begin{aligned}\delta_4 &= \delta(\text{benzene}) + 2[\Delta\delta(\text{CH}_3, m)] \\ &= 128.5 + 2(-0.1) = 128.3\end{aligned}$$

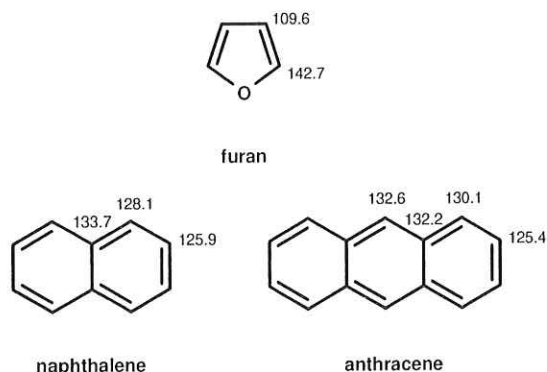
The observed chemical shift of the methyl groups (δ 21.3) could have been predicted from the data for toluene in Section 7.2. □

As we saw with metal complexed vinyl carbons, organometallic complexes of aromatic compounds exhibit ^{13}C chemical shifts upfield of the uncomplexed compound. For example, metal-coordinated benzene carbons are found in the range δ 74–111, depending on the exact structure of the complex. Similarly, metal-coordinated cyclopentadienide (C_5H_5^- , abbreviated Cp^-) appears in the range δ 75–123.

7.4.3 Heteroaromatic Compounds

As was true for the hydrogens attached to heteroaromatic rings and polycyclic aromatic hydrocarbons (Section 6.5), the carbons of such rings also appear in the aromatic region. Some examples are given below,¹ and these can be used as base values when calculating chemical shifts for substituted derivatives of these compounds:



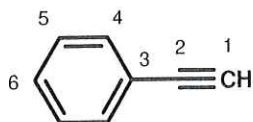


7.5 TRIPLY BONDED CARBONS

Recall (Section 6.4) that hydrogens attached to triply bonded carbons (*acetylenic* hydrogens) are unusually shielded because of the magnetic field anisotropy in the region of the triple bond. Exactly the same is true of acetylenic carbons themselves. Triply bonded (*sp*-hybridized) carbons usually appear in the δ 70–90 region, significantly upfield of typical vinyl and aromatic carbons. This is a region of the spectrum where relatively few other types of carbons are found. Acetylenic carbons are classified as either *terminal* (if they have a hydrogen directly attached) or *internal* (if they have a carbon attached). Signals for internal acetylenic carbons are usually downfield of and less intense than the signals for terminal ones. This is because of the deshielding effect of the carbon substituent (Table 7.2) and the absence of the intensity-increasing NOE (Section 5.4.1) due to the attached hydrogen.

■ **EXAMPLE 7.11** Propose a structure for the compound C_8H_6 whose ^{13}C spectrum exhibits signals at δ 77.4, 83.8 (the latter being only 20% as intense as the former), 122.4, 128.3, 128.7, and 132.2. Assign all signals by calculating expected chemical shifts.

□ **Solution:** The IOU is 6. We note immediately that there are four signals in the aromatic region and two in the acetylenic region. Thus, a likely candidate would be a monosubstituted aromatic ring with one acetylenic substituent:



Carbons 1 and 2 can be assigned on the basis of relative position and intensity (remember the NOE: fewer attached hydrogens, weaker signal) to the signals at δ 77.4 and 83.8, respectively. To assign the aromatic signals, let us predict where each should appear, with observed values:

$$\delta_3 = \delta(\text{benzene}) + \Delta\delta(-\text{C}\equiv\text{CH}, \alpha)$$

$$= 128.5 + (-5.8) = 122.7$$

$$\delta_4 = \delta(\text{benzene}) + \Delta\delta(-\text{C}\equiv\text{CH}, o)$$

$$= 128.5 + 6.9 = 135.4$$

$$\delta_5 = \delta(\text{benzene}) + \Delta\delta(-\text{C}\equiv\text{CH}, m)$$

$$= 128.5 + 0.1 = 128.6$$

$$\delta_6 = \delta(\text{benzene}) + \Delta\delta(-\text{C}\equiv\text{CH}, p)$$

$$= 128.5 + 0.4 = 128.9$$

The signals for carbons 5 (of which there are two) and 6 (of which there is one) are so close that assignments based on calculated chemical shifts alone are not likely to be 100% reliable. But notice that relative signal intensity is also consistent with the above assignment.

Look back at Example 6.18. Notice once again how the relative chemical shifts of the hydrogens parallel the relative chemical shifts of the carbons to which they are bonded. □

Another important triply bonded carbon is the one in a **cyano** group ($-\text{C}\equiv\text{N}$). Because of the higher electronegativity (and hence deshielding effect) of the nitrogen, cyano carbons occur downfield of acetylenic carbons, usually around δ 115–120. And remember: With no hydrogens attached, they usually give fairly weak signals.

Finally, in the quite unusual $-\text{C}\equiv\text{P}$ group, the carbon is deshielded to δ 185, while metal carbyne complexes ($\text{M}\equiv\text{C}-\text{R}$) are even further deshielded into the region δ 230–365. This indicates not only less shielding by the magnetic anisotropy of the CP triple bond (suggesting that there is less efficient circulation of the $\text{C}\equiv\text{P}$ triple bond electrons around the internuclear axis) but also paramagnetic deshielding by the phosphorus or metal atom.

7.6 CARBONYL CARBONS

Among the most deshielded carbon atoms are those that are doubly bonded to oxygen ($\text{C}=\text{O}$). Because of the high electronegativity of oxygen, carbonyl carbons generally appear in the δ 165–220 range. The carbonyl group occurs in many types of organic and organometallic compounds, and its ^{13}C chemical shift varies accordingly, as shown in Table 7.5. Because the regions characteristic of each functional group tend to overlap, one must usually consider the chemical shifts

TABLE 7.5 ^{13}C Chemical Shift Ranges of Carbonyl Compounds

Compound class	Structure	δ (ppm)
Ketone	$\text{R}-\text{C}(=\text{O})-\text{R}$	195–220
Aldehyde	$\text{R}-\text{C}(=\text{O})-\text{H}$	190–200
Carboxylic acid	$\text{R}-\text{C}(=\text{O})-\text{OH}$	170–185
Carboxylate ester	$\text{R}-\text{C}(=\text{O})-\text{OR}$	165–175
Anhydride	$\text{R}-\text{C}(=\text{O})-\text{O}-\text{C}(=\text{O})-\text{R}$	165–175
Amide	$\text{R}-\text{C}(=\text{O})-\text{NR}_2$	160–170
Acid halide	$\text{R}-\text{C}(=\text{O})-\text{X} (\text{X} = \text{Cl, Br, I})$	160–170
Metal-coordinated CO	$\text{M}-\text{C}=\text{O}$	150–285
Carbon monoxide	CO	183.4 ^a
Carbon dioxide	CO_2	124.8 ^b
Ketene	$\text{R}_2\text{C}=\text{C}=\text{O}$	See Table 7.6

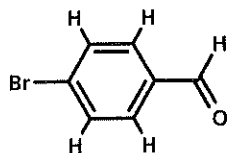
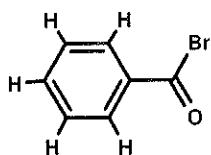
^aCO terminally coordinated to a metal in an organometallic complex ($\text{M}-\text{C}=\text{O}$) is usually deshielded and appears in the range δ 180–250 (ref. 5).

^b CO_2 -saturated CDCl_3 .

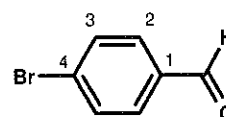
of the other carbons in order to suggest a unique structure for an unknown compound.

In addition to their characteristic downfield positions, carbonyl carbons can also be recognized by their relatively low intensity. Except in the case of a formyl carbonyl [one attached directly to a hydrogen, $-\text{C}(=\text{O})\text{H}$], there are no hydrogens attached to carbonyl carbons, so their signal cannot benefit from NOE enhancement. Carbonyl carbons also tend to have longer T_1 relaxation times than many other carbons, another cause of lower intensities in a signal-averaged pulsed-mode spectrum (Section 5.4.1).

■ **EXAMPLE 7.12** Which of the isomeric structures below has a ^{13}C spectrum consisting of signals at δ 190.6, 135.2, 132.3, 130.8, and 129.4? Assign all signals by correlating them with predicted chemical shifts:



□ **Solution:** It is easy to pick out the carbonyl signal; it is the one at δ 190.6. From Table 7.5 we can see that this signal is within the normal range for aldehydic carbons but too far downfield for an acid halide carbonyl. So, we pick the structure on the right:



$$\delta_1 = \delta(\text{benzene}) + \Delta\delta[-\text{C}(=\text{O})\text{H}, \alpha] + \Delta\delta(\text{Br}, p)$$

$$= 128.5 + 8.2 + (-1.0) = 135.7$$

$$\delta_2 = \delta(\text{benzene}) + \Delta\delta[-\text{C}(=\text{O})\text{H}, o] + \Delta\delta(\text{Br}, m)$$

$$= 128.5 + 1.2 + 2.2 = 131.9$$

$$\delta_3 = \delta(\text{benzene}) + \Delta\delta[-\text{C}(=\text{O})\text{H}, m] + \Delta\delta(\text{Br}, o)$$

$$= 128.5 + 0.6 + 3.4 = 132.5$$

$$\delta_4 = \delta(\text{benzene}) + \Delta\delta[-\text{C}(=\text{O})\text{H}, p] + \Delta\delta(\text{Br}, \alpha)$$

$$= 128.5 + 5.8 + (-5.4) = 128.9$$

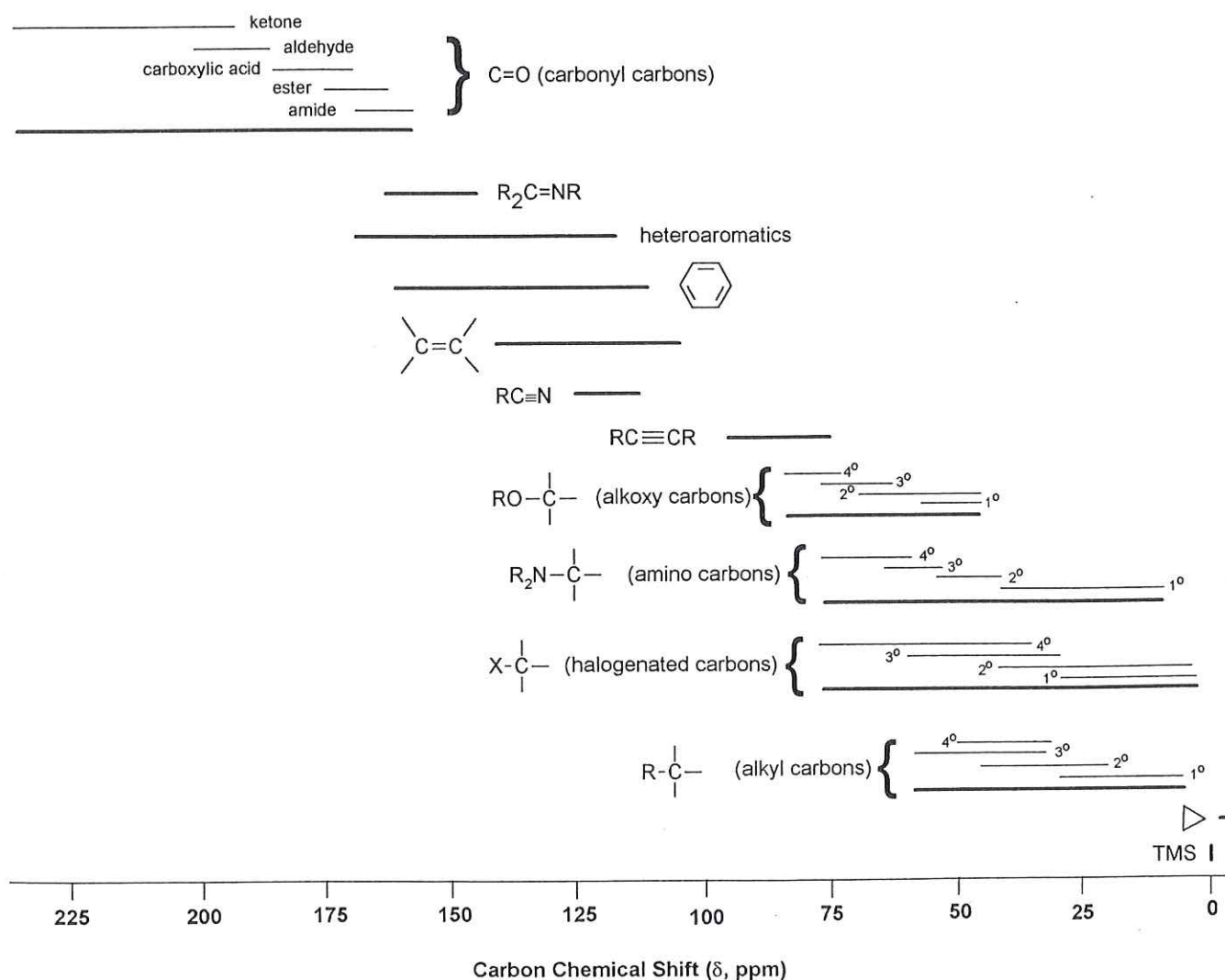
□

7.7 MISCELLANEOUS UNSATURATED CARBONS

There is a host of less common functional groups that involve unsaturated (i.e., multiply bonded) carbon and appear in the same downfield region of the ^{13}C spectrum as carbonyls, for example, the *central* (sp hybridized) carbon of an **allene** linkage ($\text{C}=\text{C}=\text{C}$). Such carbons give very weak signals

TABLE 7.6 ^{13}C Chemical Shifts of Other Functional Groups

Functional Group	Structure	$\delta(\text{ppm})$
Oxime	$\text{R}_2\text{C}=\text{N}-\text{OH}$	145–170
Isocyanate	$\text{R}-\text{N}=\text{C}=\text{O}$	110–135
Isothiocyanate	$\text{R}-\text{N}=\text{C}=\text{S}$	120–140
Metallo-carbene	$\text{M}=\text{CR}_2$	180–400
Carbenium ions	R_3C^+	212–320
Acylium ions	$\text{R}-\text{C}^+=\text{O}$	145–155
Carbon disulfide	$\text{S}=\text{C}=\text{S}$	192.3
Ketenes ^a	$\text{Z}_2\text{C}=\text{C}_\alpha=\text{O}$	$\text{Z} = \text{H, alkyl, aryl: } \alpha, 194\text{--}206; \beta, 2.5\text{--}48$
Ketenes ^a	$\text{Z}_2\text{C}=\text{C}_\alpha=\text{O}$	$\text{Z} = \text{heteroatom: } \alpha, 161\text{--}183; \beta, -20\text{--}125$

^aSee ref. 6.Figure 7.2. Pictorial representation of the ^{13}C chemical shift ranges for various classes of carbons.

(why?) in the δ 200–215 region. The two outer carbons, by contrast, are more shielded than typical vinyl carbons (Section 7.4) and appear in the δ 75–95 range. Table 7.6 lists some additional examples.

7.8 SUMMARY OF ^{13}C CHEMICAL SHIFTS

The range of ^{13}C chemical shifts is shown graphically in Figure 7.2. This is a useful place to start when trying to identify an unknown compound from its ^{13}C spectrum. But remember that these ranges represent only generalizations and that certain combinations of substituents will cause a carbon signal to show up outside the confines of its “normal” region.

Notice the similarity of Figure 7.2 with the corresponding one for hydrogen chemical shifts (Figure 6.8). This parallel behavior is because *in general* (there are exceptions) a carbon and the hydrogens attached directly to it both experience similar shielding and deshielding effects of neighboring substituents. To demonstrate the validity of this assertion, Figure 7.3 shows a plot of ^1H chemical shifts for 335 different hydrogens versus the ^{13}C chemical shifts of the carbons to which they are directly bonded.⁷ The linear relationship, expressed by Eqs. (7.1a) and (7.1b), exhibit a correlation coefficient of 0.95 over a wide variety of molecular environments:

$$\delta_{\text{H}} = 0.0479\delta_{\text{C}} + 0.472 \quad (7.1a)$$

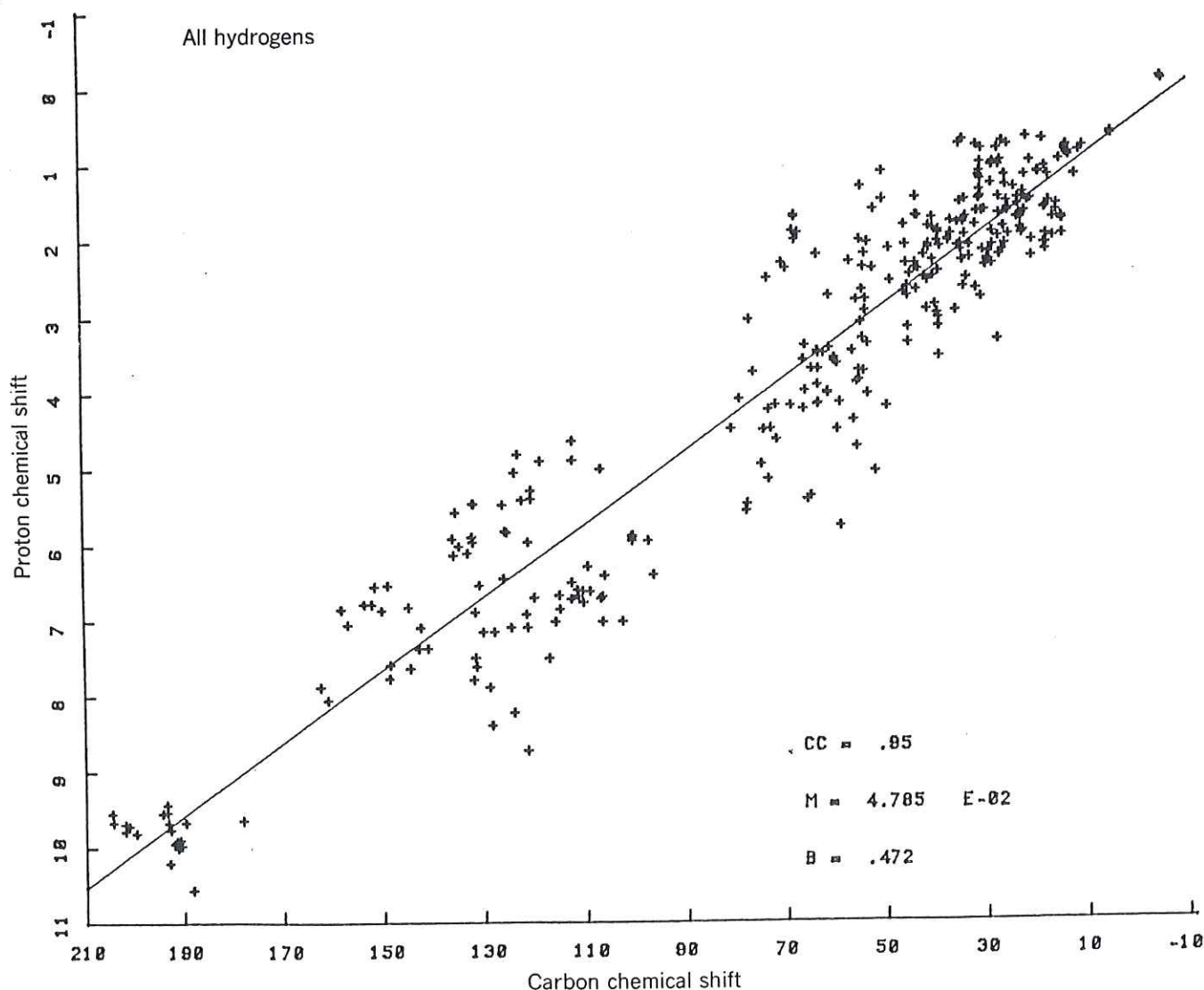


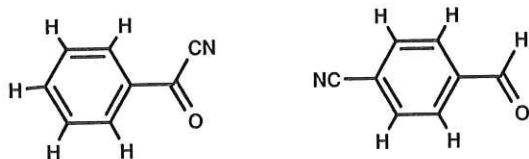
Figure 7.3. Graphical comparison of ^1H chemical shifts of C–H hydrogens versus the ^{13}C chemical shift of the attached carbon. [From “Proton–Carbon Chemical Shift Correlations,” by R. S. Macomber, *Journal of Chemical Education*, 68, 284–285 (1991). Reprinted with permission.]

$$\delta_{\text{C}} = 20.9\delta_{\text{H}} - 9.85 \quad (7.1b)$$

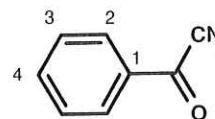
Thus, armed with only the ^1H spectrum of a molecule, one can estimate the chemical shift of the attached carbons (or vice versa) with a fair level of confidence.

■ **EXAMPLE 7.13** Suggest a structure for $\text{C}_8\text{H}_5\text{NO}$, whose ^{13}C spectrum exhibits signals at δ 112.9, 129.6, 130.3, 133.4, 136.9, and 167.8. Assign all signals by calculating the expected chemical shift of each carbon in your suggested structure.

□ **Solution:** The IOU for this compound is 7. There are six signals in this spectrum, indicative of some symmetry equivalences in the molecule. The four signals at δ 129.6, 130.3, 133.4, and 136.9 fall squarely in the aromatic carbon region, indicating either a monosubstituted benzene ring or one with two dissimilar groups para to each other. The signal at δ 167.8 is likely to be some sort of carbonyl carbon. But what kind of nitrogen-containing group would appear at δ 112.9? A cyano group! Now, see if you can put all this information into some tentative isomeric structures:



The structure on the left has a functional group we have not encountered previously, one with a cyano group attached directly to a carbonyl. It is somewhat like a ketone, whose carbonyls usually appear around δ 195–220, not δ 168. Similarly, the one on the right is an aldehyde, so its carbonyl carbon should appear around δ 190. For some reason our carbonyl signal must be unusually shielded. Perhaps the triple bond of the CN group can give rise to anisotropic shielding just like a carbon–carbon triple bond. Let us see how close the aromatic carbons in the left-hand structure come to our expectations, by treating the $-\text{C}(=\text{O})\text{CN}$ group as the closest analog to be found in Table 7.4, a $-\text{C}(=\text{O})\text{CH}_3$ group:



$$\delta_1 = \delta(\text{benzene}) + \Delta\delta[-\text{C}(=\text{O})\text{CH}_3, \alpha)$$

$$= 128.5 + 7.8 = 136.3$$

$$\delta_2 = \delta(\text{benzene}) + \Delta\delta[-\text{C}(=\text{O})\text{CH}_3, o)$$

$$= 128.5 + (-0.4) = 128.1$$

$$\delta_3 = \delta(\text{benzene}) + \Delta\delta[-\text{C}(=\text{O})\text{CH}_3, m)$$

TABLE 7.7 Representative ^{19}F Chemical Shifts^a

Compound	δ , ppm ^b	Compound	δ , ppm ^b
ClF	-441.5	CF_3H	-78.5
CH_3F	-275.4	CF_2ClH	-71.8
HF	-214.4	CF_4	-63.4
<i>trans</i> - $\text{FHC}=\text{CHF}$	-186	CF_3CN	-56.5
SiF_4	-167.6	CF_3Cl	-28.8
<i>Cis</i> - $\text{FHC}=\text{CHF}$	-165	CF_3Br	-18.2
CH_2F_2	-143.5	CF_2Cl_2	-7.0
$\text{F}_2\text{C}=\text{CF}_2$	-135.1	CF_3I	-4.0
BF_3	-131.6	CFCl_3	0
CH_3CHF_2	-110.8	ClO_2F	332.1
Ph-F	-106.3	F_2	428.4
$\text{O}=\text{PF}_3$	-92.6	XeF_4	446.6
C_2F_6	-87.4	FNO	485.6
$\text{H}_2\text{C}=\text{CF}_2$	-83.4	XeF_6	552.6
CFCl_2H	-80.7	FOOF	871.6

^aFrom ref. 8.

^bAll chemical shifts referenced to CFCl_3 .

$$= 128.5 + (-0.4) = 128.1$$

$$\delta_4 = \delta(\text{benzene}) + \Delta\delta[-\text{C}(=\text{O})\text{CH}_3, p)$$

$$= 128.5 + 2.8 = 131.3$$

Although the signal observed at δ 136.9 is assignable to C1, the remaining signals are difficult, if not impossible, to assign unambiguously among C2, C3, and C4. In Chapter 13 we will find ways to make more definite assignments. Just to set your mind at ease, the cyano-ketone structure above is the correct answer. This example demonstrates that in many real-life situations we have to use all the data at our disposal and still make some educated judgments. That, after all, is what makes life interesting! \square

7.9 CHEMICAL SHIFTS OF OTHER ELEMENTS

As stated in Chapters 2 and 5, the applications of NMR extend well beyond just hydrogen and carbon, although these two are arguably among the most commonly studied. Other nuclei subjected to *routine* NMR examination include ^2H , ^{14}N , ^{19}F , and ^{31}P ; scores of others are studied somewhat less routinely. For several of these nuclei, semiempirical chemical shift correlations of the type we have seen for ^1H and ^{13}C have been generated. In addition, there are several computer software packages now available that use these types of correlations to estimate the hydrogen and carbon chemical shifts for virtually any structure input to the program.

Table 7.7 lists the ^{19}F chemical shifts for a variety of fluorine-containing compounds; notice that these values span a range of 1300 ppm! Figures 7.4 and 7.5 show, respectively, the chemical shift ranges for ^{31}P (data from ref. 9) and ^{14}N

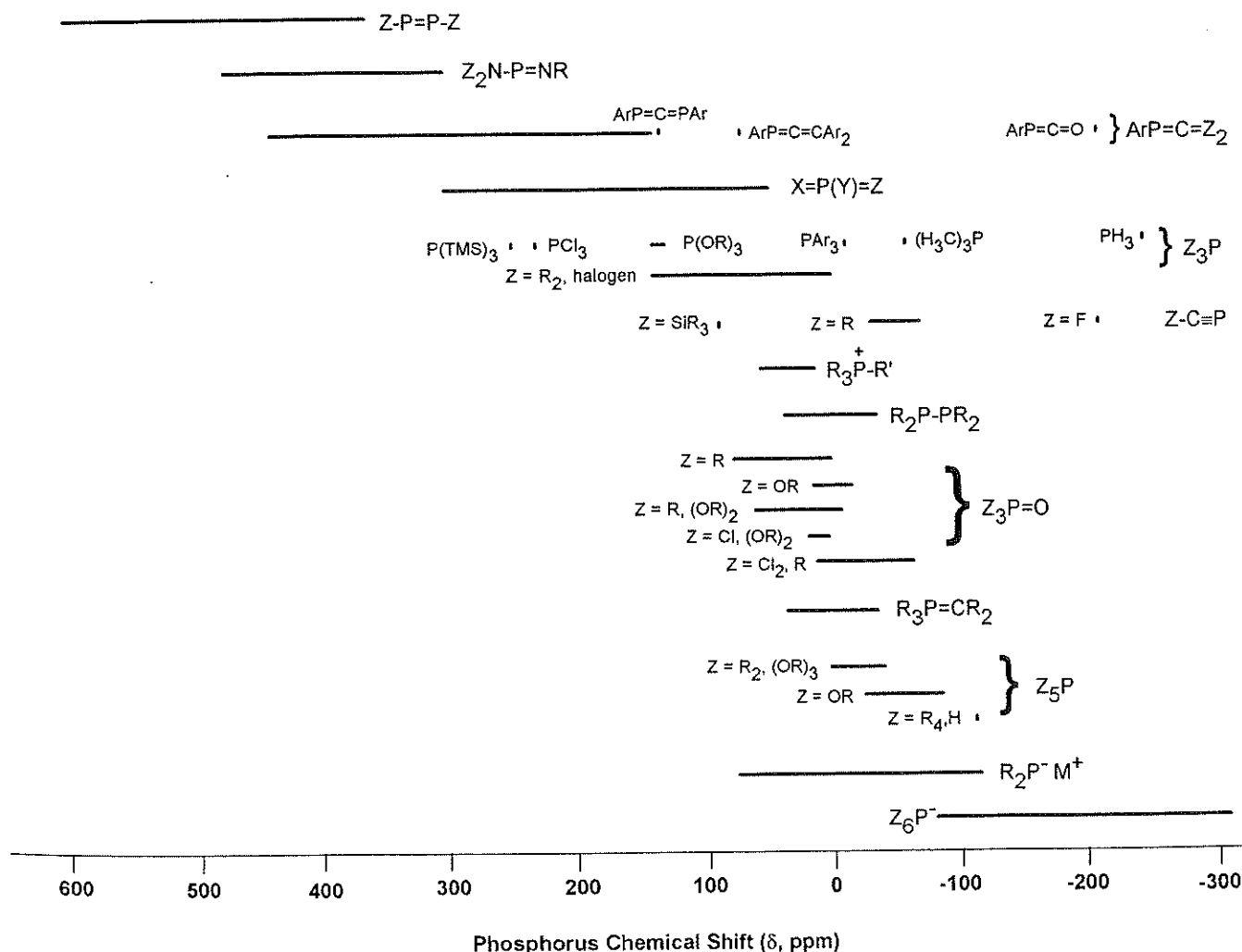


Figure 7.4. Pictorial representation of the ^{31}P chemical shift ranges for various classes of phosphorus atoms. Chemical shifts are referred to 85% H_3PO_4 .

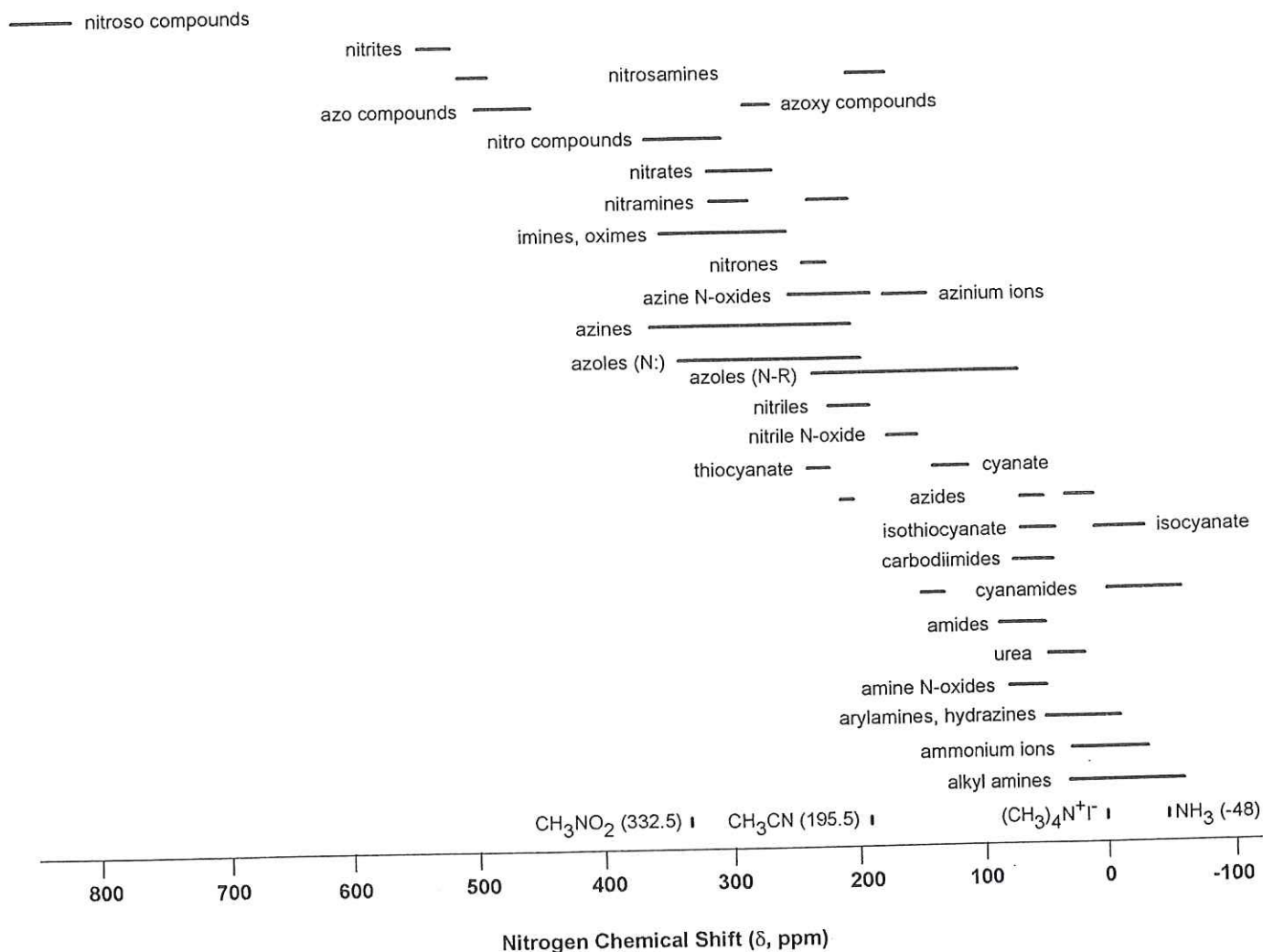


Figure 7.5. Pictorial representation of the ^{14}N chemical shift ranges for various classes of nitrogen atoms. Chemical shifts are referred to $(\text{CH}_3)_4\text{N}^+\text{I}^-$.

(data from ref. 10); both span ranges of more than 900 ppm. Compare these chemical shift ranges with those for ^1H (20 ppm) and ^{13}C (less than 400 ppm).

CHAPTER SUMMARY

1. Carbon atoms in molecules are classified, as are hydrogens, on the basis of the structural unit of which they are a part: tetrahedral (methyl, methylene, methine, or quaternary), trigonal (e.g., vinyl, aromatic, or carbonyl), and triply bonded (e.g., acetylenic).
2. Because of the low natural abundance and low sensitivity of ^{13}C , the acquisition of carbon NMR spectra requires the use of signal-averaged pulsed-mode meth-

ods. Further simplification is afforded by applying ^1H decoupling.

3. The chemical shift of each carbon in a molecule can be predicted accurately by the same type of correlations used for hydrogens, namely, an appropriate base value plus substituent parameters [Eq. (6.5b)].
4. There is a consistent parallel between the relative order of hydrogen chemical shifts and the order of chemical shifts of the carbons to which they're attached.

REFERENCES

- ¹Silverstein, R. M., Bassler, G. C., and Morrill, T. C., *Spectrometric Identification of Organic Compounds*, 5th ed., Wiley, New York, 1991.

- ²Simons, W. W., Ed., *The Sadtler Guide to Carbon-13 NMR Spectra*, Sadtler Research Laboratories, Division of Bio-Rad Laboratories, Philadelphia, 1983.
- ³Johnson, L. F., and Jankowski, W. C., *Carbon-13 NMR Spectra*, Krieger, Huntington, NY, 1978.
- ⁴Cooper, J. W., *Spectroscopic Techniques for Organic Chemists*, Wiley, New York, 1980.
- ⁵Kegley, S. E., and Pinhas, A. R., *Problems and Solutions in Organometallic Chemistry*, University Science Books, Mill Valley, CA, 1986.
- ⁶Tidwell, T. T., *Ketenes*, Wiley, New York, 1995.
- ⁷Macomber, R. S., *J. Chem. Educ.*, 68, 284 (1991).
- ⁸Mason, J., Ed., *Multinuclear NMR*, Plenum, New York, 1987.

- ⁹Verkade, J. G., and Quin, L. D., Ed., *Phosphorus-31 NMR Spectroscopy in Stereochemical Analysis. Organic Compounds and Metal Complexes*, VCH Publishers, New York, 1987.
- ¹⁰Witanowski, M., and Webb, G. A., Ed., *Nitrogen NMR*, Plenum, New York, 1973.

REVIEW PROBLEMS (Answers in Appendix I)

- 7.1. Why are aromatic carbons only slightly more deshielded than vinyl carbons, whereas aromatic hydrogens are considerably more deshielded than vinyl hydrogens.

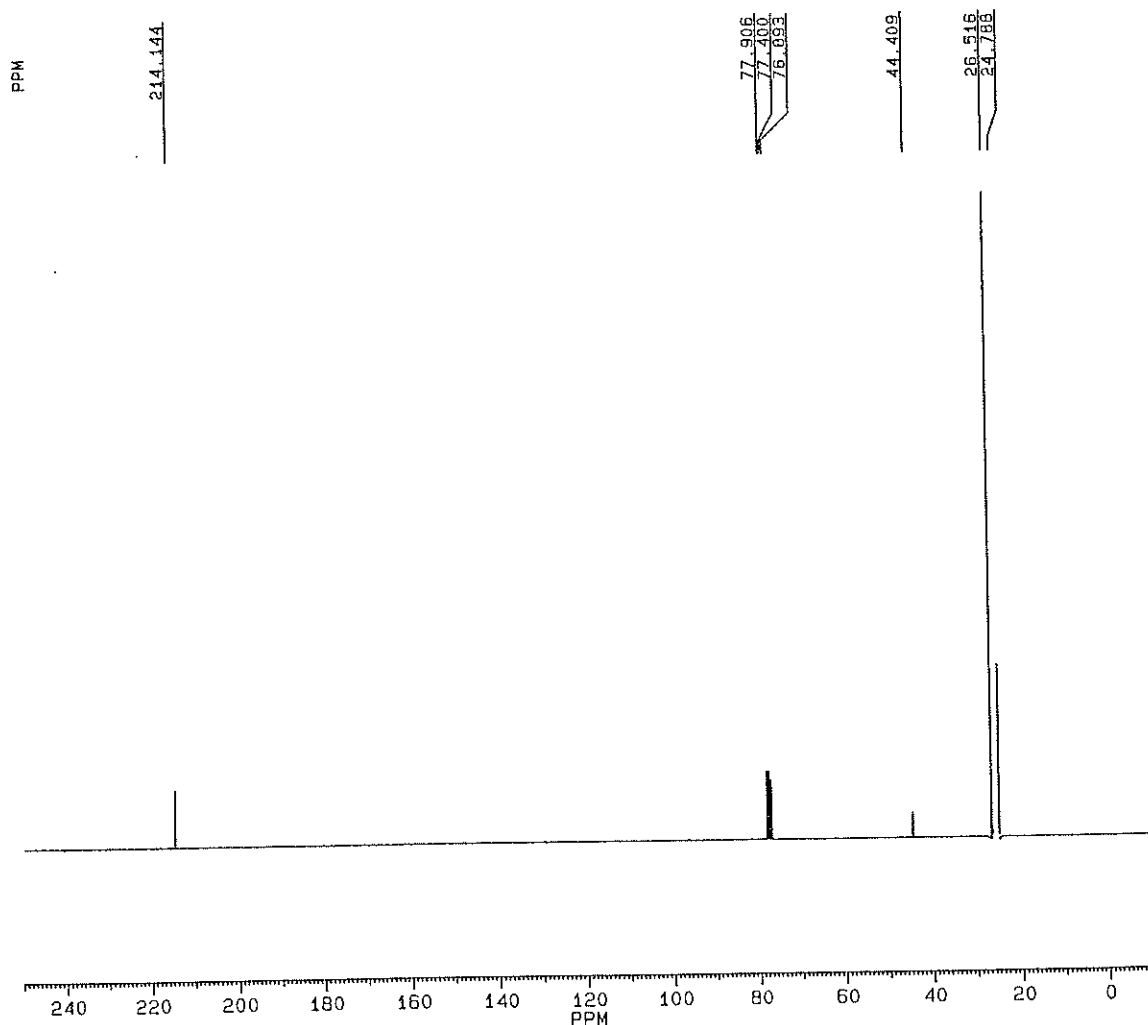


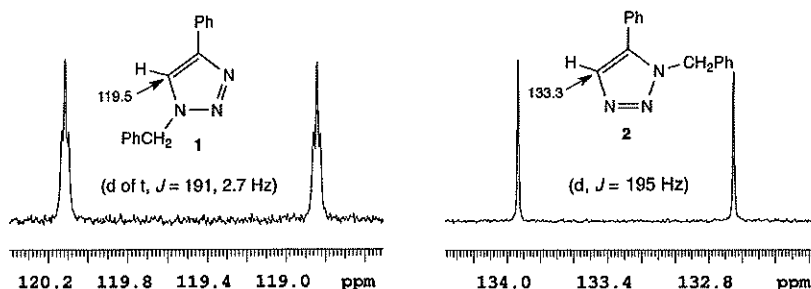
Figure 7.6. The 62.5-MHz ¹³C spectrum of C₆H₁₂O [Review Problem 7.6(a)].

Method for Assigning Structure of 1,2,3-Triazoles

Xavier Creary,* Andrew Anderson, Carl Brophy, Frances Crowell, and Zachary Funk

Department of Chemistry and Biochemistry, University of Notre Dame, Notre Dame, Indiana 46556, United States

Supporting Information



ABSTRACT: 1,4-Disubstituted-1H-1,2,3-triazoles **1** can easily be distinguished from the isomeric 1,5-disubstituted-1H-1,2,3-triazoles **2** by simple one-dimensional ^{13}C NMR spectroscopy using gated decoupling. The C_5 signal of **1** appears at δ ~120 ppm, while the C_4 signal of **2** appears at δ ~133 ppm. Computational studies also predict the upfield shift of C_5 of **1** relative to C_4 in **2**.

Triazoles are a class of compounds of much recent interest. They are generally prepared by cycloaddition reactions of azides with alkynes. The original thermal cycloaddition reaction discovered by Huisgen¹ has been largely supplanted by copper-catalyzed reactions of azides with alkynes, which give 1,4-disubstituted-1H-1,2,3-triazoles of general structure **1**.^{2,3} References to this copper-catalyzed reaction, since Sharpless first introduced the concept of the “Click Reaction” in 2001,⁴ are too numerous to list. Hence, a few general reviews are given.⁵ The regioisomeric 1,5-disubstituted-1H-1,2,3-triazoles **2** can often be prepared by a ruthenium-catalyzed reaction,⁶ or by addition of acetylide anions to azides.⁷ The structures of many of these triazoles were proven by X-ray crystallographic analysis^{2,6} or by more sophisticated NMR methods including NOE,^{2,3} HMQC, HSQC, and HMBC⁸ studies. While structures of triazoles in the Sharpless/Fokin studies and in certain other studies have been rigorously demonstrated, in many subsequent studies in the literature, the structures of triazoles are not “proven” but are simply assigned using the assumption that Cu catalysis gives isomers of type **1**, while Ru catalysis gives type **2** isomers. While these assumptions are most likely correct, a simple method for verification of structure is desirable.

X-ray, NOE, and multidimensional NMR techniques are powerful methods for structure elucidation. However, they are not always routine, rapid, simple, or inexpensive techniques. As part of another investigation, we have generated a number of isomeric triazoles for mechanistic studies. We therefore wanted a simple protocol for rapidly distinguishing between the isomeric triazoles **1** and **2**. We now report that structures can be easily assigned from simple 1-dimensional ^{13}C NMR data.

Figure 1 shows an expanded region of the ^{13}C NMR spectrum of triazole **1a** prepared by a Cu catalyzed reaction. Spectrum A is the standard proton decoupled spectrum, while

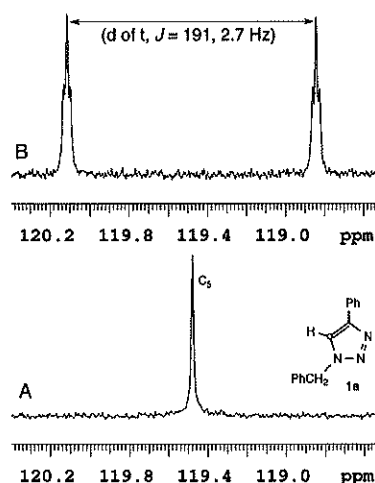


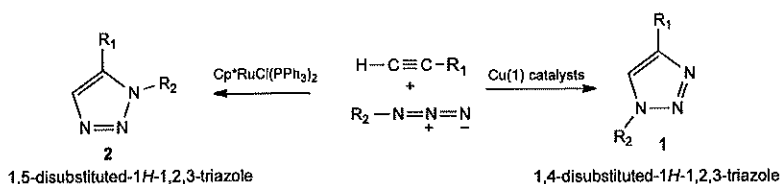
Figure 1. (A) Expanded ^{13}C NMR of **1a**. (B) ^1H coupled ^{13}C NMR of **1a**.

spectrum B uses the relatively old and simple gated decoupling sequence (decoupler off during acquisition), where coupling to neighboring hydrogens is observed. Identification of the C_5 carbon signal of **1a** is straightforward due to the relatively large C–H coupling constant of 191 Hz. The corresponding C–H coupling constants for aromatic carbons are much smaller (~155 Hz). The doublet of triplets ($J = 191, 2.7$ Hz) at δ 119.5 is due to the C_5 carbon coupled to the directly bonded hydrogen and 3-bond coupled to the two benzylic hydrogens.

Received: June 27, 2012

Published: August 15, 2012





This rapid “low tech” experiment gives the same coupling information as the more tedious HMQC and HMBC methods. It also gives precise values of coupling constants, which are used to readily assign the C_5 signal. The single frequency decoupled spectrum (not shown), where the benzylic hydrogens at $\delta = 5.57$ ppm in the ^1H NMR spectrum are irradiated, confirms that the triplet is due to long-range coupling to the benzylic hydrogens. This verifies that the carbon signal at $\delta = 119.5$ is indeed due to the C_5 carbon of 1a.

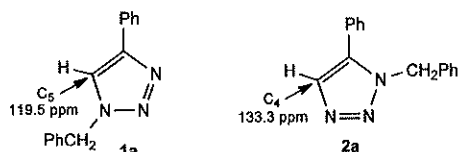


Figure 2 shows an expanded region of the ^{13}C NMR spectrum of the isomeric triazole 2a. The signal at $\delta = 133.3$

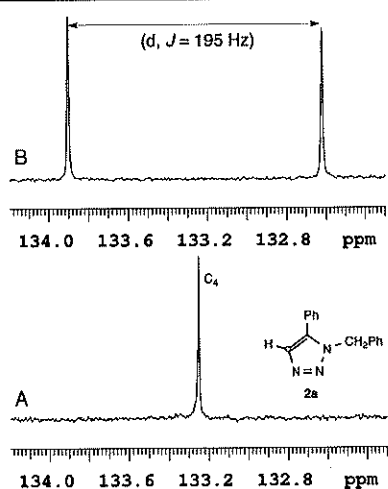


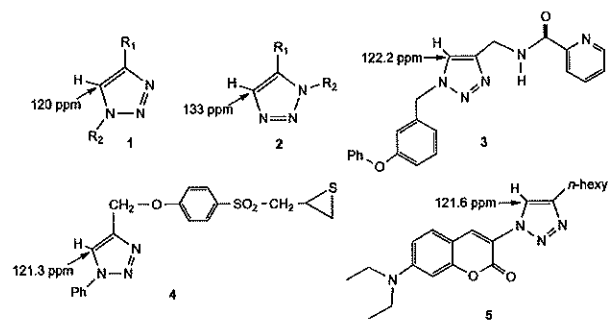
Figure 2. (A) Expanded ^{13}C NMR of 2a. (B) ^1H coupled ^{13}C NMR of 2a.

ppm is due to the C_4 carbon, and this is confirmed by the gated decoupling experiment that shows a doublet ($J = 195$ Hz) due to the directly attached hydrogen. The 4-bond coupling to the benzylic hydrogens is not observed. These ^{13}C spectra are easy to acquire and may be obtained in less than one hour using routine techniques.

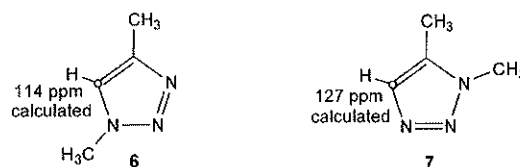
We have now prepared and analyzed the 19 pairs of triazoles in Table 1 by these simple ^{13}C NMR methods. In all of these triazoles, the C_5 carbon of 1 is always further upfield than the C_4 carbon of 2. The average chemical shift of C_5 for triazoles 1a–1o is $\delta = 120 \pm 3$ ppm, while the shift of C_4 is $\delta = 133 \pm 3$ ppm for 2a–2o. The previously reported triazoles 3,⁹ 4,¹⁰ and 5¹¹ (whose structures were based solely on the copper-catalyzed synthetic method) have also been analyzed, and the C_5 shifts also fall within the $\delta = 120 \pm 3$ ppm range.

Table 1. ^{13}C Shifts of C_5 of Triazole 1 and C_4 of Triazole 2

substrates	R_1	R_2	C_5 of 1 (ppm)	C_4 of 2 (ppm)
1a/2a	Ph	PhCH ₂	119.5	133.3
1b/2b	Ph	<i>n</i> -hexyl	119.2	133.0
1c/2c	<i>n</i> -Bu	PhCH ₂	120.4	132.5
1d/2d	<i>n</i> -Bu	<i>n</i> -hexyl	120.3	131.9
1e/2e	CH ₂ OAc	PhCH ₂	123.6	135.3
1f/2f	C(OH)Me ₂	PhCH ₂	119.0	130.9
1g/2g	Ph	Ph	117.6	133.4
1h/2h	<i>n</i> -Bu	Ph	118.8	132.3
1i/2i	C(OH)Ph ₂	<i>n</i> -hexyl	122.3	134.8
1j/2j	CH ₂ OPh	PhCH ₂	122.6	134.6
1k/2k	Ph	PhCOCH ₂	121.5	132.9
1l/2l	Ph	cyclohexyl	117.3	132.6
1m/2m	<i>n</i> -Bu	cinnamyl	120.3	132.4
1n/2n	CH(OEt) ₂	PhCH ₂	121.8	134.9
1o/2o	CH ₂ OH	PhCH ₂	121.6	136.3
1p/2p	CHO	PhCH ₂	125.1	141.2
1q/2q	CO ₂ Et	PhCH ₂	127.3	138.2
1r/2r	COCH ₃	PhCH ₂	125.2	138.6
1s/2s	OEt	PhCH ₂	105.9	113.8



Computational Studies. While ^{13}C chemical shifts of the C_5 and C_4 carbons of 1 and 2 appear to be a reliable empirical method of assigning structure, we sought a theoretical basis for these shifts. GIAO calculated shifts¹² (B3LYP/6-31G* level) of C_5 and C_4 for compounds 6 and 7 are $\delta = 114$ and 127 ppm, respectively. These calculated values are about 6 ppm upfield from the experimental values for 1 and 2. However, there is still a large difference (13 ppm) between C_5 of 6 and C_4 of 7. This calculated difference is completely consistent with the experimental findings.



Why is the C_5 carbon in isomer 1 further upfield than C_4 in isomer 2? A valence bond approach can rationalize this observation. While there are a number of resonance contributors in 1, consider the important form 1y (which

ΠΑΡΑΡΤΗΜΑ

(NMR-1 – NMR-10 & Π1 – Π9)

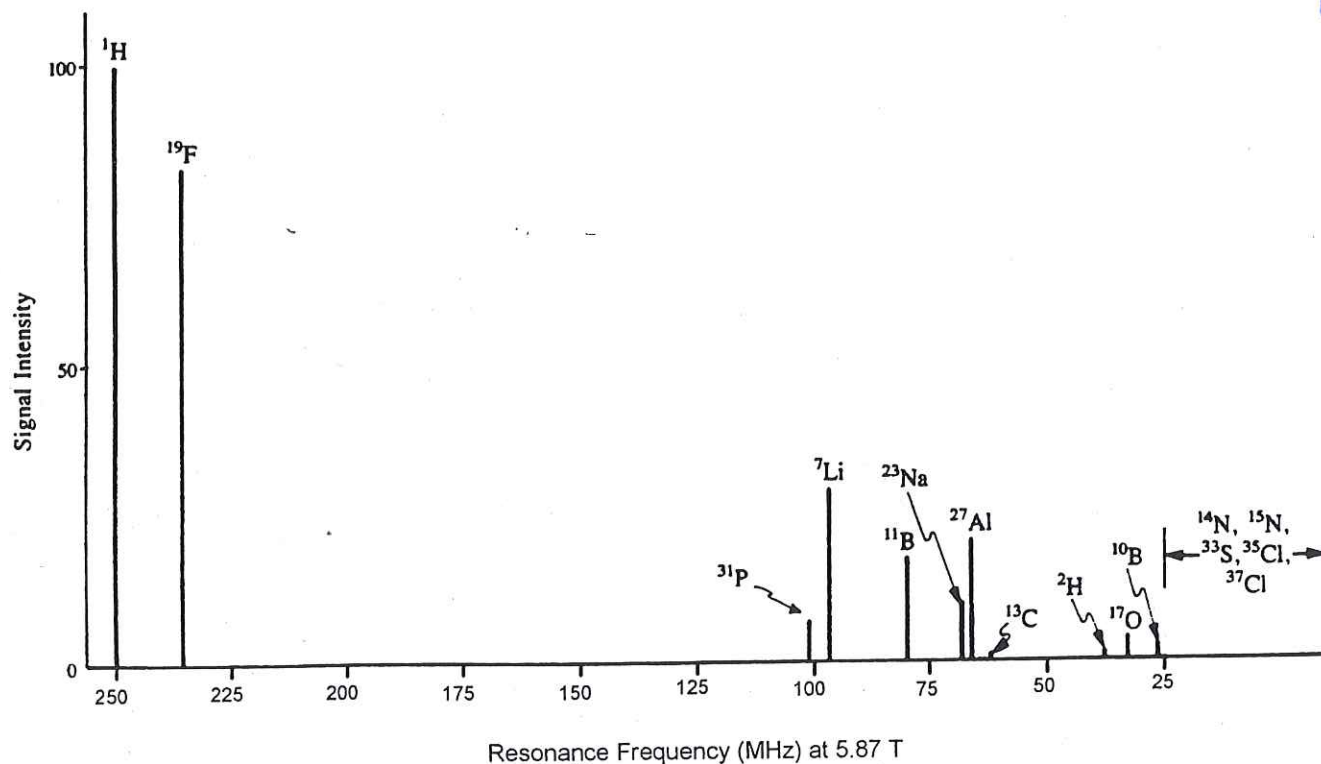


Figure 3.7. Resonance frequencies and relative sensitivities of several common isotopes at 5.87 T; compare with Table 2.1.

From the discussion in Section 3.2, it is clear that the field strength of any type of electromagnet can only be varied within an extremely narrow range. This means that the nominal operating frequency for, say, ^1H nuclei is also fixed. (In fact, the model number of most commercial NMR spectrometers is the same as the ^1H operating frequency in megahertz.) Since, for a given instrument, we cannot change B_0 , the only way to investigate nuclei other than ^1H is to switch to a different rf oscillator (B_1 source) with a frequency appropriate for the specific nucleus of interest (e.g., ^{13}C or ^{31}P). In the old days, switching oscillator circuits could be a rather tedious process, but these days it requires little more than pushing a few buttons or typing a few commands into the computer that controls the instrument.

However, as we will see in Chapter 5, the real value of NMR does not come from generating one signal for each isotope present in the sample (e.g., one signal each for ^1H , ^{13}C , or ^{31}P). Rather, we will find that even the individual nuclei of the same isotope in different molecular environments can precess at *slightly different* frequencies (on the order of parts per million), and these small differences can tell us much about the details of the molecular structure involved. Thus, we normally examine only one isotope (e.g., ^1H) in each NMR spectrum; that is, each spectrum is **homonuclear**. Since we are examining only one isotope at a time, we only have to

vary the magnetic field (field sweep) or rf frequency (frequency sweep) over narrow limits to see all of the nuclei of that specific target isotope. All older NMR spectrometers, equipped with conventional electromagnets, used either field- or frequency-sweep technology. Because both involved continuous operation of the rf (B_1) oscillator, they were both referred to as continuous-wave (cw) techniques.

3.3.1 Frequency-Sweep Mode

In the case of a frequency-sweep cw experiment, the magnetic field strength (B_0) was fixed. Suppose our sample contained two different nuclei (A and B) characterized by slightly different resonance frequencies, with $\nu_A > \nu_B$. The spin state energies of these two nuclei are depicted in Figure 3.8a. In order for nuclei A and B to generate resonance signals, Eq. (2.7) requires they be irradiated with B_1 frequencies given by

$$\nu_A = \frac{\Delta E_A}{h} \quad (3.2a)$$

$$\nu_B = \frac{\Delta E_B}{h} \quad (3.2b)$$

$$\Delta E = h\nu = \frac{\gamma h B_0}{2\pi}$$

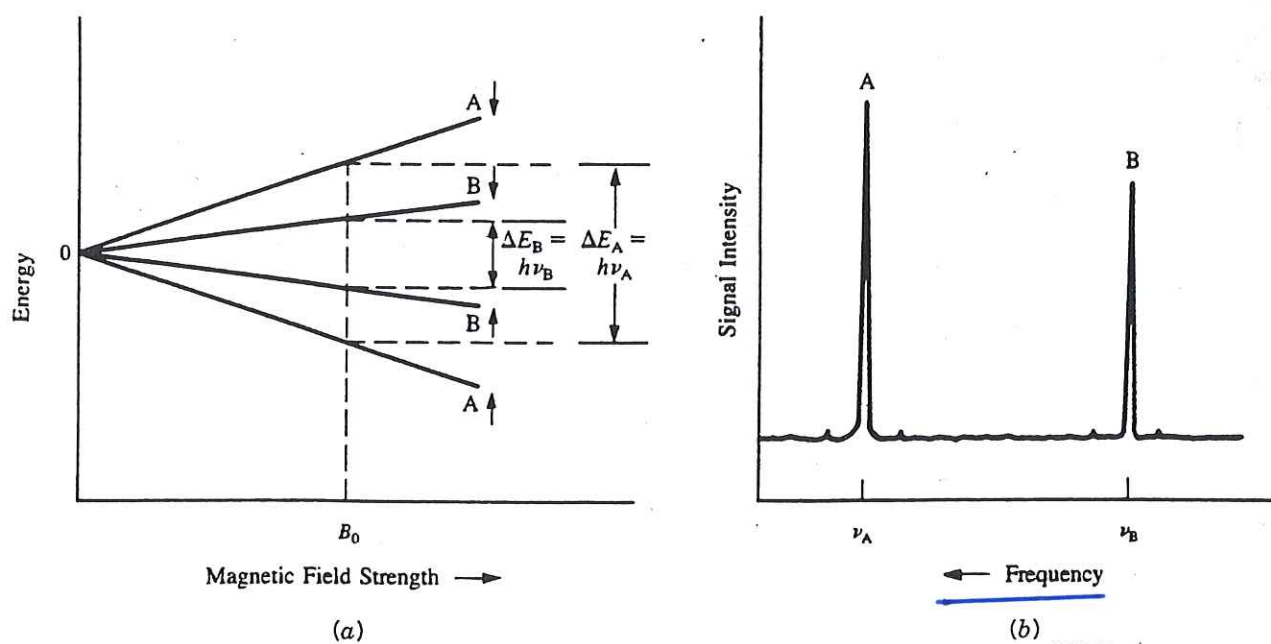


Figure 3.8. (a) Spin state energy gaps (ΔE) for two different nuclei at field strength B_0 . (b) Resulting frequency-sweep NMR spectrum.

Thus, it was necessary to sweep the operating frequency over the range ν_A to ν_B (or vice versa) using a *variable-frequency* rf transmitter. This *range* of frequencies ($\nu_A - \nu_B$) is called the **spectral width** (or sweep width), SW, of the spectrum and was limited to about 2000 Hz. Beginning at a frequency a little less than ν_B , the frequency of the continuous rf radiation was gradually increased to a value above ν_A while the receiver circuit was constantly monitored for a signal. As the frequency passed first through ν_B , then through ν_A , two separate signals were detected. A plot of the intensity of these signals versus frequency (Figure 3.8b) is our first **frequency-domain** NMR spectrum, with frequency increasing from *right to left* (as is the convention).

3.3.2 Field-Sweep Mode

Although some early NMR spectrometers did employ the frequency-sweep (at constant field) technique, it turned out to be electronically simpler to maintain the constant B_1 oscillator frequency appropriate for the target isotope and sweep (vary) the magnetic field to achieve resonance for the nuclei in the sample. By passing a slowly increasing direct current through **sweep coils**, the magnetic field B_0 could be varied through a limited range while maintaining its homogeneity in the sample area. Let us investigate how this change affected the spectrum.

Because the operating radio frequency (ν_0) was now constant, only photons of energy $h\nu_0$ were available in the experi-

ment [see Eq. (1.3)]. Thus, the *energy gap* [ΔE , Eq. (2.4)] for *each* nucleus had to be adjusted by varying the magnetic field strength B_0 . By rearranging Eq. (2.7), we can solve for the field strength at which nuclei A and B entered resonance:

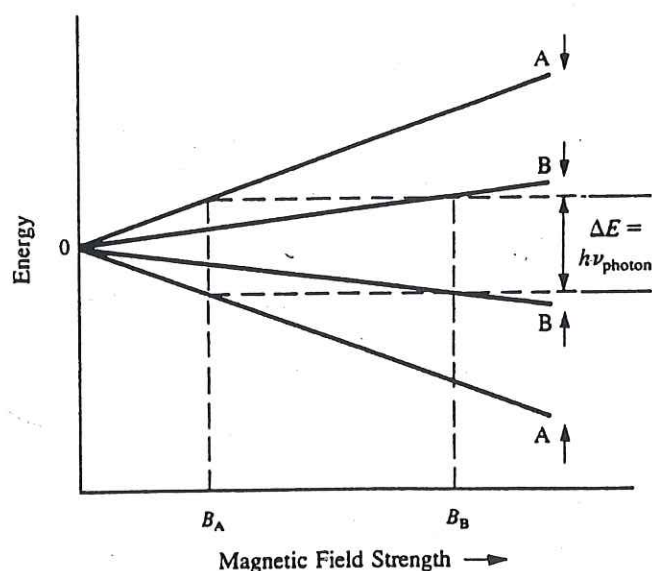
$$B_A = \frac{2\pi\nu_0}{\gamma_A} \quad (3.3a)$$

$$B_B = \frac{2\pi\nu_0}{\gamma_B} \quad (3.3b)$$

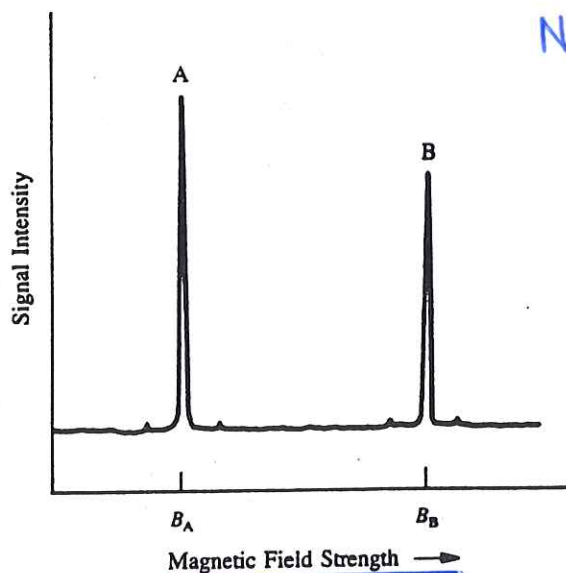
Figure 3.9a depicts the situation graphically. This time, instead of varying the B_1 frequency until it matched the precessional frequencies of nuclei A and B, we varied the precessional frequencies (by varying the field strength) until they matched the B_1 frequency. Most importantly, the resulting spectrum (Figure 3.9b) was *indistinguishable* from the frequency-sweep spectrum, except that the abscissa was calibrated in magnetic field units increasing from *left to right*.

Comparing Figure 3.8b with Figure 3.9b reveals that nucleus A enters resonance at a higher frequency (at constant field) or at a lower field (at constant frequency) than does nucleus B. For this reason, the right-hand (low-frequency) side of an NMR spectrum is often referred to as the high-field (or upfield) side, while the left-hand (high-frequency) side is called the low-field (or downfield) side.

$$\Delta E = h\nu = \frac{\hbar \gamma B_0}{2\pi}$$



(a)



(b)

Figure 3.9. (a) The B_0 field strength required for two different nuclei to attain the same spin state energy gap ΔE . (b) Resulting field-sweep NMR spectrum.

■ **EXAMPLE 3.4** Suppose that, at a nominal field strength of 2.35 T, NMR signals were detected at 100 and 25.2 MHz. (a) What are the two isotopes giving rise to the signals? (b) If the spectrum were obtained by the field-sweep method, what field strength would be required to observe the latter signal using an operating frequency of 100 MHz?

□ **Solution:** (a) By referring back to the ν column in Table 2.1, we see that isotopes are ^1H and ^{13}C , respectively. (b) Use Eq. (3.3) and the value of γ for ^{13}C from Table 2.1:

$$B_{\text{C-13}} = \frac{2\pi\nu_0}{\gamma_{\text{C-13}}} = \frac{2(3.14 \text{ rad})(100 \times 10^6 \text{ s}^{-1})}{67.3 \times 10^6 \text{ rad T}^{-1} \text{ s}^{-1}} = 9.33 \text{ T}$$

It is impossible for an NMR electromagnet designed for 2.35 T to produce a 9.33-T field! □

3.3.3 Spinning Sidebands and the Signal-to-Noise Ratio

A closer examination of the signals in Figures 3.8b and 3.9b brings up some additional points. Figure 3.10 is an enlargement of one of the peaks. Notice the two small signals symmetrically flanking the large signal. These so-called **sidebands** or **satellite peaks**, marked with asterisks in the figure, are an unavoidable result of spinning the sample to improve field homogeneity (Section 3.2.1). If the field has been well shimmed, such **spinning sidebands** rarely exceed 1% of the height of the main peak. Moreover, they will always be

separated from the main peak by *exactly* the spin rate in hertz. This is, in fact, the most direct way to measure the sample spin rate. One can, of course, completely eliminate spinning sidebands by turning off the spinner. But this would cause substantial broadening of the signal (with an accompanying decrease in signal height) because of the small inhomogeneities present in the magnetic field.

■ **EXAMPLE 3.5** Suppose the two sidebands in Figure 3.10 are each separated from the main peak by 58 Hz. (a) What

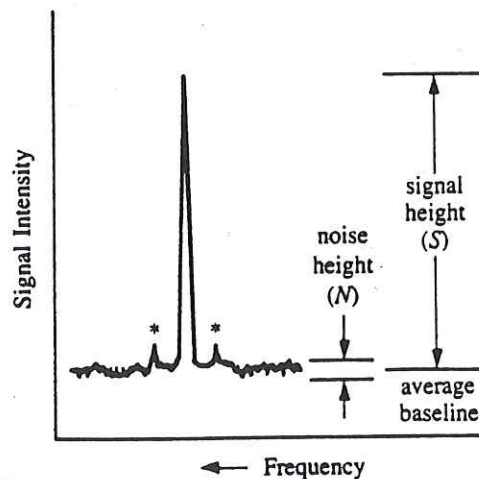


Figure 3.10. An NMR signal peak showing sidebands (*) and signal (S) to noise (N) ratio.

is the spin rate of the sample tube? (b) How could you confirm that these peaks were indeed spinning sidebands and not due to something else?

- **Solution:** (a) Because the frequency separation of a sideband from the main peak is equal to the spin rate, the latter must also be 58 Hz. (b) Varying the spin rate (by adjusting an air flow directed at the spinner paddle) causes spinning sidebands to shift position accordingly. If the peaks do not shift position, they are not spinning sidebands. There are other types of satellite peaks that we will encounter later. □

You will also notice in Figure 3.10 that the signal baseline is not perfectly flat. Instead, there is perceptible random background noise causing a continuous wiggle in the baseline. Even in the most carefully built and tuned spectrometers there will always be some electronic noise generated by the various circuits within the instrument, and the way the signal data are processed. Normally, this does not present a problem, provided the sample gives signals strong enough to be easily differentiated from the noise. But what about really weak signals? For example, a sample of natural hydrogen (Table 2.1) contains 99.985% ^1H with a relative sensitivity of 1.00, while a sample of natural carbon contains only 1.1% ^{13}C , which has a relative sensitivity of 1.59×10^{-2} . These two factors, low natural abundance and low relative sensitivity, combine to make the carbon signal only about 2×10^{-4} times as intense as a hydrogen signal for equal numbers of atoms of each element. Thus, a ^{13}C signal is much harder to distinguish from noise than is a ^1H signal.

To deal with this problem, we define a quantity called **signal-to-noise ratio** (S/N), where S and N are approximated by their respective peak heights, as shown in Figure 3.10.

■ **EXAMPLE 3.6** Using a ruler, estimate S/N in Figure 3.10.

- **Solution:** The exact values of S and N will depend on the scale of your ruler. But the ratio of the two numbers, S/N , should be about 20. □

The goal in an NMR experiment is to maximize S/N , and this can be achieved in several ways. One method is to use higher rf power and a series of rf filters to remove some of the noise. While this technique results in some improvement, care must be taken to avoid saturation problems (see Section 2.3). A far better improvement can be obtained by relying on a result of the **central limit theorem** from information theory. This theorem tells us that if the spectrum is scanned n times and the resulting data are added together, signal intensity will increase directly with n while noise (being random) will only increase by \sqrt{n} :

$$\left(\frac{S}{N}\right)_n = \left(\frac{S}{N}\right)_1 \left(\frac{n}{\sqrt{n}}\right) = \left(\frac{S}{N}\right)_1 \sqrt{n} \quad (3.4)$$

where $(S/N)_1$ is the ratio after a single scan. Thus, S/N improves linearly with \sqrt{n} .

To make use of this multiple-scan technique, we first need an extremely stable field. Then we need a computer to collect the signal data (digitally) from each scan, add the data together, and then divide the sum by n . The technique is known as **signal averaging** or **CAT** (computer-averaged transients, not to be confused with the diagnostic X-ray technique called *computer-aided axial tomography*). Because each scan of an older cw instrument could require 10 or more minutes, this process used to take hours, during which time the magnetic field had to be kept as perfectly stable and homogeneous as possible. A momentary flicker in the building power during an overnight experiment could cause all the data to be useless.

■ **EXAMPLE 3.7** A single 10-min cw NMR scan of a certain highly dilute sample exhibited S/N of 1.9. How much time would be required to generate a spectrum with S/N of 19?

- **Solution:** We can rearrange Eq. (3.4) to calculate the required number of scans:

$$\sqrt{n} = \frac{(S/N)_n}{(S/N)_1} = \frac{19}{1.9} = 10$$

$$n = 10^2 = 100$$

The time required for 100 scans is

$$t = (100 \text{ scans})(10 \text{ min per scan})$$

$$= 1000 \text{ min} = 16 \text{ h } 40 \text{ min}$$

No sleep tonight! □

3.4 THE MODERN PULSED MODE FOR SIGNAL ACQUISITION

Further improvement in S/N had to await the development of faster computer microprocessors, which was exactly what happened during the 1980s. Armed with very fast and efficient microcomputers with large memories, chemists discovered they could now generate NMR signals in an entirely new way.

Have you ever been sitting in a quiet room when suddenly a fixed pitch noise (sound waves) causes a nearby object to vibrate in sympathy? This is an example of acoustic resonance, in which the frequency of the sound waves exactly matches the frequency with which the object naturally vibrates. If the pitch of the sound changes, the resonance ceases.

This is because only when the two frequencies match can the sound waves *constructively* interfere (reinforce) the motion of the object. At any other frequency the interaction will be one of *destructive* interference and the net result will be no vibration by the object. This is exactly analogous to the continuous-wave NMR experiment. But have you not also heard how a single loud sound such as a sonic boom can set many different objects vibrating for a long period after the boom is over? This occurs because the brief sound pulse acts as though it is a mixture of all audible frequencies. Might it also be possible to generate NMR signals this way?

In a **pulsed-mode** NMR experiment, which is performed at both constant magnetic field and constant rf frequency, rf radiation is supplied by a brief but powerful computer-controlled pulse of rf current through the transmitter coil. This "monochromatic" (single-frequency) pulse, centered at the operating frequency ν_0 , is characterized by a power (measured in watts and controlling the magnitude of \mathbf{B}_1) and a **pulse width** (t_p), the duration of the pulse measured in microseconds. However, as a direct consequence of the uncertainty principle [Eq. (1.6)], this brief pulse acts as if it covers a range

of frequencies from $\nu_0 - \Delta\nu$ to $\nu_0 + \Delta\nu$ (Figure 3.11), where $\Delta\nu$ is nothing more than the inverse of t_p (Section 1.4). Thus, the shorter the pulse, the greater the range of frequencies covered.

The exact value of ν_0 is designed to be slightly offset from the range of nuclear precession frequencies to be examined (the spectral width, SW, in hertz). Therefore, the SW can be no greater (and preferably less) than $\Delta\nu$, leading to the relationship

$$\text{SW} \leq (t_p)^{-1} \quad \text{or} \quad t_p \leq (\text{SW})^{-1} \quad (3.5)$$

The power of the pulse must be sufficient to cause all sets of nuclei precessing at frequencies within the SW to become phase coherent, each set tipping their \mathbf{M} vectors toward the x', y' plane (Section 2.3). The nearer a nucleus's precession frequency is to ν_0 , the more excitation energy the nucleus receives from the pulse, and the greater its flip angle α . However, the closer α is to 90° , the stronger will be the signal generated by a set of nuclei (Section 2.3). At the powers normally used, a pulse as long as $1/\text{SW}$ causes flip angles to

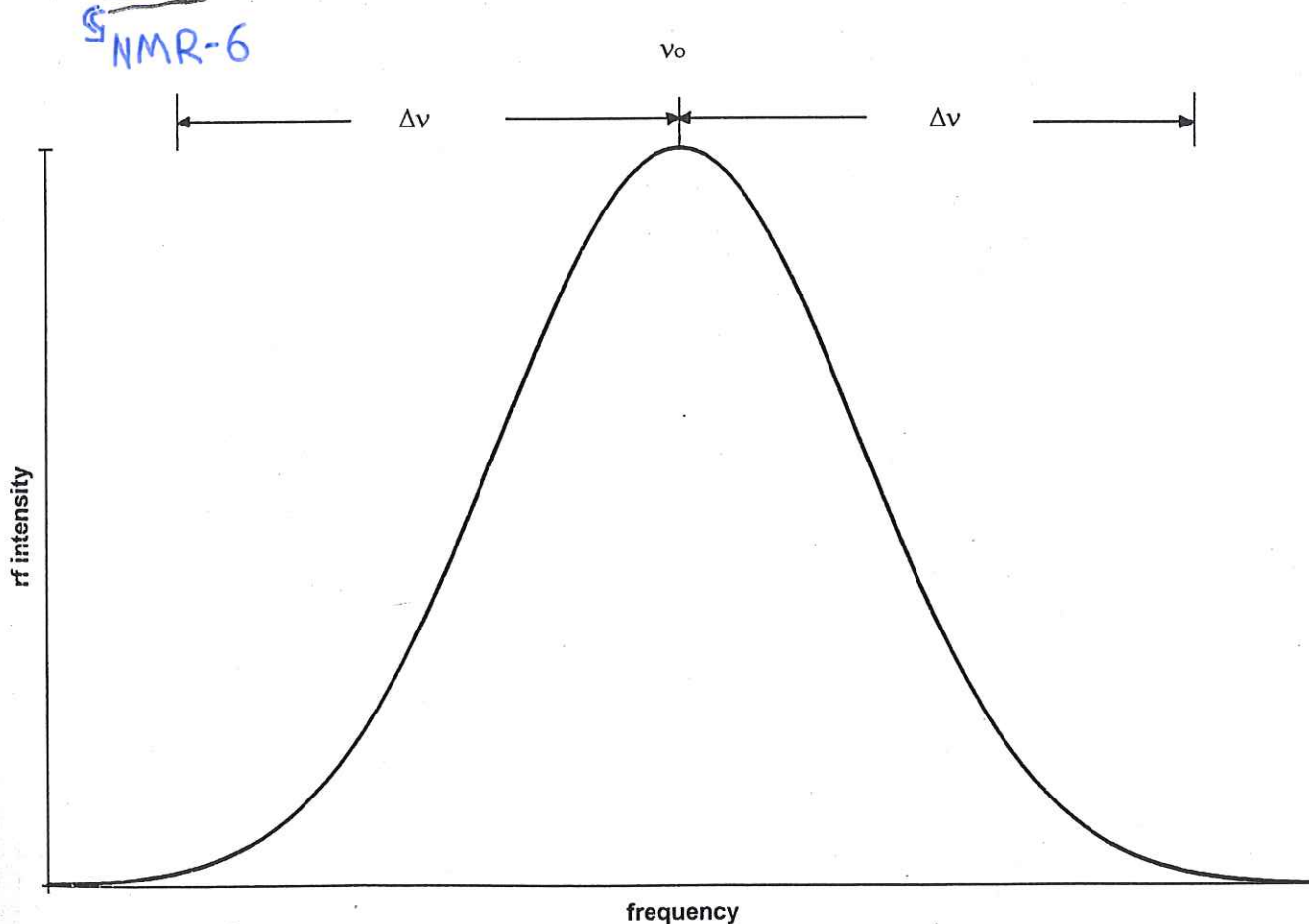


Figure 3.11. Frequency distribution profile for an rf pulse of duration (pulse width) t_p . The frequencies range from $\nu_0 - \Delta\nu$ to $\nu_0 + \Delta\nu$, where $\Delta\nu$ equals $1/t_p$. The sweep width can be either half of the curve.

■ **EXAMPLE 1.2** The C=O bond in formaldehyde vibrates (stretches, then contracts) with a frequency of 5.13×10^{13} Hz. (a) What frequency of radiation could be absorbed by this vibrating bond? (b) How much energy would each photon deliver? (c) To which region of the electromagnetic spectrum does this radiation belong? (d) Are photons of this region capable of breaking bonds?

□ **Solution:** (a) From Eq. (1.5) we know the frequencies must match; therefore, $\nu_{\text{photon}} = 5.13 \times 10^{13}$ Hz. (b) From Eq. (1.3),

$$E_{\text{photon}} = h\nu = (6.63 \times 10^{-34} \text{ J s})(5.13 \times 10^{13} \text{ s}^{-1})$$

$$= 3.40 \times 10^{-20} \text{ J} = 20.5 \text{ kJ mol}^{-1}$$

(c) From Table 1.1 we see that radiation of this frequency and energy falls in the infrared region. (d) No. This amount of energy is less than half that required to break even the weakest chemical bond. However, absorption of such a photon does create a vibrationally excited bond, which is more likely to undergo certain chemical reactions than is the same bond in its ground state. □

At this point you might think that the frequency-matching requirement places a heavy constraint on the types of absorption processes that can occur. After all, how many kinds of periodic motion can a particle have? The answer is that even a small molecule is constantly undergoing many types of periodic motion. Each of its bonds is constantly vibrating; the molecule as a whole and some of its individual parts are rotating in all three dimensions; the electrons are circulating through their orbitals. And each of these processes has its own characteristic frequency and its own set of selection rules governing absorption!

All of the above forms of microscopic motion are what we might describe as *intrinsic*. That is, the motion takes place all by itself, without intervention by any external agent. However, it is possible under certain circumstances to *induce* particles to engage in additional forms of periodic motion. Still, to achieve resonance, we need to match the frequency of this induced motion with that of the incident radiation [Eq. (1.5)].

For example, an ion (or any charged particle, for that matter) follows a curved path as it moves through a magnetic field. If we carefully adjust the strength of the magnetic field, the ion will follow a perfectly circular path, with a characteristic fixed frequency that depends on its mass, charge, velocity, and strength of the magnetic field. Matching this characteristic **cyclotron** frequency with incident electromagnetic radiation of the same frequency can lead to absorption, and this is the basis of a technique known as **ion cyclotron resonance (ICR) spectroscopy**. We will discover in Chapter 2 that a strong magnetic field can also be used to induce

certain nuclei to move with uniform periodic motion of a different type.

1.4 UNCERTAINTY AND THE QUESTION OF TIME SCALE

If you have ever tried to take a photograph of a moving object, you know that the shutter speed of the camera must be adjusted to avoid blurring the image. And, of course, the faster the object is moving, the shorter must be the exposure time to “freeze” the motion. We have very similar considerations in spectroscopy.

Suppose you owned a collection of very extraordinary chameleons that were able to change colors instantaneously from white to black or black to white every 1 s. If you took a picture of them with a shutter speed of 10 s, each of the little critters would appear to be gray. But if you decreased the exposure time to 0.01 s, the photograph would show black ones and white ones in roughly equal numbers but no gray ones! Thus, to capture the individual colors, your exposure time must be significantly shorter than the lifetimes of the species, in this case the 1-s lifetime of each colored form.

There are many types of molecular chameleons, that is, molecules that constantly undergo some sort of reversible reorganization of their structures. If absorption of the photon is fast enough, we will detect both the “black” and “white” forms of the molecule. But if the absorption process is slower than the interconversion, we will detect only some sort of *time-averaged* structure. The situation therefore boils down to the question: How long does it take for a particle to absorb a photon? Unfortunately, such a question is impossible to answer with complete precision.

In 1927, W. Heisenberg, a pioneer of quantum mechanics, stated his **uncertainty principle**: There will always be a limit to the precision with which we can *simultaneously* determine the energy and time scale of an event. Stated mathematically, the product of the uncertainties of energy (ΔE) and time (Δt) can never be less than h (our old friend, Planck’s constant):

$$\Delta E \Delta t \geq h \quad (1.6)$$

Thus, if we know the energy of a given photon to a high order of precision, we would be unable to measure precisely how long it takes for the photon to be absorbed. Nonetheless, there is a useful generalization we *can* make. Using Eq. (1.3), we can substitute $h \Delta \nu$ for the ΔE in Eq. (1.6), giving

$$\Delta \nu \Delta t \geq 1 \quad \Delta t \geq \frac{1}{\Delta \nu} \quad \text{or} \quad \Delta \nu \geq \frac{1}{\Delta t}$$

where $\Delta \nu$ is the uncertainty in frequency. As a result, the time required for a photon to be absorbed (Δt) must be approximately as long as it takes one “cycle” of the wave to pass the

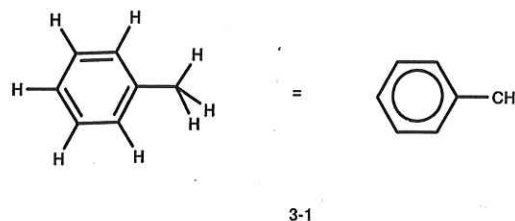
per cycle for each contributing wave. Therefore, so that frequencies of $\Delta\nu_i$ from 0 to SW hertz can be determined, the computer must collect $2 \times \text{SW}$ data points per second, which is equivalent to a dwell time no larger than the inverse of twice SW:

$$t_d \leq (2 \text{ SW})^{-1} \quad (3.6)$$

Actually, the spectroscopic data would more closely resemble the pattern in Figure 3.15, which is the same as the wave in Figure 3.14, except that the overall intensity of the signal decays exponentially with time. (Note that the decay does *not* affect the frequencies.) Such a pattern is called the modulated free induction decay (FID) signal (or time-domain spectrum). The decay is the result of spin-spin relaxation (Section 2.3.2), which reduces the net magnetization in the x, y plane. The envelope (see Section 3.6.2) of the damped wave is described by an exponential decay function whose decay time is T_2^* , the effective spin-spin relaxation time.

Most molecules examined by NMR have more than just two sets of nuclei, each set with a different frequency ($\Delta\nu_i$). Furthermore, each set has its own relaxation times (T_1 and T_2), and usually there are different numbers of nuclei within each set. These factors combine to give complex digital FID curves consisting of n data points (usually in the thousands), numbered from 0 to $n - 1$.

For example, Figure 3.16 shows the ^1H FID curve for toluene (3-1):



From the FID data the computer determines the frequency ($\Delta\nu_i$) and intensity of each component wave. How does it accomplish this magic? The computer performs a Fourier transformation (FT) of the FID data according to the equation

$$F_j = \sum_{k=0}^{n-1} T_k \exp\left(-\frac{2\pi i j k}{n}\right) \quad \text{for } j = 0, \dots, n-1 \quad (3.7)$$

where T_k represents the k th point of the time-domain (FID) data and F_j represents the j th point in the resulting frequency-domain spectrum. Thus, *each* F_j point (from 0 to $n - 1$) requires a summation over all n points in the FID curve, and the total calculation involves n^2 multiplications and additions.

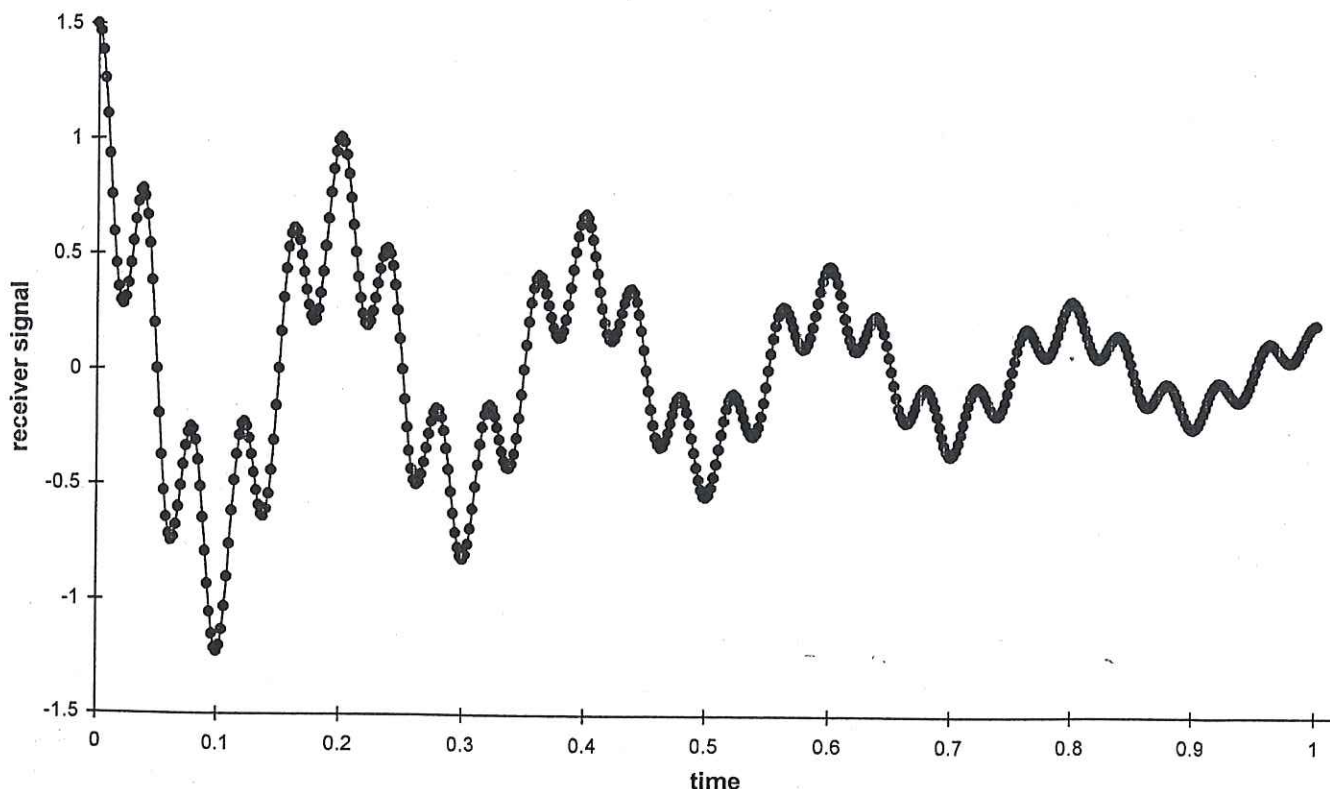


Figure 3.15. Simulated FID signal. The same data as in Figure 3.14, with exponential decay of the signal added.

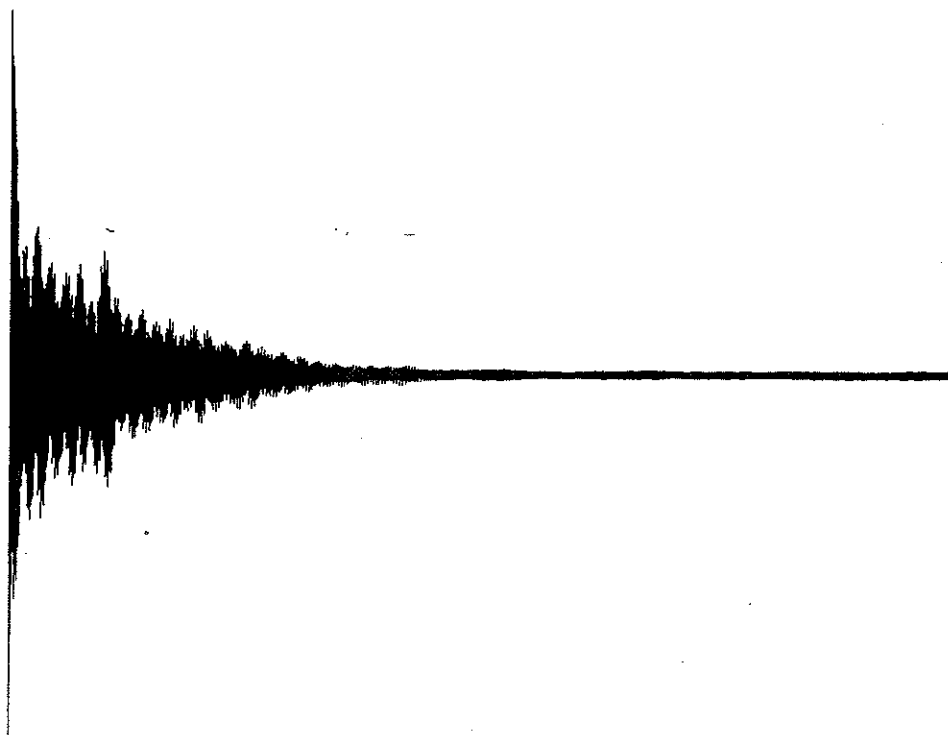


Figure 3.16. Actual ^1H FID curve for toluene (3-1).

An algorithm developed by Cooley and Tukey simplified this extremely time-consuming calculation, bringing it within the capability of modern microcomputers. Today, the transformation takes only a few seconds, after which the frequency-domain spectrum F_j can be plotted. (The frequency-domain spectrum corresponding to Figure 3.16 will be discussed in Chapter 5.)

During the FT of the FID data the computer will perform a series of additional manipulations on the time- and frequency-domain data in order to present the most accurate peak shape and spectrum appearance, including such computational techniques as **zero filling** and **apodization**. Zero filling is a process for retrieving the maximum resolution present in the FID data without increasing the RAM requirement of the computer. Apodization eliminates sinusoidal wiggles in the baseline around a frequency-domain signal peak caused by truncating the FID acquisition too soon (using a t_{acq} that is too short). Further details of these techniques are beyond the scope of this book, but the interested reader may wish to consult the Additional Resources section at the end of this chapter. With input from the operator, adjustments can also be made to the **phasing** of each signal, ensuring that the baseline on both sides is symmetrically horizontal.

In experiments with either dilute samples or insensitive nuclei (such as ^{13}C), one pulse usually does not give a sufficiently high S/N to allow the determination of the component frequencies and intensities accurately. The S/N can be improved by repeating the pulse-data acquisition sequence, then

adding the new FID data to the previously acquired data, as in a CAT experiment. The required number of pulse sequences (scans) is determined by the desired S/N . But there is an additional consideration: To avoid saturation, one must allow enough time between pulses for the nuclei to return (or nearly return) to their original equilibrium (Boltzmann) distribution. The required **delay time** (t_w) is a function of the T_1 values for each set of nuclei of interest (Sections 2.3 and 2.5).

As a typical example of the pulse-data acquisition-delay sequence (hereafter referred to as the **pulse sequence**), we consider the parameters necessary when generating a typical pulsed-mode 250-MHz ^1H NMR spectrum. First, we select a spectral width that covers all the nuclei of interest, usually around 4000 Hz. Remember that the SW determines the pulse width [$t_p \approx (4 \text{ SW})^{-1}$], which in this case would have to be 62.5 μs . Since the frequency ($\Delta\nu_i$) of each component wave can be uniquely determined by two points per cycle and our spectral width might include frequencies anywhere from 0 to 4000 Hz, we must sample points twice that fast, or 8000 Hz (a dwell time t_d of 125 μs), to ensure collecting all relevant frequencies [Eq. (3.6)]. Moreover, we are limited by our computer's memory capacity. Generating 8000 points per second will fill up 32K (32,768 locations) of the computer's RAM in 4.1 s. This fact determines the maximum **acquisition time** (t_{acq}), the length of time a given FID signal is actually monitored. Moreover, **resolution** (R), the ability to distinguish two nearby signals, is inversely proportional to acquisition time:

$$R = (t_{\text{acq}})^{-1} \quad (3.8)$$

Thus, the 4.1 s acquisition time would provide a resolution of $(4.1 \text{ s})^{-1} = 0.24 \text{ Hz}$. If we require a resolution better (smaller) than 0.24 Hz, either we need more computer RAM to accommodate a longer acquisition time or we have to decrease our spectral width window.

Because the FID signal decays due to spin-spin relaxation, there is a time limit beyond which further monitoring of the FID provides more noise than signal. The usual compromise is to have a short enough *dwell time* to cover the spectral width and a long enough *acquisition time* to provide the desired resolution, consistent with computer memory limitations.

After collecting data from one pulse, we must wait for the nuclei to relax to equilibrium. A total of at least $3T_1$ is usually adequate, but part of this is spent as acquisition time. Thus, the additional *pulse delay time* (t_w), the time between the end of data acquisition and the next pulse, is given by

$$t_w = 3T_1 - t_{\text{acq}} \quad (3.9)$$

Since ^1H nuclei normally exhibit T_1 values on the order of 1 s, we need essentially no additional delay after 4 s acquisition time. For ^{13}C and other slow-to-relax nuclei, however, substantial delay times are sometimes required. Following the pulse delay, the sample is irradiated with another pulse, and the data acquisition sequence begins anew.

Figure 3.17 depicts this sequence. After some number of pulse sequences (depending on sample concentration and isotope being studied), the data are subjected to a Fourier transformation, and the S/N of the resulting frequency-domain spectrum is ascertained. If it is not yet adequate, the pulse sequence is resumed until the desired S/N is attained.

To summarize, a pulsed-mode NMR experiment encompasses two steps: (1) the collection of FID data by a pulse-data acquisition-delay sequence, repeated enough times to yield a time-averaged signal possessing the desired S/N , and (2) a FT of the FID data followed by plotting of signal intensity as a function of frequency. The main thing to remember is that the frequency-domain spectrum generated in a pulsed-mode/Fourier transform experiment contains all the same information as the spectrum obtained in a cw experiment (e.g., Figure 3.8), but in principle all the relevant spectroscopic information can be generated in just a few seconds from a single rf pulse (S/N limitations notwithstanding). And there is one further incidental advantage to the pulse-mode technique. Because the receiver coil is off during the pulse and the transmitter coil is off during data acquisition, we can use just one coil to do both jobs (Figure 3.5b)!

■ **EXAMPLE 3.9** Suppose we are about to acquire a 62.5-MHz ^{13}C NMR spectrum. The desired spectral width window is 15,000 Hz. The nuclei have T_1 values up to 3 s and

the computer RAM has a capacity of 64K (65,536 locations). The desired resolution is 0.5 Hz. (a) Using Figure 3.17 as a guide, suggest values for the various data acquisition parameters. (b) How many data points can be collected from one pulse sequence with these values? (c) If 1000 pulse sequence repetitions (*scans*) are required for the desired S/N , how long will the total experiment take?

□ **Solution:** (a) Use Eqs. (3.5), (3.6), (3.8), and (3.9):

$$t_p \approx (4 \text{ SW})^{-1} = (4 \times 15,000 \text{ Hz})^{-1} = 17 \mu\text{s}$$

$$t_d = (2 \text{ SW})^{-1} = (30,000 \text{ Hz})^{-1} \\ = 33 \mu\text{s} \quad (30,000 \text{ data points per second})$$

$$t_{\text{acq}} = R^{-1} = (0.5 \text{ Hz})^{-1} = 2 \text{ s}$$

$$t_w = 3(T_1) - t_{\text{acq}} = 3(2 \text{ s}) - 2 \text{ s} = 4 \text{ s}$$

(b) Acquiring 30,000 data points per second for 2 s results in 60,000 points for each pulse, well within the computer's RAM limits. (c) Since the pulse time is negligible, the total pulse sequence time is essentially equal to $t_{\text{acq}} + t_w (= 3T_1)$; thus, each pulse sequence requires 6 s. If we need 1000 scans, the total time required for the experiment is 6000 s (1 h 40 min). Although this may seem like a long time, remember from Example 3.7 that just 100 cw scans required nearly 17 h! □

Lest you worry that you will have to supply each parameter in every pulse sequence each time you take an NMR spectrum, you can relax. Modern spectrometers are menu driven. For most common nuclei all you have to do is select the nucleus and the computer assigns the appropriate pulse sequence parameters for most normal cases. However, when you are dealing with an unusual structure or an uncommon nucleus, you may have to do some experimenting with the parameters to get the best spectroscopic data.

3.5 LINE WIDTHS, LINESHAPE, AND SAMPLING CONSIDERATIONS

3.5.1 Line Widths and Peak Shape

A typical signal peak in a frequency-domain NMR spectrum is characterized by several features. Most important are its frequency (its position in the spectrum, $\Delta\nu_i$) and intensity (peak height, or more accurately, the area under the peak). But it is also characterized by a *shape* and a **halfwidth**. The halfwidth ($\nu_{1/2}$) of a signal is the width (in hertz) of the peak at half height (Figure 3.18). The shape, which is determined during the FT process, is described as **Lorentzian** (as opposed to, say, Gaussian; see review problem 3.3). A Lorentzian signal peak (L_ν) conforms to the lineshape equation

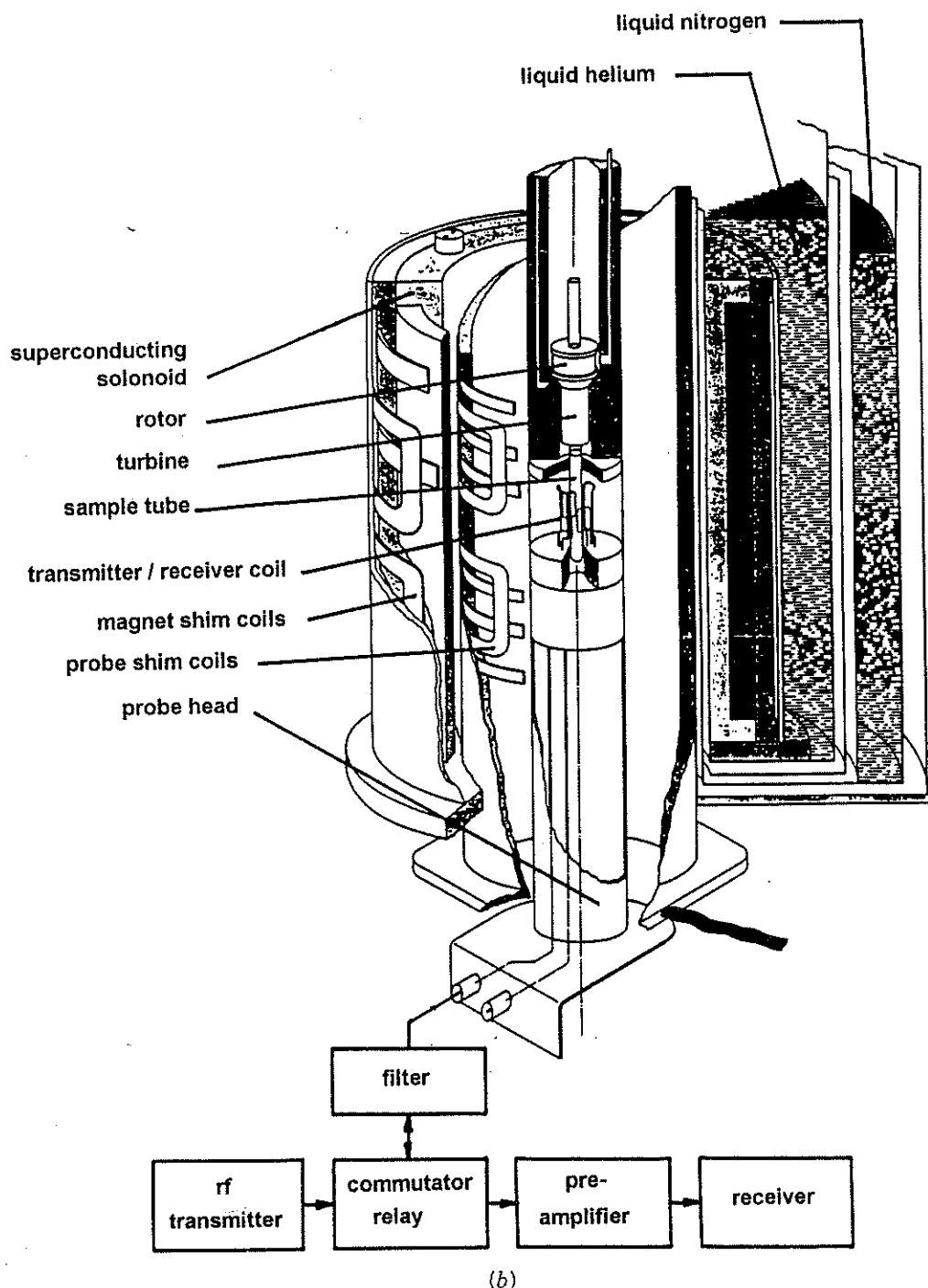


Figure 3.5. (b) Cutaway diagram of the cryostat, showing the essential parts of the magnet and probe.
(Courtesy of Bruker Instruments, Inc.)

This spinning helps to "average out" any slight inhomogeneities of the field in the sample region.

Second, the contour (shape) of the field itself can be varied (within very narrow limits) by passing extremely small currents through a complex series of **shim coils** located around

the probe cavity. The resulting small fields in these coils can be adjusted to further improve the homogeneity of the field. This process, called **shimming** or **tuning** the magnet, is accomplished by adjustment of a dizzying series of shim controls (labeled by the field axis most affected, e.g.,

Η σταθερά σ (*sigma*) του Hammett



$$\log K - \log K_0 = \rho \sigma$$




K_0 είναι η σταθερά ιονισμού του βενζοϊκού οξέος, το οποίο είναι το μόριο αναφοράς

K είναι η σταθερά ιονισμού του παραγώγου του βενζοϊκού οξέος που φέρει τον υποκαταστάτη που μελετάται

ρ (*rho*) είναι σταθερά που στην περίπτωση των χημειοτύπων βενζοϊκού οξέος έχει τιμή=1,00

σ (*sigma*) είναι η σταθερά που αποδίδεται στον υποκαταστάτη. Η σταθερά σ ποσοτικοποιεί τη συνολική ηλεκτρονιακή επίδραση (συζυγιακή και επαγωγική) του υποκαταστάτη και έχει διαφορετική τιμή ανάλογα με το εάν αυτός βρίσκεται σε θέση παρα-, μετα- ή ορθο- ως προς την καρβοξυλική-ομάδα.

Η σταθερά σ^* (*sigma-star*) του Taft



$$\sigma^* = (-\Delta pK_a - 0,06) / 0,63$$



το ΔpK_a υπολογίζεται με αφαίρεση από το pK_a του οξικού οξέος το pK_a του παραγώγου του οξικού οξέος που έχει ως υποκαταστάτη την ομάδα που θέλουμε να προσδιορίσουμε την τιμή σ^* . Η τιμή σ^* ποσοτικοποιεί την αλειφατική επαγωγική επίδραση του υποκαταστάτη και έχει προσαρμοστεί με βάση την παραδοχή ότι το σ^* του μεθυλίου έχει τιμή 0,00.

Παραδείγματα τιμών σ (Hammett) και σ^* (Taft)

Σημείωση: Οι αρνητικές τιμές αναφέρονται σε δότες ηλεκτρονίων ενώ οι θετικές σε δέκτες.

Table 17.4 Sigma substituent constants

	From benzoic acid		From acetic acid
	Meta substituents σ_m	Para substituents σ_p	σ^*
—NHMe	−0.30	−0.84	−0.81
—CH ₂ SiMe ₃	−0.17	−0.27	−0.31
—NMe ₂	−0.15	−0.83	0.32
— <i>t</i> -Bu	−0.09	−0.15	−0.30
—Me	−0.06	−0.14	0.00
—NH · OH	−0.04	−0.34	0.30
—NH · CO · NH ₂	−0.03	−0.24	1.31
—NH · NH ₂	−0.02	−0.55	0.40
—H	0.00	0.00	
<hr/>			
—NH ₂	0.00	−0.57	0.62
—C ₆ H ₅	0.05	−0.01	0.75
—OMe	0.11	−0.28	1.81
—NH · COMe	0.12	−0.09	1.40
—OH	0.13	−0.38	1.34
—SMe	0.14	0.00	1.56
—SH	0.25	0.15	1.68
—N ₃	0.27	0.15	2.62
—CO · NH ₂	0.28	0.31	1.68
—CO · OMe	0.32	0.39	2.00
—CO · OH	0.35	0.44	2.08
—CHO	0.36	0.44	2.15
—COMe	0.36	0.47	1.81
—OCF ₃	0.36	0.33	
—SCF ₃	0.38	0.50	2.75
<hr/>			
—F	0.34	0.06	3.21
—Cl	0.37	0.24	2.96
—Br	0.39	0.22	2.84
—I	0.35	0.21	2.46
<hr/>			
—O · COMe	0.39	0.31	2.56
—CCl ₃	0.40	0.46	2.65
—SCN	0.41	0.52	3.43
—CF ₃	0.46	0.53	2.61
—SO ₂ NH ₂	0.46	0.57	2.61
—CN	0.62	0.70	3.30
—SO ₂ Me	0.64	0.73	3.68
—NO ₂	0.74	0.78	4.25
—SO ₂ CF ₃	0.76	0.95	4.50
<hr/>			
<i>Ions</i>			
—S [−]	−0.36		
—CO ₂ [−]	0.09	−0.05	−1.06
—NH ₃ ⁺	0.67	0.53	3.76
—NMe ₃ ⁺	0.99	0.96	4.55

(Perrin, Dempsey and Serjeant, 1981.)

Σημείωση: Τιμές με αρνητικό (-) πρόσημο αναφέρονται σε μετατοπίσεις upfield (προστασία) ενώ αυτές με θετικό (+) πρόσημο αναφέρονται σε μετατοπίσεις downfield (αποπροστασία).

TABLE 6.2 ^1H Substituent Parameters ($\Delta\delta_X$, ppm) for Substituents on Tetrahedral Carbons

Group X^b	$\Delta\delta_{\alpha-X}$	$\Delta\delta_{\beta-X}^c$	Group X^b	$\Delta\delta_{\alpha-X}$	$\Delta\delta_{\beta-X}^c$
-R	0.62	0.01	-SPh	2.27	
-CF ₃	1.2		-S(=O) _{1,2} R	2.37	
-CH=C(R/H) ₂	1.37	0.15	-Br	2.47	0.95
-C \equiv C(R/H)	1.50	0.35	-SC \equiv N	2.47	
-C(=O)OR	1.77	0.33	-N=CR ₂	2.67	
-C(=O)N(R/H) ₂	1.77	0.25	-N ⁺ (R/H) ₃	2.72	0.55
-C(=O)OH	1.87	0.33	-NHC(=O)R	2.72	0.25
-S(R/H)	1.87	0.43	-SO ₃ (R/H)	2.77	
-C(=O)R	1.87	0.20	-Cl	2.80	0.70
-C \equiv N	1.92	0.43	-O(R/H)	2.97	0.35
-I	1.94	0.90	-P ⁺ Cl ₃	3.07	
-C(=O)H	1.97	0.25	-N=C=S	3.17	
-NR ₂	2.00	0.20	-OC(=O)(R/H)	3.40	0.45
-Ph	2.00	0.33	-OSO ₂ R	3.47	
-PR ₂ , -P(=O)R ₂	2.00		-OPh	3.60	0.45
-C(=O)Ph	2.17	0.33	-OC(=O)Ph	3.60	0.80
-SSR	2.17		-NO ₂	3.82	0.75
-NH ₂	2.27		-F	4.00	0.70

αρχικό $\delta = 0.23$

TABLE 6.4 Substituent Parameters ($\Delta\delta_X$, ppm) for Vinyl Hydrogen Chemical Shifts

-X	$\Delta\delta_{\text{gem}}$	$\Delta\delta_{\text{cis}}$	$\Delta\delta_{\text{trans}}$
-C \equiv N	0.23	0.78	0.58
-R (alkyl)	0.44	-0.26	-0.29
-C \equiv CR	0.50	0.35	0.10
-CH ₂ SR	0.53	-0.15	-0.15
-CH ₂ NR ₂	0.66	-0.05	-0.23
-CH ₂ OR	0.67	-0.02	-0.07
-CH ₂ I	0.67	-0.02	-0.07
-NR ₂	0.69 (2.30)	-1.19 (-0.73)	-1.31 (-0.81)
-Cycloalkenyl ^b	0.71	-0.33	-0.30
-CH ₂ Cl	0.72	0.12	0.07
-CH ₂ Br	0.72	0.12	0.07
-C(=O)OR	0.84 (0.68)	1.15 (1.02)	0.56 (0.33)
-CH=CH ₂	0.98 (1.26)	-0.04 (0.08)	-0.21 (-0.01)
-C(=O)OH	1.00 (0.69)	1.35 (0.97)	0.74 (0.39)
-Cl	1.00	0.19	0.03
-SR	1.00	-0.24	-0.04
-C(=O)H	1.03	0.97	1.21
-Br	1.04	0.40	0.55
-C(=O)R	1.10 (1.06)	1.13 (1.01)	0.81 (0.95)
-C(=O)Cl	1.10	1.41	0.99
-OR	1.18 (1.14)	-1.06 (-0.65)	-1.28 (-1.05)
-Ph	1.35	0.37	-0.10
-C(=O)NR ₂	1.37	0.93	0.35
-SO ₂ R	1.58	1.15	0.95
-OC(=O)R	2.09	-0.40	-0.67

απρίκο δ=5.28

TABLE 6.5 Aromatic Substituent Parameters ($\Delta\delta_X$, ppm)^a

X	H _{ortho}	H _{meta}	H _{para}	X	H _{ortho}	H _{meta}	H _{para}
-CH ₃	-0.17	-0.09	-0.18	-I	0.40	-0.26	-0.03
-CH ₂ CH ₃	-0.15	-0.06	-0.18	-OH	-0.50	-0.14	-0.4
-CH(CH ₃) ₂	-0.14	-0.09	-0.18	-OR	-0.27	-0.08	-0.27
-C(CH ₃) ₃	0.01	-0.10	-0.24	-OC(=O)R	-0.22	0	0
-CH=CH ₂	0	0	0	-OSO ₂ Ar	-0.26	-0.05	0
-C≡CH	0.20	0	0	-C(=O)H	0.58	0.21	0.27
-Ph	0.18	0	0.08	-C(=O)R	0.64	0.09	0.3
-CF ₃	0.25	0.25	0.25	-C(=O)OH	0.8	0.14	0.20
-CH ₂ Cl	0	0.01	0	-C(=O)OR	0.74	0.07	0.20
-CHCl ₂	0.10	0.06	0.10	-C(=O)Cl	0.83	0.16	0.3
-CCl ₃	0.8	0.2	0.2	-C≡N	0.27	0.11	0.3
-CH ₂ OH	-0.10	-0.10	-0.10	-NH ₂	-0.75	-0.24	-0.63
-CH ₂ OR	0	0	0	-NR ₂	-0.60	-0.10	-0.62
-CH ₂ NH ₂	0.0	0.0	0.0	-NHC(=O)R	0.23		
-SR	-0.03	0	0	-N ⁺ H ₃	0.63	0.25	0.25
-F	-0.30	-0.02	-0.22	-NO ₂	0.95	0.17	0.33
-Cl	0.02	-0.06	-0.04	-N=C=O	-0.20	-0.20	-0.20
-Br	0.22	-0.13	-0.03				

"NMR Chemical Shifts of Common Laboratory Solvents as Trace Impurities" *J. Org. Chem.*, 62, 7512-7515 (1997).

Notes

J. Org. Chem., Vol. 62, No. 21, 1997 7513

Table 1. ¹H NMR Data

	proton	mult	CDCl ₃	(CD ₃) ₂ CO	(CD ₃) ₂ SO	C ₆ D ₆	CD ₃ CN	CD ₃ OD	D ₂ O
solvent residual peak			7.26	2.05	2.50	7.16	1.94	3.31	4.79
H ₂ O		s	1.56	2.84 ^a	3.33 ^a	0.40	2.13	4.87	
acetic acid	CH ₃	s	2.10	1.96	1.91	1.55	1.96	1.99	2.08
acetone	CH ₃	s	2.17	2.09	2.09	1.55	2.08	2.15	2.22
acetonitrile	CH ₃	s	2.10	2.05	2.07	1.55	1.96	2.03	2.06
benzene	CH	s	7.36	7.36	7.37	7.15	7.37	7.33	
tert-butyl alcohol	CH ₃	s	1.28	1.18	1.11	1.05	1.16	1.40	1.24
	OH ^c	s			4.19	1.55	2.18		
tert-butyl methyl ether	CCH ₃	s	1.19	1.13	1.11	1.07	1.14	1.15	1.21
	OCH ₃	s	3.22	3.13	3.08	3.04	3.13	3.20	3.22
BHT ^b	ArH	s	6.98	6.96	6.87	7.05	6.97	6.92	
	OH ^c	s	5.01		6.65	4.79	5.20		
	Ar-CH ₃	s	2.27	2.22	2.18	2.24	2.22	2.21	
	ArC(CH ₃) ₃	s	1.43	1.41	1.36	1.38	1.39	1.40	
chloroform	CH	s	7.26	8.02	8.32	6.15	7.58	7.90	
cyclohexane	CH ₂	s	1.43	1.43	1.40	1.40	1.44	1.45	
1,2-dichloroethane	CH ₂	s	3.73	3.87	3.90	2.90	3.81	3.78	
dichloromethane	CH ₂	s	5.30	5.63	5.76	4.27	5.44	5.49	
diethyl ether	CH ₃	t, 7	1.21	1.11	1.09	1.11	1.12	1.18	1.17
	CH ₂	q, 7	3.48	3.41	3.38	3.26	3.42	3.49	3.56
diglyme	CH ₂	m	3.65	3.56	3.51	3.46	3.53	3.61	3.67
	CH ₂	m	3.57	3.47	3.38	3.34	3.45	3.58	3.61
	OCH ₃	s	3.39	3.28	3.24	3.11	3.29	3.35	3.37
1,2-dimethoxyethane	CH ₃	s	3.40	3.28	3.24	3.12	3.28	3.35	3.37
	CH ₂	s	3.55	3.46	3.43	3.33	3.45	3.52	3.60
dimethylacetamide	CH ₃ CO	s	2.09	1.97	1.96	1.60	1.97	2.07	2.08
	NCH ₃	s	3.02	3.00	2.94	2.57	2.96	3.31	3.06
	NCH ₃	s	2.94	2.83	2.78	2.05	2.83	2.92	2.90
dimethylformamide	CH	s	8.02	7.96	7.95	7.63	7.92	7.97	7.92
	CH ₃	s	2.96	2.94	2.89	2.36	2.89	2.99	3.01
	CH ₃	s	2.88	2.78	2.73	1.86	2.77	2.86	2.85
dimethyl sulfoxide	CH ₃	s	2.62	2.52	2.54	1.68	2.50	2.65	2.71
dioxane	CH ₂	s	3.71	3.59	3.57	3.35	3.60	3.66	3.75
ethanol	CH ₃	t, 7	1.25	1.12	1.06	0.96	1.12	1.19	1.17
	CH ₂	q, 7 ^d	3.72	3.57	3.44	3.34	3.54	3.60	3.65
	OH	s ^{c,d}	1.32	3.39	4.63		2.47		
ethyl acetate	CH ₃ CO	s	2.05	1.97	1.99	1.65	1.97	2.01	2.07
	CH ₂ CH ₃	q, 7	4.12	4.05	4.03	3.89	4.06	4.09	4.14
	CH ₂ CH ₃	t, 7	1.26	1.20	1.17	0.92	1.20	1.24	1.24
ethyl methyl ketone	CH ₃ CO	s	2.14	2.07	2.07	1.58	2.06	2.12	2.19
	CH ₂ CH ₃	q, 7	2.46	2.45	2.43	1.81	2.43	2.50	3.18
	CH ₂ CH ₃	t, 7	1.06	0.96	0.91	0.85	0.96	1.01	1.26
ethylene glycol	CH	s ^e	3.76	3.28	3.34	3.41	3.51	3.59	3.65
"grease" ^f	CH ₃	m	0.86	0.87		0.92	0.86	0.88	
	CH ₂	br s	1.26	1.29		1.36	1.27	1.29	
n-hexane	CH ₃	t	0.88	0.88	0.86	0.89	0.89	0.90	
	CH ₂	m	1.26	1.28	1.25	1.24	1.28	1.29	
HMPA ^g	CH ₃	d, 9.5	2.65	2.59	2.53	2.40	2.57	2.64	2.61
methanol	CH ₃	s ^h	3.49	3.31	3.16	3.07	3.28	3.34	3.34
	OH	s ^{c,h}	1.09	3.12	4.01		2.16		
nitromethane	CH ₃	s	4.33	4.43	4.42	2.94	4.31	4.34	4.40
n-pentane	CH ₃	t, 7	0.88	0.88	0.86	0.87	0.89	0.90	
	CH ₂	m	1.27	1.27	1.27	1.23	1.29	1.29	
2-propanol	CH ₃	d, 6	1.22	1.10	1.04	0.95	1.09	1.50	1.17
	CH	sep, 6	4.04	3.90	3.78	3.67	3.87	3.92	4.02
pyridine	CH(2)	m	8.62	8.58	8.58	8.53	8.57	8.53	8.52
	CH(3)	m	7.29	7.35	7.39	6.66	7.33	7.44	7.45
	CH(4)	m	7.68	7.76	7.79	6.98	7.73	7.85	7.87
silicone grease ⁱ	CH ₃	s	0.07	0.13		0.29	0.08	0.10	
tetrahydrofuran	CH ₂	m	1.85	1.79	1.76	1.40	1.80	1.87	1.88
	CH ₂ O	m	3.76	3.63	3.60	3.57	3.64	3.71	3.74
toluene	CH ₃	s	2.36	2.32	2.30	2.11	2.33	2.32	
	CH(o/p)	m	7.17	7.1-7.2	7.18	7.02	7.1-7.3	7.16	
	CH(m)	m	7.25	7.1-7.2	7.25	7.13	7.1-7.3	7.16	
triethylamine	CH ₃	t, 7	1.03	0.96	0.93	0.96	0.96	1.05	0.99
	CH ₂	q, 7	2.53	2.45	2.43	2.40	2.45	2.58	2.57

^a In these solvents the intermolecular rate of exchange is slow enough that a peak due to HDO is usually also observed; it appears at 2.81 and 3.30 ppm in acetone and DMSO, respectively. In the former solvent, it is often seen as a 1:1:1 triplet, with ²J_{H,D} = 1 Hz.

^b 2,6-Dimethyl-4-*tert*-butylphenol. ^c The signals from exchangeable protons were not always identified. ^d In some cases (see note a), the coupling interaction between the CH₂ and the OH protons may be observed (*J* = 5 Hz). ^e In CD₃CN, the OH proton was seen as a multiplet at δ 2.69, and extra coupling was also apparent on the methylene peak. ^f Long-chain, linear aliphatic hydrocarbons. Their solubility in DMSO was too low to give visible peaks. ^g Hexamethylphosphoramide. ^h In some cases (see notes a, d), the coupling interaction between the CH₃ and the OH protons may be observed (*J* = 5.5 Hz). ⁱ Poly(dimethylsiloxane). Its solubility in DMSO was too low to give visible peaks.

Magnetic anisotropy

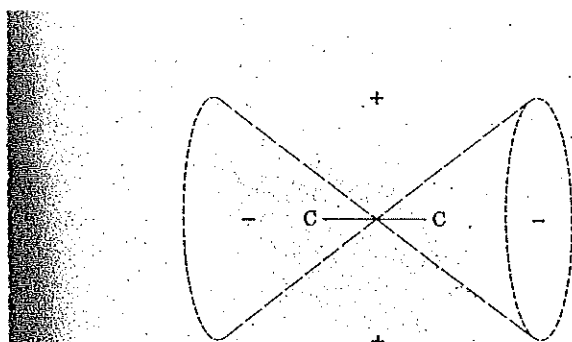


Fig. 16.

Shielding (+) and deshielding (-) zones of C—C.

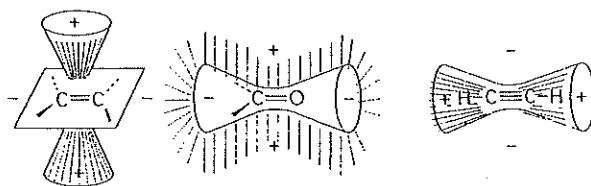


Fig. 3.32 Magnetic anisotropy of (C=C)-, and (C=C)- bonds

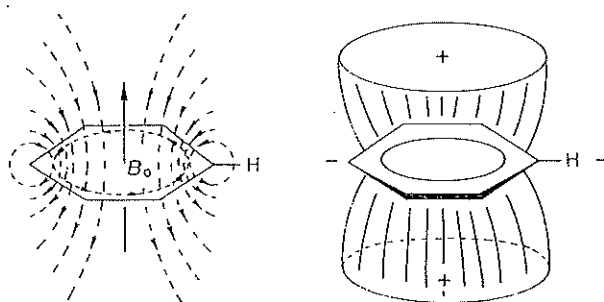


Fig. 3.33 Ring current model for aromatic systems (example: benzene)

- **Solution:** Using a base value of δ 1.51 for a CH_2 group in cyclopentane (Table 6.3) and the $\Delta\delta_{\alpha-\text{Cl}}$ value of 2.80 (Table 6.2), we predict a chemical shift of δ 4.31. The observed value is δ 4.37.³ □

By comparing the $\Delta\delta_\alpha$ and $\Delta\delta_\beta$ for substituents in Table 6.2, you have probably noted that the (de)shielding effect of a substituent normally decreases as the number of intervening bonds increases. The chlorine is separated from the underlined hydrogen in Example 6.11 by *two* bonds; this is called a **geminal** relationship, and here the effect is greatest ($\Delta\delta_{\alpha-\text{Cl}} = 2.80$). The hydrogens (H^β) *three* bonds away from the chlorine (called a **vicinal** relationship) are deshielded only slightly ($\Delta\delta_{\beta-\text{Cl}} = 0.70$), while the deshielding effect on those hydrogens (H^γ) separated by four bonds is negligible.

Before we proceed any further, there is something else that might be troubling you. Why do we need all these correlations and tables if we can simply look up the actual spectra of so many compounds? There are two answers to this question. First, in trying to identify an unknown compound, we need to start somewhere, and acquiring its NMR spectrum is the best place. With only that information, we can usually (if it is not too complicated a molecule) make a decent guess about its structure, then go to the literature for confirmation. But what if the spectrum of our compound has never been reported before? In that case our main evidence for its structure may be how well its NMR spectrum matches expectations based on the above correlations.

6.2.4 Index of Unsaturation and the Nitrogen Rule

In the course of this book we are going to be solving many problems like the one in Example 6.7. Here is a little “trick” to make the process a little easier. Whenever you encounter a molecular formula $\text{C}_c\text{H}_h\text{N}_n\text{O}_o\text{X}_x$ (where X represents halogen: F, Cl, Br, or I), begin by calculating its **index of unsaturation (IOU)** from the equation

$$\text{IOU} = \frac{1}{2} [2c + 2 + n - (h + x)] \quad (6.7)$$

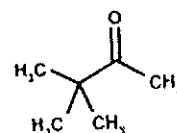
This equation derives from the normal valences of (number of bonds to) atoms of carbon, nitrogen, hydrogen, and halogen (4, 3, 1, and 1, respectively) in molecules where all valences are satisfied (divalent atoms such as oxygen and sulfur do not appear in the equation). The IOU tells us how many rings plus π bonds there must be in any legitimate isomer with that molecular formula. Recall that a double bond is usually pictured as one cylindrically symmetric σ bond and one π bond between two parallel p orbitals. A triple bond consists of one σ bond and two π bonds. The IOU, therefore, is very useful in quickly eliminating from consideration any structures that do not possess the correct number of rings plus π bonds. Thus, the IOU of $\text{C}_7\text{H}_5\text{N}$ (Example 6.7) is $[2(2) + 2 +$

$1 - 3]/2 = 2$, so the correct structure must have either two rings or one ring and one π bond (i.e., one double bond) or two π bonds (two double bonds or one triple bond). The $\text{CH}_3\text{C}\equiv\text{N}$ molecule fits in the last category.

The “nitrogen rule” applies to molecules made up of carbon, hydrogen, nitrogen, oxygen, sulfur, and halogen. When the number of nitrogens in the molecular formula is *even*, the number of hydrogens plus halogens, as well as the nominal molecular mass, must both be even. When the number of nitrogens is *odd*, the number of hydrogens plus halogens, as well as the nominal molecular mass, must both be odd (zero is considered even in this context). This rule can be useful in making guesses about an unknown molecular formula, when the number of hydrogens plus halogens is known (e.g., from NMR data).

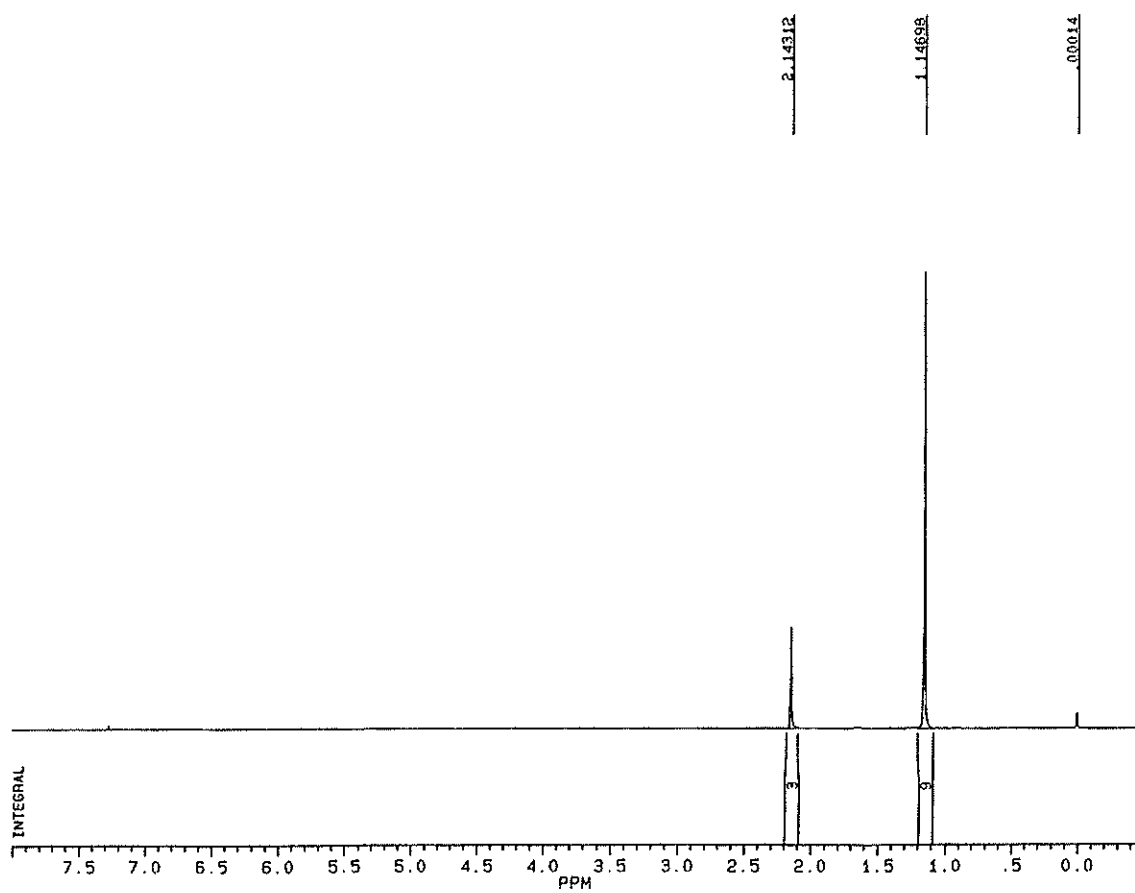
■ **EXAMPLE 6.12** Deduce the structure of the compound whose 250-MHz ^1H NMR spectrum is reproduced in Figure 6.3, given only that its molecular formula is $\text{C}_6\text{H}_{12}\text{O}$.

- **Solution:** Begin by calculating the IOU: $[2(6) + 2 - 12]/2 = 1$. The molecule must therefore possess one ring or one π (that is, double) bond. We note immediately that there are 12 hydrogens, and therefore an even number (zero) of nitrogens. These 12 are divided into 9 equivalent hydrogens at δ 1.15 and 3 other equivalent ones at δ 2.14. Whenever you encounter a 9-proton signal near δ 1.0, it is probably due to 3 equivalent methyl groups, such as those in a *tertiary* butyl group $[(\text{CH}_3)_3\text{C}-]$. Note how all 3 of the methyls in such a group are equivalent, just as the 3 hydrogens in a methyl group are equivalent (Section 4.2). The δ 2.14 signal fits well for a methyl group connected directly to a $\text{C}(=\text{O})\text{R}$ group (see Table 6.2 and Example 6.5). The correct structure, therefore, is pinacolone (3,3-dimethyl-2-butanone):



6.3 VINYL AND FORMYL HYDROGEN CHEMICAL SHIFTS

Two carbons connected by a double (i.e., $\sigma + \pi$) bond are called **vinyl** or **olefinic** carbons. Each vinyl carbon is nominally sp^2 hybridized and attached to three atoms (one of which is the other vinyl carbon). These three atoms describe an approximately equilateral triangle, which is why vinyl carbons are also described as **trigonal**. Hydrogens attached directly to vinyl carbons are called vinyl (or olefinic) hydrogens.



The 250-MHz ^1H NMR spectrum of $\text{C}_6\text{H}_{12}\text{O}$